PHYSICOCHEMICAL INTERACTIONS AT THE BINDER-AGGREGATE INTERFACE

A Dissertation

by

MARIA LORENA GARCIA CUCALON

Submitted to the Office of Graduate and Professional Studies of
Texas A&M University
in partial fulfillment of the requirements for the degree of

DOCTOR OF PHILOSOPHY

Chair of Committee,	Dallas N. Little
Co-Chair of Committee,	Eyad Masad
Committee Members,	Amy Epps Martin
	Robert Lytton
	Bruce Herbert
	Emad Kassem
Head of Department,	Robin Autenrieth

August 2016

Major Subject: Civil Engineering

ABSTRACT

Asphalt mixtures undergo chemical and mechanical changes with environmental weathering, most specifically due to moisture damage and oxidative aging. Degradation through weathering compromises asphalt mixture integrity and leads to early failure. It has been reported that potential for moisture damage is related to physicochemical properties of binder, aggregate, and resulting interface. Oxidative aging literature suggests that the aggregate could be a catalyst to the oxidation process and/or that the aggregate could selectively absorb softer functional groups from within the asphalt binder, resulting in an additional age-hardening effect of the asphalt mixture.

This study characterized mechanical and physicochemical properties of asphalt binders and aggregates and resulting mechanical responses of corresponding asphalt mixtures subjected to moisture and aging effects. The experimental plan involved 20 binder-aggregate combinations including warm-mix asphalt technologies, neat and polymer-modified binders, and two aggregates with different mineralogies and morphologies. Experiments were conducted at various length scales: full mixtures, fine aggregate mixtures, asphalt binder, and aggregates. Additionally, this study proposes a modified microcalorimetry experiment to evaluate binder-aggregate interaction over the range of in-service temperatures and with moisture present at the interface.

This study concludes that physicochemical characteristics of the binder-aggregate interface and aggregate microtextural features affect moisture damage. It was found that increasing temperature reduces binder-aggregate bond strength and that a uniform layer

of moisture prevents binder-aggregate interfacial bonding. Inclusion of warm-mix asphalt additives with adhesion promoters can improve mixture performance in terms of moisture resistance, and additive dosage should be optimized. In terms of age-hardening, it was found that warm-mix asphalt can exhibit greater age-hardening in the first 3 months of laboratory aging, but longer-term aging is comparable to that of hot-mix asphalt. Additional findings conclude that aggregate type can significantly alter the age-hardening process of asphalt mixtures. Gabbro aggregate catalyzes the oxidation process of the asphalt binder, while inclusion of limestone aggregate produces increased stiffening of the asphalt mixture, possibly due to selective absorption. Based on these findings, it is recommended to pursue a deeper understanding of an interphase region formed due to binder interlocking with the aggregate surface and with diffusion of binder into the aggregate.

DEDICATION

I dedicate this work to my family.

To my parents, my grandparents, and my beloved sister and her beautiful family—thanks for raising me with strong values and for loving me unconditionally.

I thank God for giving me patience, endurance, and strength to achieve this goal.

ACKNOWLEDGEMENTS

First, I want to thank my doctoral advisors, Dr. Dallas Little and Dr. Eyad Masad, for the opportunity, guidance, and resources toward execution and completion of my PhD study. Gratitude is extended to my undergraduate and masters academic advisors, Mrs. Paola Carvajal Ayala and Dr. Amy Epps Martin (who also served diligently as a member of my PhD committee). Thank you for giving me strong foundations, preparing me for the PhD road, and for continuing to mentor me throughout my academic path.

I greatly appreciate the guidance and teachings provided by my committee members, Dr. Robert Lytton, Dr. Emad Kassem, and Dr. Bruce Herbert. Appreciation is extended to Dr. Amit Bhasin, Dr. David Allen, Dr. Troy Pauli, Dr. Gayle King, and Dr. David Newcomb for their contribution to my research studies and professional development. This extensive research was made possible thanks to financial support from the Qatar National Research Fund (QNRF) through National Priority Research Program project no. 5-506-2-203. Collaboration in laboratory tasks was provided by Rezwan Jahangir, Tejas Baid, Amanda Hampton, Nikhil Mandhana, and Benjamin Slater.

Last but not least, I want to thank my dear friends and colleagues, Eisa Rahmani, Edith Arambula, Fan Yin, Rafael Menendez, Charles Gurganus, Kamilla Vasconcelos, Silvia Caro, Ilaria Menapace, Ahmed Awed, Cindy Estakhri, Rick Canatella, Barbara Hein, Juliana Cammarata, Karthik Sridhara, Mohammed Sadeq, Jackie Kafie, Javier Grajales, and Maria Alejandra Hernandez-Saenz. Each one of you has enriched my graduate school experience.

NOMENCLATURE

AASHTO	American Association of State Highway and Transportation Officials
ASTM	American Society for Testing and Materials
AFM	Atomic Force Microscopy
AMPT	Asphalt Mixture Performance Tester
ATR	Attenuated Total Reflectance
BET	Branauer, Emmet, and Teller
CA	Carbonyl Area
CI	Confidence Interval
DMA	Dynamic Mechanical Analyzer
DMR	Dynamic Modulus Ratio
DPSE	Dissipated Pseudostrain Energy
DSR	Dynamic Shear Rheometer
ER	Energy Ratio
FAM	Fine Aggregate Matrix
FTIR	Fourier Transform Infrared Spectroscopy
GR	Glover-Rowe
HMA	Hot-Mix Asphalt
LVE	Linear Viscoelastic
LTOA	Long-Term Oven Aging
LW	Lifshitz–van der Waals

MPK	Methyl Propyl Ketone
MSR	Moisture Susceptibility Ratio
NCHRP	National Cooperative Highway Research Program
NPRP	National Priority Research Program
PANDA	Pavement Analysis Using a Nonlinear Damage Approach
PAV	Pressure-Aging Vessel
PG	Performance Grade
RAP	Reclaimed Asphalt Pavement
RH	Relative Humidity
RTFOT	Rolling Thin Film Oven Test
SARA	Saturates, Aromatics, Resins, and Asphaltenes
SBS	Styrene-Butadiene-Styrene
SE	Standard Error
SEM	Scanning Electron Microscopy
SFE	Surface Free Energy
SGC	Superpave Gyratory Compactor
SHRP	Surface Highway Research Program
SSA	Specific Surface Area
STOA	Short-Term Oven Aging
USD	Universal Sorption Device
UV	Ultraviolet
VE	Viscoelastic

WMA	Warm-Mix Asphalt
WRI	Western Research Institute
QNRF	Qatar National Research Fund
XRD	X-ray Diffraction
XRF	X-ray Fluorescence

TABLE OF CONTENTS

Page

LIST OF FIGURES

Page

LIST OF TABLES

Page

CHAPTER I

INTRODUCTION

Asphalt mixtures are a well-established paving material and provide the wearing course in about 93% of United States roads (NAPA). These mixtures are composed of three main phases: mineral aggregates, asphalt binder, and air voids. The viscoelastic (VE) nature of asphalt binder allows for a workable material at production and placement temperatures (130 to 163°C), while rendering a tough, flexible material at operational temperatures. The general industry trend to develop more-resistant, longer-lasting, and ecofriendly materials has led to a broad range of technological alternatives to produce asphalt concrete in the past two decades, thus challenging mixture design methodologies and experience-based prediction models for asphalt pavement performance.

Asphalt mixtures degrade with time due to weathering, specifically moisture damage and oxidative aging (Little and Jones 2003, Caro et al. 2008a, Petersen 2009). Traditional experimental methods (D'Angelo and Anderson 2003) and recently developed modeling techniques (Shakiba et al. 2014, Rahmani 2015) involve extensive laboratory testing in order to account for the effect of weathering degradation in asphalt mixtures. Consideration of interactions between binder and aggregates have shown promise in identifying more compatible asphalt binder-aggregate systems and the ability to develop better micromechanical models of asphalt mixtures subjected to moisture damage (Caro et al. 2008a, Masad et al. 2008, Caro et al. 2009). Oxidative aging of asphalt binder has been thoroughly studied (Liu et al. 1998, Petersen 2009, Petersen and Glaser 2011, Cui et

al. 2014), but the role of aggregate in the age-hardening process of asphalt mixtures remains unclear.

1.1 Literature Review

This section summarizes a literature review and current practices to address moisture damage and age-hardening of asphalt mixtures, most specifically for hot-mix asphalt (HMA). Additionally, one recently implemented technological alternative, warm-mix asphalt (WMA), is detailed, including the current state-of-the-art.

1.1.1 Moisture Damage

Moisture damage in asphalt pavements refers to the deterioration of asphalt mixtures due to moisture effect. Moisture damage compromises the integrity of asphalt mixtures and exacerbates other forms of pavement distresses, so it is a major concern for pavement engineers and researchers (McGennis et al. 1984, D'Angelo and Anderson 2003, Caro et al. 2008a). A wide range of test methods have been developed in an effort to characterize moisture damage in asphalt mixtures (Solaimanian et al. 2003). To prevent moisture-induced early failure in asphalt pavement, the industry has developed a variety of chemical adhesion promoters, including lime and other aggregate treatments that have proved effective over the years (Hunter and Ksaibati 2002, Epps et al. 2003, Little et al. 2006). Nevertheless, these techniques cannot be applied as a universal recipe for improved performance. Susceptibility to moisture damage is related to the particular asphalt binder-aggregate combination, which should be considered during mixture design (Parker Jr and Wilson 1986, D'Angelo and Anderson 2003).

Previously identified mechanisms for moisture damage include detachment, displacement, spontaneous emulsification, pore pressure–induced damage, hydraulic scour, and environmental effects on the asphalt binder-aggregate system (Little and Jones 2003). Detachment and displacement can be explained by interfacial interactions occurring between asphalt binder and aggregate and by the potential for water to disrupt the interface. Caro et al. (2008) summarized theories explaining adhesive bond mechanisms including weak boundary layers, electrostatic forces, chemical bonding (absorption), mechanical bonding, and surface free energy (SFE). The SFE approach provides a sound methodology for ranking compatible systems, and it can be used in micromechanics-based computational simulations of moisture damage, so this study focuses mainly on the SFE theory.

When a particular combination of asphalt binder and aggregate experiences a stronger interaction or bond, it can be referred to as a more compatible system. Such systems are expected to be less likely to exhibit early failure due to moisture effects. Asphalt binder-aggregate compatibility can be optimized by binder modifications or by selection of an alternative aggregate source. Such optimization can be performed through mechanical evaluation of asphalt mixture laboratory specimens with and without moisture-induced damaged or, alternatively, by evaluating the adhesive characteristics of the binder-aggregate system (Little and Bhasin 2006, Bhasin et al. 2007, Howson et al. 2007, Bhasin and Little 2009) based on their respective SFEs.

SFE is defined as the energy required to create a new unit of surface area of a material. For one particular material, the total SFE (γ^{total}) can be described as a function

of three SFE components: monopolar acidic (γ^+), monopolar basic (γ^-), and apolar, or Lifshitz–van der Waals (LW) (γ^{LW}), as described in Equation (1).

$$\gamma^{total} = \gamma^{LW} + 2\sqrt{\gamma^+\gamma^-} \quad (1)$$

Based on SFE components of asphalt binder and mineral aggregates, the asphalt binder-aggregate adhesive bond energy can be calculated using Equation (2). The work of debonding in the presence of moisture can be calculated by Equation (3), and the cohesive bond energy within the asphalt binder itself can be calculated using Equation (4). Additionally, an energy ratio (ER), shown in Equation (5), was proposed as an energy-based indicator of moisture susceptibility (Bhasin et al. 2006, Bhasin and Little 2007). The ER parameter was found to correlate well with laboratory and field performance.

$$\Delta G_{AS} = 2\sqrt{\gamma_A^{LW}\gamma_S^{LW}} + 2\sqrt{\gamma_A^+\gamma_S^-} + 2\sqrt{\gamma_A^-\gamma_S^+} \quad (2)$$

$$\begin{aligned}\Delta G_{AWS} = {} & 2\gamma_W^{LW} + 4\sqrt{\gamma_W^+\gamma_W^-} + 2\sqrt{\gamma_A^{LW}\gamma_S^{LW}} - 2\sqrt{\gamma_A^{LW}\gamma_W^{LW}} - 2\sqrt{\gamma_S^{LW}\gamma_W^{LW}} \\ & -2\sqrt{\gamma_W^+}\left(\sqrt{\gamma_A^-} + \sqrt{\gamma_S^-}\right) - 2\sqrt{\gamma_W^-}\left(\sqrt{\gamma_A^+} + \sqrt{\gamma_S^+}\right) + 2\sqrt{\gamma_A^+\gamma_S^-} + 2\sqrt{\gamma_A^-\gamma_S^+}\end{aligned} \quad (3)$$

$$\Delta G_{AA} = 2\gamma_A^{LW} + 4\sqrt{\gamma_A^+\gamma_A^-} \quad (4)$$

$$ER = \left|\frac{\Delta G_{AS} - \Delta G_{AA}}{\Delta G_{AWS}}\right| \quad (5)$$

where subscripts *A, S,* and *W* correspond to asphalt, aggregate (stone), and water, respectively.

Follow-up studies at Texas A&M University proposed the use of isothermal microcalorimetry to evaluate binder-aggregate adhesion and aggregate hydrophilicity by

directly measuring heat of immersion (Bhasin and Little 2009, Vasconcelos et al. 2010, Miller et al. 2011). Microcalorimetry has the advantage of being a direct measurement of binder-aggregate interactions and offers the flexibility for pretreating aggregates in order to evaluate realistic conditions. To date, studies on asphalt binder-aggregate adhesion by contact angle techniques and microcalorimetry have reported measurements at room temperature and are assumed to be representative of bond strength at an in-service temperature range.

Research studies on moisture susceptibility of asphalt mixtures are generally rank mixtures with susceptibility to moisture damage based on mechanical evaluation before/after moisture conditioning or by conducting the experiment in wet conditions directly. Various studies have found incongruence in ranking asphalt mixture potential for moisture damage when different experimental methods/conditions are used in ranking the same mixtures (Parker Jr and Wilson 1986, Izzo and Tahmoressi 1999, Epps Martin et al. 2014). Among other experimental variables, the different temperatures among the various test methods or conditioning protocols could contribute to the observed differences. Binder-aggregate mechanical interlock depends on aggregate textural features and binder interlocking with surface texture. Asphalt binders are temperature-dependent (fluid-like VE materials); therefore, their capacity to interlock with aggregate particles is also expected to be temperature-dependent. In addition to mechanical features, the binder-aggregate work of adhesion (interfacial bonding) could decrease with increasing temperature, analogous to reduced surface tension of asphalt binder. It is important to

explore adhesive characteristics of binder-aggregate systems at a representative in-service temperature range.

Another important factor exacerbating moisture damage in asphalt mixtures is residual moisture from incomplete drying of aggregates during the production process. It has been noted in previous studies using microcalorimetric techniques that aggregate condition or pretreatment may have a significant impact on binder-aggregate adhesion, most specifically when conditions are such that aggregates are not fully dried prior to testing. Results from measuring binder-aggregate enthalpy of immersion revealed that lower pretreatment temperatures result in less bonding; the authors attributed this observation to residual moisture attached to the aggregate surface (Miller et al. 2011). It is known that the vast majority of aggregates utilized in asphalt mixtures are hydrophilic (Miller et al. 2012), so it is thermodynamically favorable for water to displace (or detach) binder from the aggregate surface (Little and Bhasin 2006, Caro et al. 2008a). It is important to quantify the effect of moisture in binder-aggregate interfacial bonding; such measurements can be conducted by microcalorimetric techniques.

1.1.2 Age-Hardening of Asphalt Mixtures

Oxidative aging is a primary cause of asphalt pavement failures and early cracking. It can be observed mechanically as hardening and embrittlement of the asphalt binder that reflects on the mixture (age-hardening of the asphalt mixture). Extensive research has been conducted to investigate the chemistry of asphalt binders, develop characterization techniques, and investigate changes in binder chemistry occurring with oxidative aging and oxidation kinetics (Davidson et al. 1989, Liu et al. 1998, Petersen and Harnsberger

1998, Petersen 2009, Petersen and Glaser 2011, Cui et al. 2014). Aging changes the relative proportions of saturates, aromatics, resins and asphaltenes (SARA fractions) within the asphalt binder, causing a shift of aromatics and resins toward the subsequent class. VE properties of asphalt binders are altered with changes in colloidal structure (Mastrofini and Scarsella 2000). Formation of oxidation products, principally carbonyl groups, has proved to cause changes in binder rheology by various studies (Lau et al. 1992, Liu et al. 1998, Glover et al. 2005, Petersen 2009, Pauli and Huang 2013). Aging occurs at two different stages for an asphalt mixture: (i) at production (short-term aging), which involves loss of volatile components and binder oxidation during storage, mixing, transport, and placement, and (ii) in-service (long-term aging), involving further oxidation of the asphalt binder (Airey 2003). The generally accepted assumption is that age-hardening of asphalt mixtures results directly from binder aging. Current practices for binder characterization and quality assurance include the use of accelerated aging protocols such as the rolling thin film oven test (RTFOT) to simulate short-term aging, as well as the pressure-aging vessel (PAV) to simulate long-term aging.

The majority of research involving age-hardening of asphalt binders and mixtures focus on either binder or mixtures separately. Studies by the Strategic Highway Research Program (SHRP) were strongly oriented toward (i) characterization of binder chemistry and rheology with aging (Branthaver et al. 1993, Petersen at al. 1994, Anderson et al. 1994) or (ii) simulating mixture aging during production and/or service life under field conditions using laboratory short- and long-term oven aging (STOA and LTOA) protocols for the purpose of mechanically characterizing asphalt mixtures (Bell 1989, Bell et al.

1994). Limited studies were conducted before and during the SHRP to investigate the impact of mineral aggregate in binder aging. It was suggested that the aggregate fraction could be a catalyst to the oxidation process (Barbour et al. 1974, Petersen et al. 1974). Additionally, the aggregate's surface morphology, most specifically porosity, was suggested as possibly impacting asphalt mixture age-hardening and binder oxidation processes. The lighter oily fractions found within the asphalt binders may enter porous aggregates, while the highly associated polar fractions remain at the surface of the aggregate, resulting in a stiffer material surrounding the aggregate (Lee et al. 1990). In the event of selective absorption, the "fractionated" binder may follow different oxidation paths as compared to the "complete" binder (Usmani 1997). As a material can adsorb a greater amount of polar components from the binder, it may also protect the adsorbed components from further oxidation (Petersen et al. 1974).

Later studies turned to investigating the impact of mineral aggregates on the mechanical age-hardening process of asphalt mixtures. Experimental comparisons of mixture and binder aging report contradictory results (Airey and Wu 2009). In this study, a particular mixture demonstrated the most severe stiffening upon aging, while the binder extracted from the same mixture showed the least stiffening, challenging the common assumption that mixture age-hardening results directly from binder age-hardening. A more recent study confirmed that aggregate has an impact on binder and mixture aging (Wu et al. 2014). As pavement engineers, our priority is to characterize mixtures at the initial stage and account for the age-hardening effect throughout the service life of a pavement structure. Ideally, such information should be available upon binder characterization in

terms of oxidation and/or age-hardening, but limited correlations between binder and mixture aging are found in the literature (Morian et al. 2011, Glover et al. 2014, Newcomb et al. 2015). It is possible that this lack of conclusiveness results from ignoring the role of the aggregate fraction neighboring the asphalt binder and possibly affecting the oxidation and age-hardening processes.

Within the Pavement Analysis Using Nonlinear Damage Approach (PANDA), a continuum-based aging state variable was developed and validated in order to account for progressive change in the properties of asphalt concrete due to age-hardening throughout the lifespan of asphalt pavement. Calibration of model parameters is based on linear viscoelastic (LVE) properties changing with aging time and consideration of oxygen content and temperature variation (Rahmani 2015); the model is described by Equation (6).

$$\dot{A} = \frac{dA}{dt} = \Gamma^{a}\theta^{\alpha_1}(1-A)^{\alpha_2} f(T) \tag{6}$$

where $\dot{A}$ is the time rate of the aging state variable, A ($0 \leq A \leq 1$), Γ^{a} is the fluidity parameter controlling growth rate of A; θ is the oxygen content ($0 \leq \theta \leq 1$); α_1 is the model parameter controlling the effect of oxygen content on aging rate; α_2 is the model parameter controlling the effect of the aging history term, (1-A); and $f(T)$ is the aging temperature coupling parameter.

Within PANDA, the mechanical behavior of an asphalt mixture is defined in terms of creep compliance, as defined by Equation (7). With aging, the compliance terms (D_i) and retardation times (λ_i) are shifted as a function of the aging state variable (A), as

indicated by Equation (8) and Equation (9), respectively, where k_1 and k_2 are material parameters. The instantaneous compliance (D_0) is assumed not to vary with aging.

$$D(t) = D_0 + \sum_{n=1}^{n} D_i[1 - \exp(-\lambda_i t)] \quad (7)$$

$$\mathrm{D_i^A} = (1 - \mathrm{A})^{\mathrm{k_1}} \mathrm{D_i} \quad (8)$$

$$\lambda_\mathrm{i}^\mathrm{A} = (1 - \mathrm{A})^{\mathrm{k_2}} \lambda_\mathrm{i} \quad (9)$$

Note that creep behavior is defined as a function of loading time, while the aging state variable is a function of aging time. It is assumed that the material in a roadway does not age within the time period that a load is applied. Ideally, the aging state variable (A) should be determined from binder age-hardening. Further research is needed to describe mechanistically the relationship between binder and mixture age-hardening processes.

1.1.3 Warm-Mix Asphalt Technologies

WMA consists of a technological innovation that allows asphalt mixtures to be produced and placed at reduced temperatures, as compared to the conventional HMA (i.e., 15°C minimum). Reduced mixing and compaction temperatures can be achieved by using different mechanisms that involve microstructural, physicochemical, and mechanical changes to asphalt binders. Some WMA additives are advertised to reduce viscosity at mixing temperatures while maintaining or slightly increasing the viscosity at operational temperatures (e.g., organic waxes). Other chemical WMA additives reduce the surface tension of the binder to improve wettability (ability to coat) over the aggregate, enabling reduction of production temperatures (e.g., surfactants). Foaming technologies are based on water injection at high pressures to expand the volume of binder and provide better

coating. Concerns remain regarding WMA performance and long-term durability because of reduced production and compaction temperatures (e.g., early rutting and moisture damage).

Several studies have compared the performance of WMA to HMA (Table 1). Most studies show that HMA outperforms WMA in the laboratory, while WMAs demonstrate satisfactory and comparable field performance. Researchers recommend optimizing selection of WMA technology to improve compatibility with mixture constituents for reduced risk of moisture damage. Polymer modification, inclusion of anti-stripping agents, and use of recycled materials have also been evaluated for WMA with satisfactory results. Recommendations for mixture design to preclude moisture damage in WMA, including experimental methods and pass/fail thresholds, were proposed by Garcia Cucalon et al. (2014) and validated by Yin et al. (2016). Satisfactory field performance of WMA validates the continued use of the technology and promotes further implementation (Jones et al. 2011, Estakhri 2012, Epps Martin et al. 2014).

Table 1. Previous research on WMA performance

Topic	Findings	References
Laboratory Evaluation, Moisture Susceptibility	WMA is more moisture-susceptible than HMA	Wasiuddin 2008 Austerman et al. 2009 Diefenderfer and Clark 2011 Kim et al. 2011 Caro et al. 2012
	WMA production at reduced temperatures potentially increases moisture susceptibility	Goh and You 2011 Mejias-Santiago et al. 2011 Alavi et al. 2012
	Inclusion of reclaimed asphalt pavement (RAP) improves WMA resistance to moisture-induced damage	Doyle et al. 2011 Mogawer et al. 2011 Solaimanian et al. 2011
	Optimization of mixture constituents (i.e., WMA additive, binder type, aggregate type, anti-stripping agent) produces best results	Prowell et al. 2007 Hearon and Diefenderfer 2008 Xiao et al. 2011 Bennert et al. 2011 Garcia Cucalon et al. 2015
Laboratory Evaluation, Rutting Potential	WMA has increased rutting potential	Rashwan and Williams 2012 Bower et al. 2012
	Inclusion of anti-stripping agents, polymers, or RAP improves WMA in terms of rutting potential	Hurley and Prowell 2006 Mogawer et al. 2012
Laboratory Evaluation, Fatigue, WMA vs. HMA	WMA shows improved fatigue resistance	Goh and You 2011 Caro et al. 2012 Sadeq et al. 2016a
	WMA shows equivalent fatigue resistance	Bonaquist 2011
	WMA shows decreased fatigue resistance	Bower et al. 2012
Field Performance	WMA reports satisfactory field performance	Diefenderfer and Clark, 2011 Jones et al. 2011 Kim et al., 2011 Estakhri 2012 Epps Martin et al. 2014

In addition to WMA-versus-HMA comparisons at one selected time-frame or specimen condition, National Cooperative Highway Research Program (NCHRP) studies 9-49 and 9-52 evaluated the evolution of WMA mechanical properties with STOA and LTOA protocols. It was found that WMA is generally less stiff than HMA during early life, but it is able to "catch up" with HMA over time. Equivalency is reached, not only in terms of stiffness but in terms of resistance to moisture damage (Epps Martin et al. 2014, Newcomb et al. 2015). To understand the causation of the observed mechanical response in WMA mixtures (Table 1) and the evolution of WMA mechanical properties with time, it is important to understand the technological changes imposed on the binder and mixture from a fundamental perspective.

For WMA surfactant additives, the reduction in binder surface tension (or SFE) enhances wettability of the aggregate surface. A previous study on the effectiveness of reducing surface tension at mixing temperatures revealed that WMA additives may or may not effectively contribute to the expected reduction in binder surface tension (Osmari et al. 2015). Nevertheless, the term "wettability" involves considering the aggregate; therefore, it is possible that surface mineralogy and microtextural features of the aggregate fraction contribute to the effectiveness of WMA additives in reducing production temperatures. It is important to develop a deeper understanding of binder-aggregate interactions with temperature changes. A general recommendation from previous studies (Table 1) is to characterize and optimize compatibility of constituent materials (i.e., WMA additive, anti-stripping agents, binder type, and aggregate type), which should be addressed upon understanding the fundamental material properties that are altered by

technological changes. It is important to evaluate the effect of WMA technologies on SFE components of asphalt binders (and binder-aggregate interaction) with consideration of short- and long-term aging.

1.2 Objectives of Study

Previous research has established a relationship between the potential for moisture damage and interactions occurring at the binder-aggregate interface (i.e., adhesion, cohesion, and debonding work due to moisture) based on surface energy components of constituents (Bhasin et al. 2006, Little and Bhasin 2006, Bhasin et al. 2007). Oxidative aging has been thoroughly explored in terms of binder chemistry, kinetics, and mechanisms for oxidation with proven empirical correlation to mixture performance (Liu et al. 1998, Petersen 2009, Glover et al. 2014), although the effect of aggregate type on the age-hardening process of asphalt concrete remains unclear. With the current availability of numerous technological alternatives to asphalt mixtures, it is important to pursue a deeper understanding of binder-aggregate interactions contributing to weathering degradation processes.

The specific objectives of this study are as follows:

1. Evaluate the effect of modifications (i.e., WMA additives and dosages) and laboratory aging on binder SFE and potential for moisture damage.
2. Quantify the effect of temperature and moisture on binder-aggregate interfacial bonding.
3. Quantify the contribution of aggregate type and binder modifications to the age-hardening of asphalt mixtures.

1.3 Description of Contents

To fulfill the objectives of the study, it was required to conduct extensive laboratory testing at various length scales, considering physicochemical, chemical, and mechanical characterization of constituents and composites. Chapter II describes the research approach, including materials, experimental methods, and research tasks, which are objective-specific.

Results are discussed with respect to each objective in separate chapters (III, IV, and V). The effect of WMA additives on binder SFE and potential for moisture damage is discussed in Chapter III. Additionally, the effect of laboratory aging on SFE is discussed. The effects of temperature and moisture on binder-aggregate interfacial bonding are discussed in Chapter IV. Chapter V describes the age-hardening process of asphalt mixtures under laboratory aging conditions. Binder extraction and recovery were conducted for assessment of age-hardening and investigating chemical factors contributing to binder and mixture age-hardening processes. Finally, conclusions and recommendations for future research are provided in Chapters VI and VII, respectively.

CHAPTER II

RESEARCH APPROACH

This chapter provides details on the materials, experimental methods, and research tasks executed to meet the proposed objectives.

2.1 Materials

This study considered two different binder types, unmodified performance grade (PG) 64-22 and polymer-modified PG 76-22, commonly utilized in Qatar. Mixtures were fabricated with two different aggregate types, gabbro and limestone. The aggregates were thoroughly characterized in previous studies (Masad et al. 2011, Al-Ansary and Iyengar 2013).

Masad et al. (2011) evaluated characteristics of the aggregates, including angularity and textural features before and after laboratory-induced degradation (microdeval). The researchers concluded that gabbro is a tough, highly wear-resistant, siliceous igneous rock that can be used in pavement structural layers and wearing courses. Limestone aggregate is a good-quality material, but is weaker in terms of wear resistance, limiting its use to structural layers rather than wearing courses. Al-Ansary and Iyengar (2013) characterized fundamental physiochemical properties of aggregates utilized in the construction industry in Qatar. Qualitative and semiquantitative chemical analyses by X-ray diffraction (XRD) and X-ray fluorescence (XRF) are summarized in Table 2 and Table 3 for the materials relevant to this study. Additionally, Al-Ansary and Iyengar (2013) reported scanning electron microscopy (SEM) evaluation of the surface of both

aggregates; results indicated that gabbro has a densely sealed surface morphology, while limestone has a relatively highly porous surface morphology.

Table 2. Qualitative analysis based on XRD (Al-Ansary and Iyengar 2013)

Mineral/Phase	Notation	Chemical Formula	Relative % Composition of Sample	
			Gabbro	Limestone
Antigorite	a	$Mg_3Si2O_5(OH)_4$	28.54	
Clinopyroxene	x	$Ca(Ti,Mg,Al)(Si,Al)_2O_6$	14.06	
Edenite	e	$NaCa_2Mg_5AlSi_7O_{22}(OH)_2$	11.24	
Plagioclase	p	$Ca_{0.63}Na_{0.37}(Al_{1.63}Si_{2.37}O_8)$	28.81	
Fosterite	f	Mg_2SiO_4	16.35	
Dolomite	d	$CaMg(CO_3)_2$	-	55.01
Calcite	c	$CaCO_3$	-	34.15
Quartz	q	SiO_2	-	10.77

Table 3. Semi-quantitative analysis based on XRF (Al-Ansary and Iyengar 2013)

Element	Component	Mass (%)	
		Gabbro	Limestone
Carbon	CO_2	8.25	40.8
Sodium	Na_2O	1.32	0.176
Magnesium	MgO	13.1	16.3
Aluminum	Al_2O_3	13.2	1.11
Silicon	SiO_2	39.4	11.0
Phosphorous	P_2O_5	0.0685	0.114
Sulfur	SO_3	0.0858	0.0875
Chlorine	Cl	0.11	0.108
Potassium	K_2O	0.0558	0.0219
Calcium	CaO	12.4	29.8
Titanium	TiO_2	0.810	-
Chromium	Cr_2O_3	0.104	-
Manganese	MnO	0.191	0.0315
Iron	Fe_2O_3	10.9	0.343
Nickel	NiO	0.0655	-
Strontium	SrO	0.0209	0.0109
Barium	BaO	-	0.0972

WMA technologies were evaluated in combination with both binders PG 64-22 and PG 76-22. One WMA laboratory foaming technology and three different WMA additives were utilized (Sasobit®, Rediset® LQ, and Evotherm® MA3). Sasobit is an organic wax that melts at high temperatures and reduces asphalt binder viscosity, consequently lowering mixing and compaction temperatures of WMA. Rediset LQ (Akzo Nobel) and Evotherm MA3 (Mead Westvaco) are chemical additives, surfactants designed to reduce the surface tension of asphalt binders for improved coating of aggregates at lower production temperatures. Both additives include active adhesion promoters (amine-based), similar to commonly marketed liquid anti-stripping agents. The percentages recommended by the producers of Rediset, Evotherm, and Sasobit are 0.5%, 0.5%, and 2.0% over binder weight, respectively. For the foaming technology, water content was selected to be 1% over binder weight upon determination of the optimum foam ability index, as recommended by Yin et al. (2014a).

One aggregate gradation was selected for all asphalt mixtures, including both aggregate types in combination with both PG binders and WMA technologies. The aggregate gradation (shown in Figure 1) is a mixture with a 25-mm maximum nominal aggregate size. Selection of aggregate gradation and initial binder content was previously reported by FUGRO Middle East in a mixture design utilizing gabbro and binder PG 76-22. Binder contents were then adjusted for the other three HMA mixtures (gabbro PG 64-22, limestone PG 64-22, and limestone PG 76-22) based on a target 5.2% air void content, as assigned by FUGRO. No further binder content adjustments were conducted for WMA mixtures. Production temperatures were defined for the HMA based on the PG of the

binder. For WMA mixtures, it was required to reduce mixing temperature by at least 15°C compared to the base PG binder. Conditioning times and temperatures prior to compaction were selected to mimic the initial condition of a pavement, as recommended by Yin et al. (2013). Specimens were compacted to a 150mm diameter by 170mm height using a Superpave gyratory compactor (SGC) and then were cored and trimmed to 100mm diameter by 150mm height. The final specimens were prepared based on a target 7% air void content, which is common for performance testing. A general description of the specimens tested in this study is provided in Table 4. The binder content is expressed as a percent of the total mixture weight.

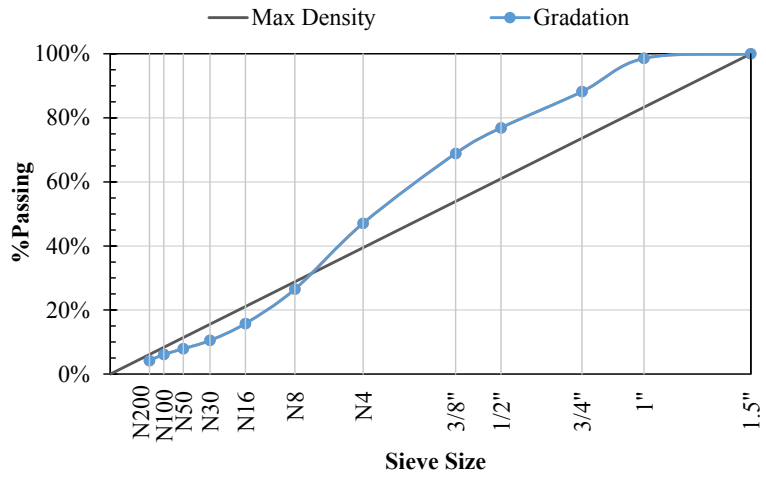

Figure 1. Gradation asphalt mixture

Table 4. Mixture characteristics

Aggregate	Binder	Additive	Binder Content %	Air Voids %	Absorbed Binder %	Effective Binder %	Mix/Compact Temperatures °C
Gabbro	PG 64-22	None	4.3	7.3	0.6	3.7	143/135
		Rediset	4.3	7.0	0.5	3.8	128/116
		Sasobit	4.3	7.3	0.3	4.0	128/116
		Evotherm	4.3	7.3	0.5	3.8	128/116
		Foaming	4.3	6.6	0.4	3.9	128/116
	PG 76-22	None	3.9	7.2	0.1	3.8	163/135
		Rediset	3.9	6.7	0.1	3.8	145/116
		Sasobit	3.9	7.1	0.0	3.9	145/116
		Evotherm	3.9	7.4	0.2	3.7	145/116
		Foaming	3.9	7.1	0.3	3.6	145/116
Limestone	PG 64-22	None	5.1	7.0	1.7	3.4	143/135
		Rediset	5.1	7.1	1.3	3.8	128/116
		Sasobit	5.1	6.8	1.6	3.5	128/116
		Evotherm	5.1	6.7	1.2	3.9	128/116
		Foaming	5.1	7.1	1.4	3.7	128/116
	PG 76-22	None	4.9	7.0	1.5	3.4	163/135
		Rediset	4.9	7.1	1.6	3.3	145/116
		Sasobit	4.9	6.8	1.5	3.4	145/116
		Evotherm	4.9	7.1	1.5	3.4	145/116
		Foaming	4.9	7.0	1.5	3.4	145/116

To select the corresponding fine aggregate matrix (FAM) portions for a given mixture, the percentage passing sieve no. 16 was taken as 100% (Figure 1), and individual retained fractions for all smaller sieve sizes were recalculated proportionally (Figure 2). The gradation for the corresponding FAM proportion is shown in Figure 2, which is also the same for all 20 mixtures considered in this study. Binder contents for the FAMs were determined based on the procedure presented by Sousa et al. (2013). For limestone aggregates, the optimum binder content was 10.5% by weight of mix, while it was 7.3% by weight of mix for gabbro mixtures.

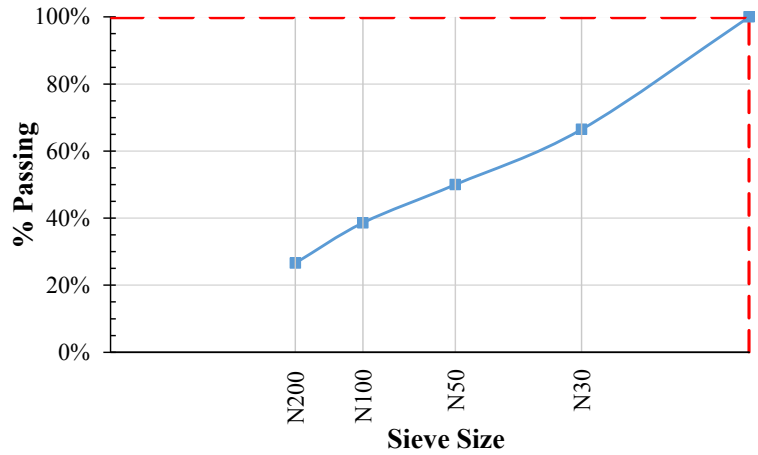

Figure 2. Gradation FAM

FAM specimens were conditioned for short-term aging, as recommended by Yin et al. (2013), and were compacted with an SGC, from which the specimens were cored to cylinders of 25mm diameter by 50mm height. All FAM specimens had air void contents below 3%.

2.2 Experimental Methods

This section includes a description of each experimental method considered in this study to characterize constituents, adhesion, and asphalt concrete.

2.2.1 Surface Free Energy by Wilhelmy Plate

The Wilhelmy plate test method is a contact angle technique used to determine the surface energy component of a material. The experimental setup is shown in Figure 3.

(a) Equipment and Data Acquisition **(b) Detailed View**

Figure 3. Wilhelmy plate

To measure surface characteristics of asphalt binder, a plate coated with binder was immersed into a probe liquid of known characteristics. The contact angle of asphalt binder was determined from the measured force (ΔF) through simple equilibrium equations considering the weight of the plate in the air (ρ_{air}) and partially submerged (ρ_L) in a probe liquid with known surface energy (γ_L^{Tot}), as described in Equation (10). In Equation (10), P_t is the perimeter of the bitumen-coated plate, and V_{im} is the volume immersed in the probe liquid.

$$\cos\theta = \frac{\Delta F + V_{im}(\rho_L - \rho_{air} g)}{P_t \gamma_L^{Tot}} \quad (10)$$

The SFE of a material (γ^{Total}) can be defined by three components: monopolar acidic (γ^+), monopolar basic (γ^-), and apolar or LW (γ^{LW}), as given in Equation (1). Considering two materials, solid and liquid, in contact, Van Oss et al. (1988) related Gibbs free energy of adhesion, the contact angle (θ) of the probe liquid (L) with a solid (S), and surface energy characteristics (γ) of liquid and solid. Hefer et al. (2006) utilized this theory

in order to calculate the surface energy components of asphalt binders based on contact angle measurements with probe liquids (Equation 11).

$$\gamma_L^{total}(1+\cos\theta) = \left(2\sqrt{\gamma_L^{LW}}\right)x_1 + \left(2\sqrt{\gamma_L^{-}}\right)x_2 + \left(2\sqrt{\gamma_L^{+}}\right)x_3 \quad (11)$$

where x_1, x_2, and x_3 are the unknown surface energy components for the asphalt binder.

A system of at least three equations was needed to solve for the three unknown SFE components of the asphalt binder. Five probe liquids (distilled water, formamide, glycerol, ethylene glycol, and methylene iodide) were used in experimental measurements in order to minimize the effect of possible experimental errors in the calculated surface energy components, as recommended by Hefer et al. (2006).

2.2.2 Surface Free Energy by Universal Sorption Device

The SFE components of aggregates can be obtained by the Universal Sorption Device (USD) (Figure 4). The clean aggregate was placed in a closed system at low pressure. A probe vapor was released and allowed to adsorb onto the aggregate surface, while the mass of adsorbed probe vapor was measured with a high-precision magnetic scale. The adsorption isotherm is the relation between vapor pressure of the probe vapor and adsorbed mass (n). The equilibrium spreading pressure (π_e) of a probe vapor on the solid surface can be obtained by measuring the adsorption isotherm at several pressures (p). Equation (12) defines the spreading pressure as a function of the universal gas constant (R), temperature (T), molecular weight of the probe vapor (M), and specific surface area (SSA) of the aggregate (A). The Branauer, Emmett, and Teller (BET) procedure, shown in Equation (13), is recommended to calculate the SSA of the aggregate.

In Equation (13), n_m is the monolayer capacity of the aggregate surface, N_0 is Avogadro's number, and $\propto$ is the projected area of a single molecule.

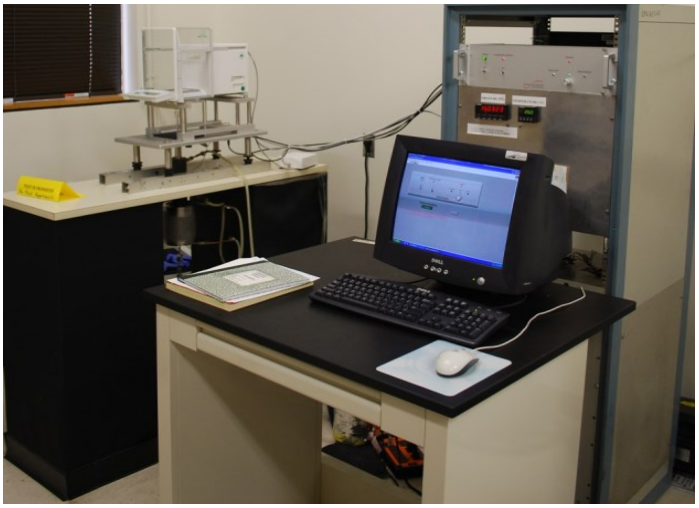

Figure 4. USD

Work of adhesion between solid and vapor can also be calculated as a function of the equilibrium spreading pressure of the vapor over the solid surface, as shown in Equation (14). To calculate each SFE component of the aggregate, the experimental measurements included three probe liquids (n-hexane, methyl propyl ketone [MPK], and water) in order to solve for the unknowns in Equation (11).

$$\pi_e = \frac{RT}{MA}\int_0^{P_n}\frac{n}{p}dp \tag{12}$$

$$\mathrm{A} = \left(\frac{n_m N_0}{M}\right)\propto \tag{13}$$

$$\mathrm{W}_{S,V}^{a} = \pi_e + 2\gamma_V^{Total} \tag{14}$$

2.2.3 Dynamic Mechanical Analysis of Moisture Damage in Fine Aggregate Matrix

The model proposed for evaluating crack growth within a FAM was described by Masad et al. (2008). Based on this approach, crack growth can be expressed in terms of the J-integral, as shown in Equation (15).

$$\frac{dr}{dN} = A[J_R]^n \tag{15}$$

where $\frac{dr}{dN}$ is the crack extension per load cycle; R is the average crack radius; A and n are experimentally determined material constants; and J_R is the J-integral, calculated by Equation (16).

$$J_R = \frac{\partial DPSE}{\partial(crack\ surface\ area)} = \frac{\frac{\partial W_R}{\partial N}}{\frac{\partial(crack\ surface\ area)}{\partial N}} \tag{16}$$

where, csa is the crack specific area, and W_R is the dissipated pseudostrain energy (DPSE).

W_R was calculated on the basis of the area of hysteresis loop of pseudostrain against measured stress. The relationship between W_R and *N* is given in Equation (17).

$$W_R = a + cN^b \tag{17}$$

The pseudostrain energy release rate ($\partial W_R/\partial N$) was calculated using Equation (17) and was then substituted in Equation (16) to calculate the J-integral (J_R). The J-integral (J_R) was substituted in Equation (15) to calculate crack size and define a crack size index. After some mathematical manipulations (Masad et al. 2008), the model for calculating crack growth radius (ΔR) is as follows:

$$\Delta R(N) = \left[\left(\frac{2n+1}{nb+1}\right)^{n+1}\left(\frac{E_R bc}{4\pi E_1 \Delta G_f}\right)^{n} N^{nb+1}\right]^{\frac{1}{2n+1}} \quad (18)$$

where a, b, and c are the model parameters used to define DPSE; E_R is a reference modulus; E_1 is the initial modulus from the relaxation test; ΔG_f is the work of adhesion; and n is a material constant correlated to the m value from the relaxation modulus (Schapery 1984). A wet-over-dry ratio of the crack radius (ΔR) at 5000 load cycles was selected as a moisture susceptibility ratio (MSR) for comparison of all FAM mixtures, as indicated in Equation (19) .

$$\text{MSR} = \frac{\Delta R(5000)_{wet}}{\Delta R(5000)_{dry}} \quad (19)$$

When tensile strength and surface energy are constants during fracture, the relation between n and m can be described by Equation (20).

$$\text{n} = 1 + \frac{1}{m} \quad (20)$$

To account for ΔG_f, I considers that specimens in dry and wet conditions will have different bond energies. The maximum ΔG_f occurs in the dry condition (Equation (21), and it can be obtained directly from the measurements utilizing the Wilhelmy plate and USD for binders and aggregates, respectively, as described in Equation (2).

$$\Delta G_{f(dry)} = \Delta G_{AS} \quad (21)$$

After moisture conditioning, the asphalt binder-aggregate interface is partially saturated (Lytton et al. 1993, Kim et al. 2004). Therefore, ΔG_f, representing a partially saturated interface, results in a lower value than that in the dry condition, which can be assumed to degrade proportionally due to a degradation in mechanical properties

accounted for by a wet/dry dynamic modulus ratio (DMR), as described in Equation (22) and Equation (23).

$$\Delta G_{f(wet)} = \Delta G_{f(dry)} \times DMR \tag{22}$$

$$DMR = \frac{\left(\frac{|E^*|_i}{|E^*|_0}\right)_{wet}}{\left(\frac{|E^*|_i}{|E^*|_0}\right)_{dry}} \tag{23}$$

where $|E^*|_i$ is the dynamic modulus at i cycles, i.e., 1000 cycles, and $|E^*|_0$ is the reference modulus.

The testing protocol for FAM mixtures was conducted utilizing a Bose® ElectroForce® dynamic mechanical analyzer (DMA) (Figure 5a). The test specimens were carefully gripped into the DMA (Figure 5b) and then were subjected to dynamic loading. Figure 5c shows a typical test specimen after failure.

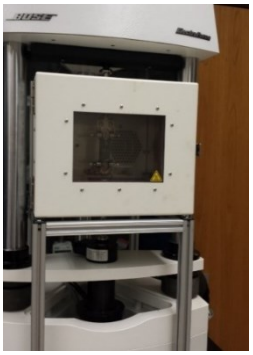

(a) Bose ElectroForce DMA

(b) Gripping the Specimen

(c) Specimen After Testing

Figure 5. DMA

The first step in the DMA testing sequence was to obtain the relaxation modulus for each material. For this purpose, a FAM specimen was subjected to a constant tensile strain level of 200 με, small enough to avoid any damage to the FAM specimens. The

strain was held constant for 10 minutes, and both load and displacement were measured. The relaxation modulus (Figure 6a) was calculated using Equation (24) and Equation (25). In addition, the model parameters E_1 (initial modulus) and m (relaxation speed) were obtained using Equation (26).

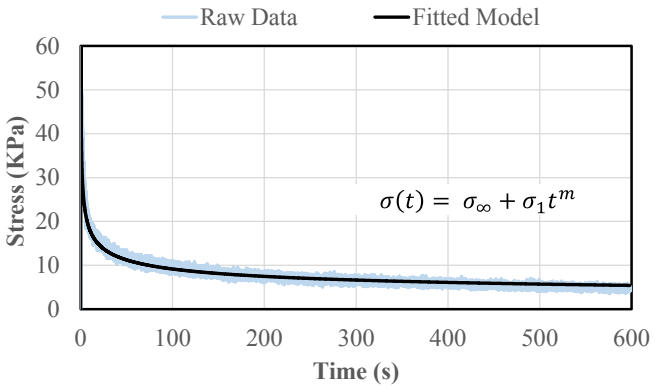

(a) Relaxation Modulus

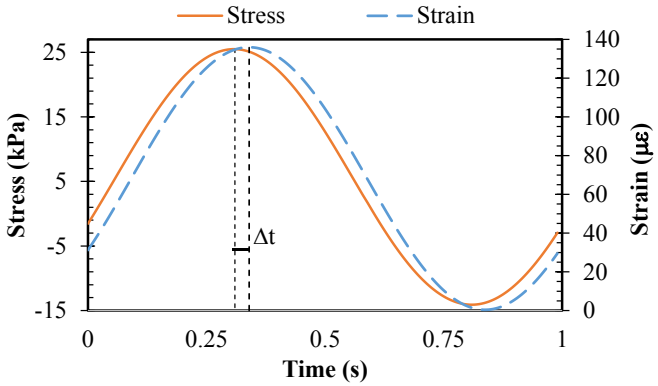

(b) Dynamic Modulus

Figure 6. DMA testing sequence

$$\sigma(t) = \sigma_\infty + \sigma_1 t^m \tag{24}$$

$$E(t) = \frac{\sigma(t)}{\varepsilon_0} \tag{25}$$

$$E(t) = E_\infty + E_1 t^m \tag{26}$$

The relaxation modulus test was followed by a repeated sinusoidal tensile strain test (Figure 6b) at 130 με (nondestructive). After a 20-minute rest period, the FAM was subjected to a sinusoidal tensile strain of 3000 με to induce gradual damage to the test specimen. Sinusoidal tensile tests were performed at a frequency of 1 Hz. Load and displacement outputs from the DMA were filtered using a Fourier fit in MATLAB prior to calculating the stress, strain, and phase angle (Figure 6b). DPSE was defined as the area in the stress-pseudostrain hysteresis loop (Figure 7), which increases with load applications as the sample is damaged (Figure 8). Data were fitted to Equation (17).

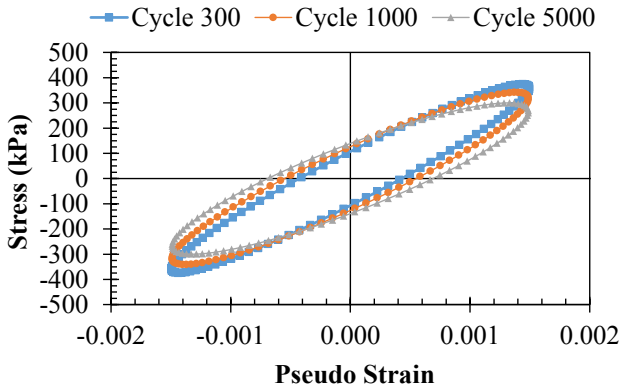

Figure 7. Stress vs. pseudostrain for different load cycles.

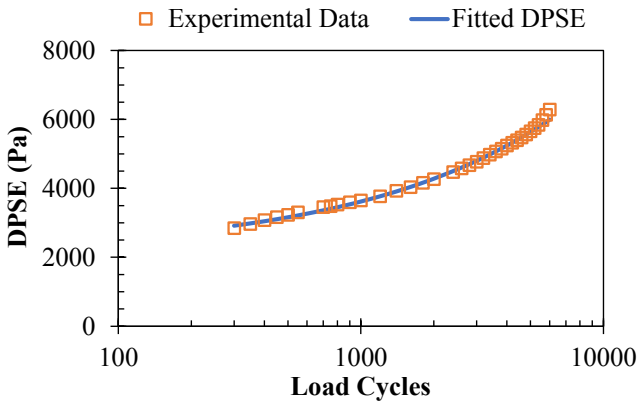

Figure 8. Change in DPSE with load cycles.

Calculation of DPSE (Equation 27) was conducted as detailed by Masad et al. (2008), considering DPSE components related to phase angle increase (Equation (28)) and modulus decrease (Equation (29)).

$$\text{DPSE} = W_{R1} + W_{R3} \tag{27}$$

$$W_{R1} = \pi E^*_{VE} \gamma^2_{0F} \sin(\delta_{NF} - \delta_{VE}) \tag{28}$$

$$W_{R3} = \frac{1}{2} \gamma^2_{0F} (E^*_{VE} - E^*_{NF}) \tag{29}$$

where E^*_{VE} is the VE dynamic modulus at the nondestructive strain level; δ_{VE} is the VE phase angle at the nondestructive strain level; γ_{0F} is the strain amplitude during the destructive test; δ_{NF} is the phase angle changing with load cycles during the destructive test; E^*_{NF} is the dynamic modulus changing with load cycles during the destructive test.

2.2.4 Enthalpy of Immersion by Microcalorimeter

The experimental procedure summarized in this section has been utilized in previous studies (Bhasin and Little 2009, Vasconcelos et al. 2010). The system utilized in this study was a differential isothermal microcalorimeter manufactured by Omnical Inc. The system is presented in Figure 9a, including a microcalorimeter device and a water temperature controller. The microcalorimeter unit measures heat change or differential heat between two cells, a reaction and a reference cell (Figure 9b). The reference cell consisted of an empty vial while the reaction cell contained aggregate particles. The binder was injected in both reaction and reference cells simultaneously, and the heat transferred between both was measured. The use of a reference cell allowed one to exclude heat

generated from the sole injection process or other experimentally induced heat differentials, which do not correspond to the heat generated during the wetting process.

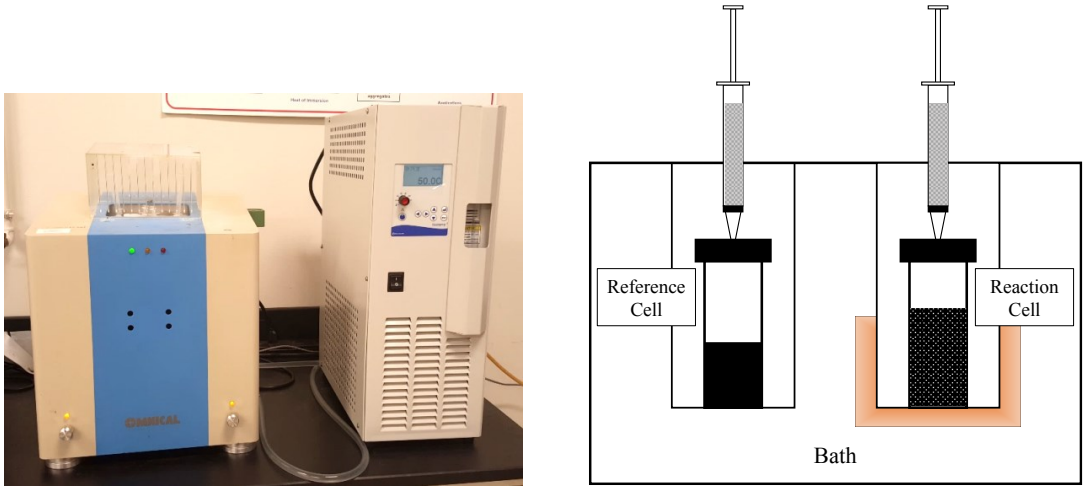

(a) Microcalorimeter (b) Schematics

Figure 9. Microcalorimeter

The system was set to a constant temperature. Once thermal equilibrium was reached (i.e., no heat flow observed), the binder solution was injected into the sample and reference vials simultaneously, and heat flow was recorded, as shown in Figure 10. The enthalpy of immersion (ΔH) was determined by integrating the area between the heat-flow-versus-time curve and the baseline. The measurements were normalized considering the amount of material inside the vial and the SSA of the aggregates obtained by experimental measurements in the USD, with N-hexane as the probe vapor. During the progress of each experiment (i.e., 45 to 60 minutes), the system was kept at a constant temperature. Upon completion of the experiment, the entire system was set to the next test temperature.

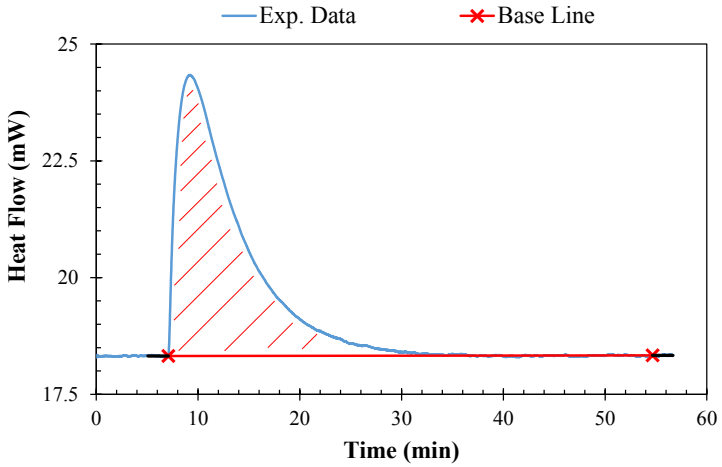

Figure 10. Microcalorimeter output data

The materials required to conduct the experiment are illustrated in Figure 11.The aggregate fraction evaluated corresponds to the size passing sieve no. 100 and that retained on sieve no. 200 (Figure 11a). A consistent particle size was required to minimize data variability. The small aggregate fraction allowed for a larger surface area so that the heat produced was sufficient to be detected by the microcalorimeter. The binder was injected in the form of a solution in a toluene solvent in the empty cell and in the cell containing aggregate (Figure 11b). Previous research by the Western Research Institute (WRI) indicated that toluene does not compromise the integrity of the asphalt molecule, but disperses the molecules, thus affecting mobility (Robertson et al. 2001). The aggregate can be pretreated with heat (3 hours at 150°C) to ensure complete drying (Figure 11c). Alternatively, the aggregates can also be pretreated to create a uniform distribution of water on the surface. This is typically achieved by allowing the sample to equilibrate inside a desiccator at a predetermined relative humidity (RH) until constant weight is reached (Figure 11d).

(a) Aggregate Fraction

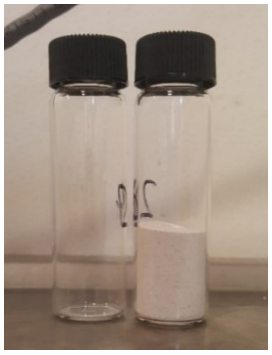

(b) Vials: Reference and Reaction

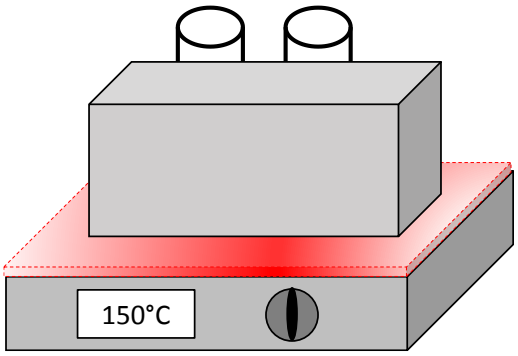

(c) Heating System

(d) Desiccator

Figure 11. Materials description—microcalorimeter

The experimental procedure utilized is summarized in the following steps:

1. Prepared the binder solution and tested within 12 to 24 hours.
2. Prepared aggregate vials with 8g of material (±0.01g).
3. Pretreated the aggregate to dry condition or to the desired RH.
4. Recorded aggregate weight before and after treatment.
5. Set the materials in the microcalorimeter and allowed for the system to reach thermal equilibrium.
6. Injected 4 ml of solution in the reference cell and 4 ml of solution in the reaction cell simultaneously.
7. Recorded the heat flow over time.

2.2.5 Linear Viscoelastic Characterization of Asphalt Mixtures and Binders

The evaluation of dynamic properties at a variety of frequencies and temperatures (e.g., modulus and compliance) is a common technique for VE characterization of asphalt binders and mixtures. The dynamic shear rheometer (DSR) was used to characterize the asphalt binder, while asphalt mixtures were tested in accordance with AASHTO TP-79 using an asphalt mixture performance tester (AMPT). Test methods consisted of temperature and frequency sweeps to construct a master curve from the dynamic response; details on test temperatures and frequencies are provided in Table 5.

Table 5. Experimental conditions—LVE characterization

Material	Temperature (°C)	Frequency (Hz)	Test Method	Strain Level
Asphalt Binder	10, 20, 30	35, 30, 25, 15, 10, 5, 1, 0.5, 0.1	DSR 8-mm plate	1% rotation
	40, 50, 60, 70	35, 30, 25, 15, 10, 5, 1, 0.5, 0.1	DSR 25-mm plate	10% rotation
Asphalt Mixture	4, 20	25, 10, 5, 1, 0.1	AMPT	85–115 με
	40	25, 10, 5, 1, 0.1, 0.01	AMPT	85–115 με

Considering a thermorheological simple material, a time-temperature superposition was applied to the experimental data to define the material properties over a wider frequency range. The reference temperature was selected to be 20°C, and the time-temperature shift is described in Equation (30). In addition, the optimization of the time-temperature shift was performed by simultaneously fitting a simple sigmoidal smoothening function, described in Equation (31).

$$log[a(T)] = C_1T^2 + C_2T + C_3 \quad (30)$$

$$log|D^*| = \delta - \frac{\alpha}{1 + e^{\beta+\gamma log\omega_r}} \quad (31)$$

where $|D^*|$ is the dynamic compliance, $a(T)$ is the temperature-dependent shift factor; C_1, C_2, and C_3 are fitting parameters; and T is the test temperature (°C). In the sigmoidal smoothening, ω_r corresponds to the reduced frequency, and $\delta, \alpha, \beta,$ and γ are fitting parameters. The process of constructing a master curve is illustrated in Figure 12(a) for asphalt binder and Figure 12(b) for asphalt mixtures. Additional details on the optimization process were documented by Rahmani et al. (2013). The experimental conditions to characterize asphalt binders consisted of applying shear stress; therefore, the material properties were given in terms of shear compliance. When referring to asphalt binders, all the equations presented for mixtures followed the same form, but accurate notation required replacing compliance terms (D) with shear compliance terms (J) throughout.

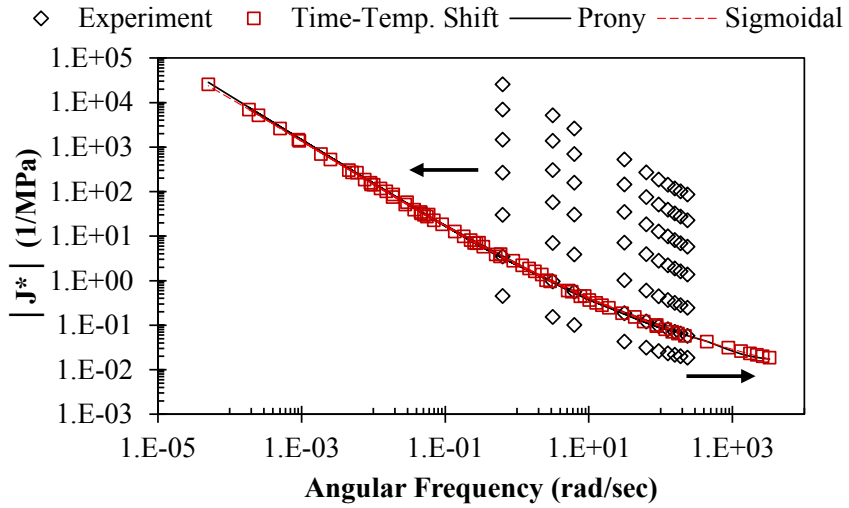

(a) Asphalt Binder (20°C Reference Temperature)

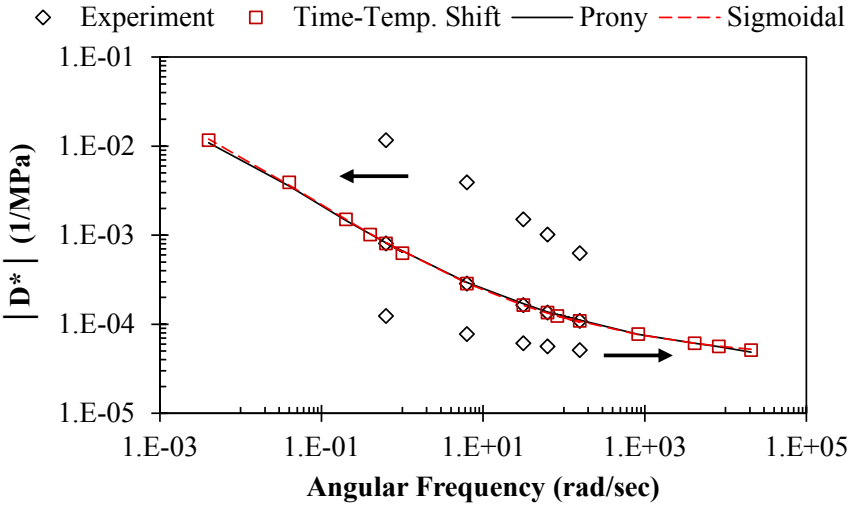

(b) Asphalt Mixture (20°C Reference Temperature)

Figure 12. Construction of dynamic compliance master curve

The mechanical behavior of mixtures and binders was represented by arrangements of mechanical analog models (Prony series), as shown in Figure 13 for an LVE solid (a) and LVE fluid (b). To obtain the model parameters with the Prony series, Equation (33) and Equation (34), and Equation (32) were fitted to the sigmoidal smoothening within the frequency range at which the experiments were conducted.

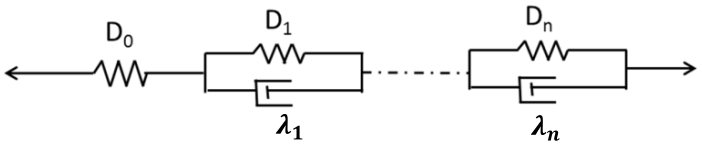

(a) Solid-Like LVE—Asphalt Mixtures

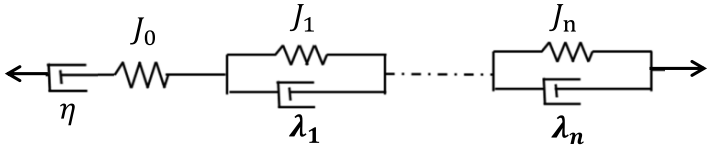

(b) Fluid-Like LVE—Asphalt Binders

Figure 13. Mechanical analog models

$$|D^*(\omega)| = \sqrt{D'^2 + D"^2} \tag{32}$$

$$D'(\omega) = D_0 + \sum_{i=1}^{n} \frac{D_i}{\left(\frac{\omega}{\lambda_i}\right)^2 + 1} \tag{33}$$

$$D"(\omega) = \frac{1}{\eta\omega} + \sum_{i=1}^{n} \frac{\frac{\omega}{\lambda_i} D_i}{\left(\frac{\omega}{\lambda_i}\right)^2 + 1} \tag{34}$$

where $|D^*(\omega)|$ is the dynamic compliance; $D'(\omega)$ is the storage compliance; $D"(\omega)$ is the loss compliance; D_i is the compliance terms (Kelvin springs); ω is the angular frequency; λ_i is the retardation times (Kelvin dashpots); and η is the viscosity of the Maxwell dashpot (infinity for a solid-like material).

The model parameters D_i and λ_i corresponded to those in Equation (7), Equation (8), and Equation (9), which were required at the material's initial condition prior to applying Rahmani's age-hardening model. Further details for calibrating the aging state variable (A) and the extension of the model to binder age-hardening are provided later in Section 2.3.3. The dashpot η was considered for characterization of the binder only.

2.2.6 Chemical Composition by Fourier Transform Infrared Spectroscopy

Chemical composition of asphalt binders can be assessed by experimental measurements with an attenuated total reflectance (ATR) Fourier transform infrared spectroscopy (FTIR), shown in Figure 14. Due to the simplicity and speed of the technique, FTIR has become a common practice in the study of asphalt oxidation. Several peaks at specific regions have been attributed to chemical compounds commonly found within asphalt binders before and after oxidative aging; the most common parameter to quantify binder aging is the carbonyl area (CA), which consists of the 1650- to 1820-cm^{-1} band area with baseline at the magnitude of the absorbance at 1820 cm^{-1} (Liu et al. 1998). Other studies have considered the added carbonyl and sulfoxide peak height as a measure of binder aging. Absorbance data were collected over a frequency range of 400 cm^{-1} to 4000 cm^{-1}, and the regions of interest were evaluated. Table 6 presents a list of FTIR peaks attributed in previous studies to specific chemical compounds present in asphalt binders.

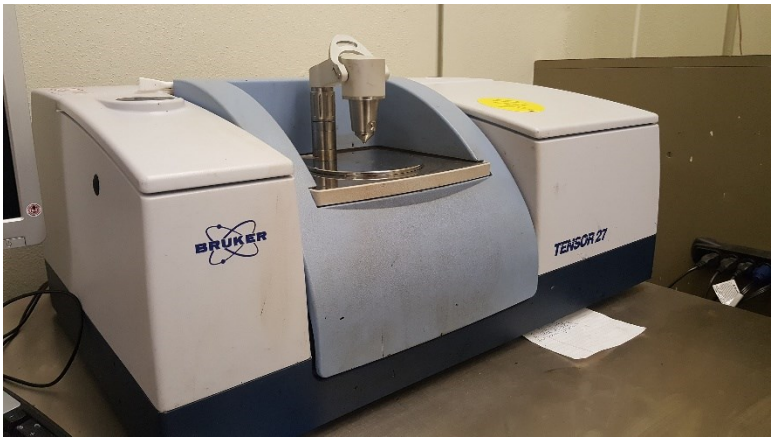

Figure 14. ATR FTIR

Table 6. FTIR peaks attributed to chemical compounds in asphalt binders

Peak (cm^{-1})	Description	Reference
1700 1700 1730 1725 and 1765	ν C=O Ketones Carboxylic acids dimer Carboxylic acids "free" Dicarboxylic anhydrides	Petersen 2009
1030	ν S=O Sulfoxides	
620	Sulfates	Usmani 1997
1320–1000	Upshift baseline due to formation of sulfoxides, sulfones, and sulfates	
1180	Aliphatic sulfur–containing groups	
1350–1300 1160–1140	Sulfones	Thomas et al. 2006
1210–1150 1060–1030 650	Sulfonic acids	
2953	ν_{as} CH_3 X, CH_3 Aryl	Lamontagne et al. 2000
2923	ν_{as} CH_2, CH_3	
2862	ν_s CH_2, CH_3	
1460	δ_{as} CH_2, CH_3	
1376	δ_s CH_3 Methyl	
724	r(CH_{2n})	
1600	ν C=C	
864, 814, 743	γ CH aromatics	
930 and 870	Presence of trichloroethylene in extracted binders	Farrar et al. 2015
966	Transdisubstituted –CH=CH= (butadiene block)	Larsen et al. 2009
748	δC-H aromatic monosubstituted (styrene block)	
690	δC-H aromatic monosubstituted (styrene block)	
721	δC-H aromatic	
995	δC-H (terminal vinyl) styrene-butadiene-styrene (SBS)	Cortizo et al. 2004
910		
700 965	SBS polymer	Lu and Isacsson 1998
723	Wax	Robertson et al. 2001

ν: stretching; δ: in-plane bending; γ: out-of-plane bending

2.3 Research Tasks

Research tasks described in this section are specific to achieving each objective of study.

2.3.1 Effects of Warm-Mix Asphalt on Surface Free Energy and Potential for Moisture Damage

This task explored the effect of WMA technologies, additive dosages, and laboratory aging in the binder SFE characteristics and the asphalt binder-aggregate adhesive bond. SFE parameters and compatibility of binder-aggregate systems were then compared to results from mechanical characterization of moisture damage for FAMs. The experimental plan to accomplish Objective 1 is shown in Figure 15. The USD was utilized to characterize SFE components of the aggregates. Measurements were conducted using the Wilhelmy plate methodology for determining SFE components of asphalt binders before aging and after RTFOT plus 20 hours of PAV aging. The effect of WMA additives was evaluated with both PG 76-22 and PG 64-22 binders. The effect of additive dosage was only explored for PG 64-22 binder (i.e., the dosage recommended by the manufacturer plus one higher and one lower value). Data analysis focused on work of cohesion (Equation 4), work of adhesion (Equation 2), and ER (Equation 5) to evaluate the potential for moisture damage with WMA additives before and after laboratory aging.

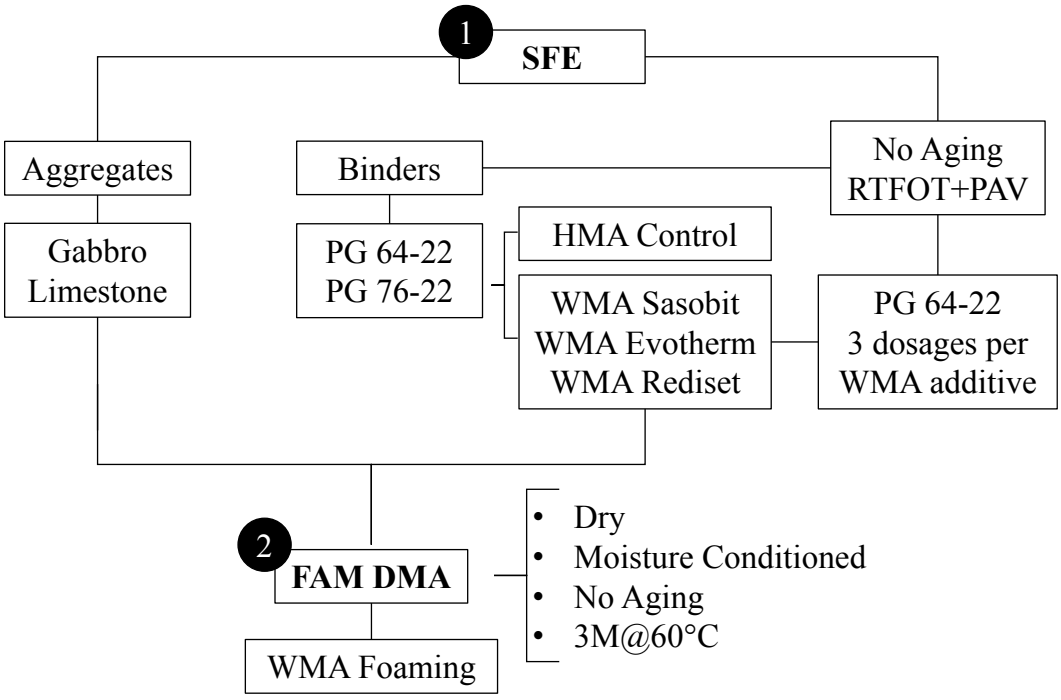

Figure 15. Experimental matrix—Objective 1

Mechanical testing was conducted to characterize moisture damage (before and after aging) affecting crack growth in the FAM specimens. Moisture susceptibility was quantified by an MSR and a DMR, parameters that are detailed in Equation (19) and Equation (22), respectively. A total of 20 mixtures in both unaged and aged conditions was tested, as detailed in Figure 15. Moisture damage was induced by conditioning the specimens under a vacuum for 3 hours, reaching saturation levels of 70% to 80%. The average percent of air voids of the FAM test specimens was less than 3%. The aging process consisted of placing the large, 150-mm SGC specimens in a temperature-controlled room (60°C) for 3 months, followed by coring the 25mm specimens after aging. The same moisture conditioning protocol was applied to the aged samples.

2.3.2 Effects of Temperature and Moisture on Binder-Aggregate Interfacial Bonding

In order to evaluate the effects of temperature and moisture on the asphalt binder-aggregate interfacial bond, the following subtasks were accomplished:

1. Developed a simple methodology capable of evaluating asphalt binder-aggregate interfacial bonding over the in-service temperature range.
2. Evaluated the effect of binder modification and use of alternative mineral aggregates on binder-aggregate adhesion over the range of in-service temperatures.
3. Measured asphalt binder-aggregate adhesion with moisture at the interface.
4. Provided recommendations to assess moisture damage based on microcalorimetry experiments.

The experimental variables considered include WMA binder modifications, two aggregates, various temperatures, and moisture conditioning, as detailed in Table 7.

Table 7. Experimental variables

Solution	Aggregate	Test Temperature (°C)	Moisture Condition	Subtasks
PG 64-22 Control	Gabbro, Limestone	10, 20, 35, 50	Dry	1, 2
WMA Rediset	Gabbro, Limestone	10, 20, 35, 50	Dry	1, 2
WMA Sasobit	Gabbro, Limestone	10, 20, 35, 50	Dry	1, 2
PG 64-22 Control	Gabbro, Limestone	20	Dry, RH 33%, 76%, 100%	3
Water	Gabbro, Limestone	20	Dry	3

Revisiting classical thermodynamic equations (Wilson 1966, McPhail and Cooper 1997), the energy available to do work (ΔG) can be described as a function of the enthalpy (ΔH) and entropy of the system (ΔS) varying with temperature (T), considering a system at constant pressure, as described by Equation (35). The enthalpy (ΔH) corresponds to the total heat produced during a process. The term TΔS is related to molecular mobility; it can be visualized as a measurement of disorder in the system, and it represents energy that is not available to do work. Considering a system at constant pressure, the change in enthalpy (ΔH) with temperature is given by the heat capacity (ΔC_P), as described by Equation (36). The temperature-dependent enthalpy and entropy in a system at constant pressure can be calculated from the heat capacity (ΔC_P) and known properties at a reference temperature (T_{ref}), as described by Equations (37) and (38).

$$\Delta G(T) = \Delta H(T) - T\Delta S(T) \tag{35}$$

$$\Delta C_P = \frac{d(\Delta H)}{dT} \tag{36}$$

$$\Delta H(T) = \Delta H_{ref} + \int_{T_{ref}}^{T} \Delta C_P dT \tag{37}$$

$$\Delta S(T) = \Delta S_{ref} + \int_{T_{ref}}^{T} \frac{\Delta C_P}{T} dT \tag{38}$$

If the heat capacity (ΔC_P) is assumed to be constant within a limited temperature range, then Equations (37) and (38) can be simplified into Equations (39) and (40). Then, the expression for a temperature-dependent ΔG in Equation (35) can be rewritten into Equation (41).

$$\Delta H(T) = \Delta H_{ref} + \Delta C_P\left(T - T_{ref}\right) \tag{39}$$

$$\Delta S(T) = \Delta S_{ref} + \Delta C_P ln\left(\frac{T}{T_{ref}}\right) \tag{40}$$

$$\Delta G(T) = \Delta H_{ref} + \Delta C_P\left(T - T_{ref}\right) - T\left(\Delta S_{ref} + \Delta C_P ln\left(\frac{T}{T_{ref}}\right)\right) \tag{41}$$

Considering the experimental measurements for asphalt binder-aggregate systems by heat of immersion or contact angle methods, the enthalpy of immersion (ΔH) and work of adhesion (ΔG) were given in terms of energy by area of contact (erg/cm^2). In a similar manner, the heat capacity calculated from the enthalpy of immersion (ΔH) was given in units of energy by area per degree Kelvin (erg/cm^{2}K); therefore, it was referred to as a specific heat capacity. Typical experimental results for asphalt binder-aggregate systems are presented in Figure 16, showing the linear fit and determination of the specific heat capacity. This process enabled calculation of enthalpy at any given temperature from 10°C to 50°C (283K to 323K) by Equation (39).

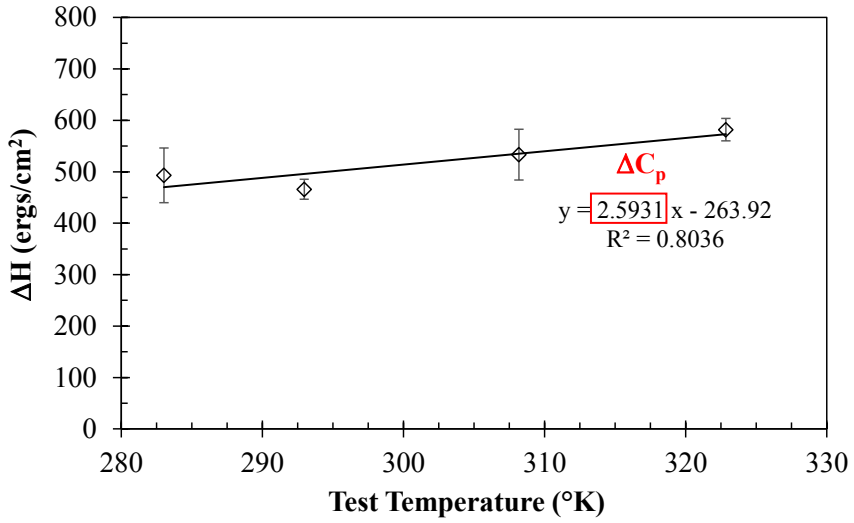

Figure 16. Specific heat capacity

In order to obtain ΔS_{ref}, it was required to measure or estimate ΔG at one reference temperature (ΔG_{ref}). For asphalt binder-aggregate systems, the work of adhesion (ΔG_{AS}) is commonly calculated based on binder and aggregate SFE components, as described in Equation (2), at one room temperature. Previous studies on binder-aggregate adhesion based on microcalorimetry have assumed that ΔG can be approximated to half the enthalpy of wetting (ΔH) at room temperature (Bhasin and Little 2009). The estimation of $\Delta G_{ref} = \frac{1}{2}\Delta H$ at 300K was originally proposed by Douillard et al. (1995), who reported the assumption to be reasonable based on experimental measurements of pure minerals and probe vapors. Both methodologies were considered in this study when modeling temperature-dependent binder-aggregate ΔG, and results were compared and are discussed.

Additional experiments were conducted with respect to aggregate-water affinity: (1) measuring the total enthalpy of immersion when water was wetting the aggregate surface and (2) measuring binder-aggregate heat of immersion with moisture uniformly distributed at the aggregate surface. The testing procedure was the same as previously described, with the only variant being preconditioning aggregates at 33%, 76% and 100% RH until constant weight was reached.

2.3.3 Age-Hardening of Asphalt Mixtures and Binders

In this task, the aging state variable (A) was calibrated for a total of 20 asphalt mixtures, including WMA modifications within two aggregate sources, as detailed in Figure 17. In addition, a subset of asphalt binders was extracted and recovered at different

aging conditions, as indicated in Figure 17, for mechanical and chemical characterization. The LVE behavior of the binders at different aging stages was evaluated, and its contribution to the aging state variable of the asphalt mixture was established. It is important to highlight that the extraction and recovery process ensured that the binder aging stage corresponded to that from the mixture. Any contribution of the aggregate type to the oxidation process could be inferred from the relative difference of binder stiffness keeping all mixture variables constant, but with different aggregate types.

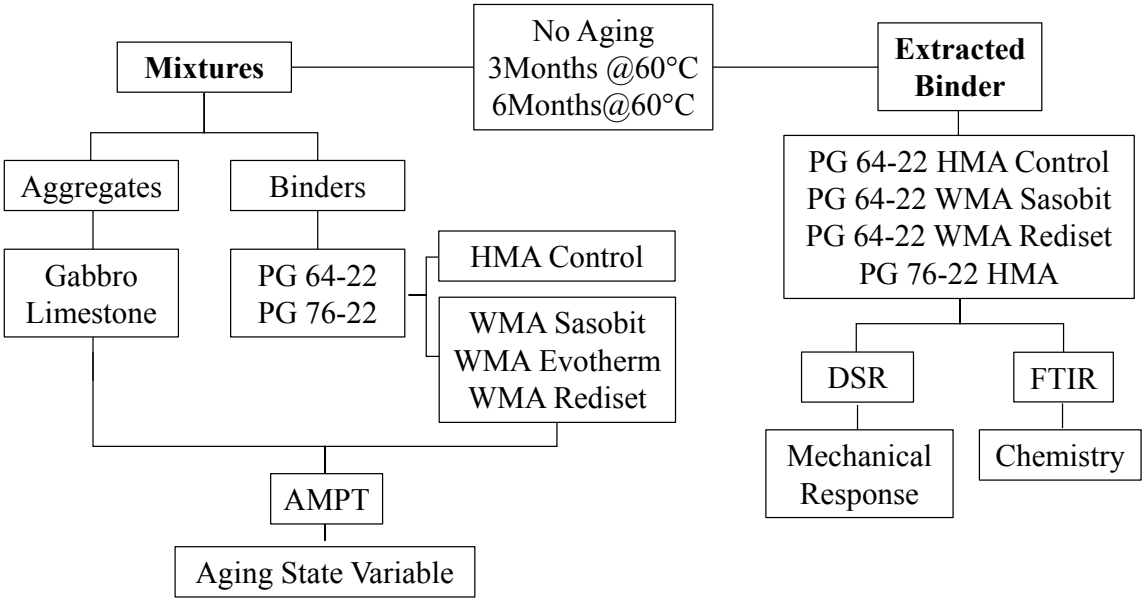

Figure 17. Experimental matrix—Objective 3

To quantify age-hardening of asphalt mixtures, the dynamic LVE response of the mixtures was evaluated using the AMPT at three stages: initial condition and after 3 months and 6 months of LTOA at 60°C. Compliances and retardation times were defined for the material at its initial condition, as previously detailed in Section 2.3.5. The aging state variable (A) was taken as a means to transition the LVE material properties to a given

aged condition (i.e., 3 months and 6 months of aging), as detailed in Equation (8) and Equation (9), for compliances and retardation times, respectively. Based on the experiments reported by Rahmani (2015) and the 20 mixtures characterized at three aging conditions in this study, it was determined that the dynamic response of asphalt mixtures with aging could be fitted considering the parameters k_1 and $k_2$to be equal to 1. The A parameter was utilized in this study to quantify the degree of age-hardening experienced by one particular asphalt mixture during a specific aging condition; therefore, statistical meaningfulness for the fitting parameter was required.

In order to fit the A parameter, an optimization process was conducted with the Microsoft® Excel® Solver by minimizing the function described in Equation (42). The optimization add-in called "functions" (Jensen 2004) was utilized to obtain the Hessian matrix involved in the optimization of A. When minimizing the error function, the diagonal of the inverse of the Hessian matrix (which is a scalar for this case) was used to calculate a standard error (SE) for fitted parameter A (Equation (43)). Equation (44) was used to determine the confidence interval (CI) for A, where $\hat{A}$ corresponds to the value obtained by optimization, the Z value corresponds to the desired confidence level (i.e., 1.96 for $\alpha = 0.05$) and the estimated SE, as shown in Equation (43). The statistical meaningfulness for the A parameter relies on the estimation that $\hat{A}$ would land within that calculated interval 95% of the time. The assumptions behind this statistical approach include (1) $\hat{A}$ is a maximum likelihood estimate, and it is asymptotically normally distributed, and (2) the errors are normally distributed. Given the complexity of the Prony equations and the optimization function, validating such assumptions would constitute a

research project on its own. An example of the fitting materials LVE response with aging is given in Figure 18, where the markers are experimental data and the continuous lines are the modeled response.

$$Error = \sum\left[\left(\frac{D'Fit}{D'Exp} - 1\right)^2 + \left(\frac{D^{"}Fit}{D^{"}Exp} - 1\right)^2\right] \times 100 \quad (42)$$

$$SE = \sqrt{\frac{1}{H}} \quad (43)$$

$$CI(A) = \hat{A} \pm ZSE \quad (44)$$

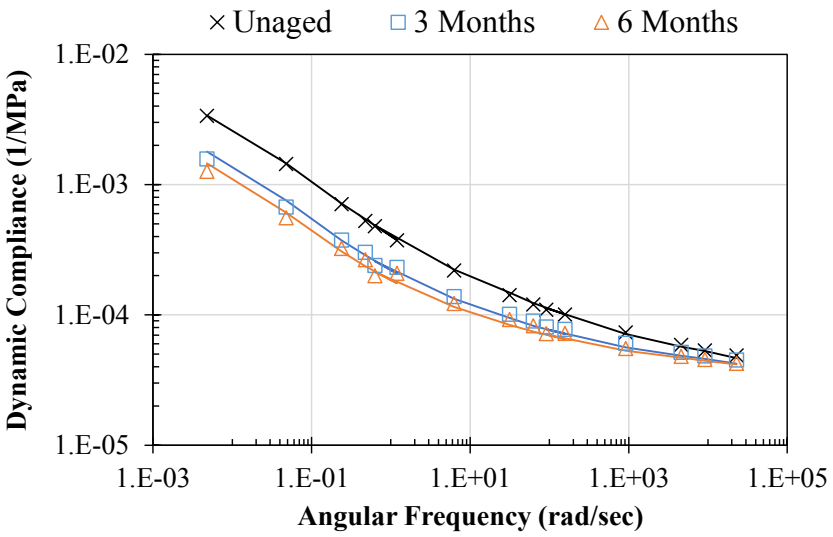

Figure 18. LVE characterization of aged asphalt mixtures

The model proposed by Rahmani (2015) does not incorporate the viscosity term in the Prony model, as his study comprised exclusively asphalt mixtures. In order to account for change in viscosity of asphalt binders with aging, this study incorporated one additional aging variable, A_2, which affects viscosity, as described by Equation (45). Note

that the A from Equation (8) and Equation (9) was denominated A_1 for the case of asphalt binder. The fitting of A_1 was performed using the storage compliance (J'), which was not affected by the viscosity term (η), as described in Equation (33) . Upon fitting A_1, the only variable left in Equation (34) for the case of asphalt binder was η, for which A_2 was optimized. The statistical approach for CIs with A_1 and A_2 was similar to that for asphalt mixtures considering Equation (46) and Equation (47) when minimizing the error.

$$\eta^A = \frac{\eta}{(1 - A_2)} \tag{45}$$

$$Error\ A_1 = \sum \left[\left(\frac{J'Fit}{J'Exp} - 1 \right)^2 \right] \times 100 \tag{46}$$

$$Error\ A_2 = \sum \left[\left(\frac{J''Fit}{J''Exp} - 1 \right)^2 \right] \times 100 \tag{47}$$

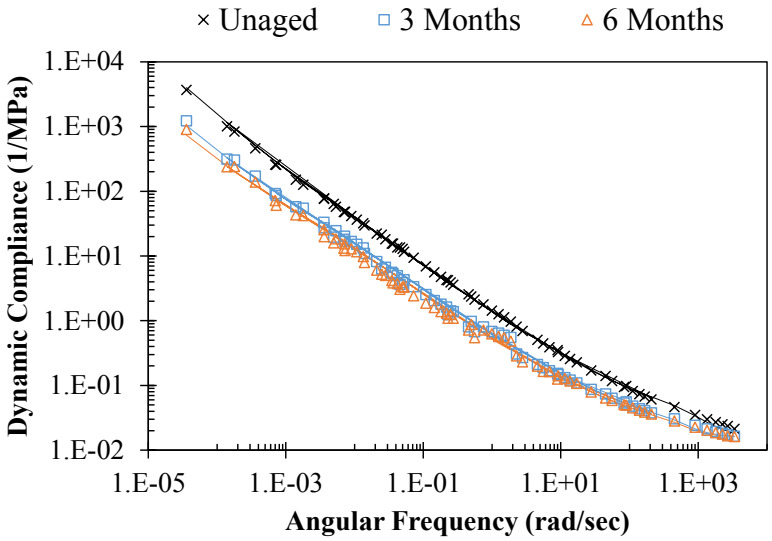

Figure 19. LVE characterization of aged asphalt binders

In addition to the mechanical model proposed in this study, one common approach for characterization of binder age-hardening was considered, the Glover-Rowe (GR) approach. The mechanical concept within this approach is to plot in the black space (phase angle versus log dynamic shear modulus) the material LVE response for one temperature and frequency (i.e., 15°C at 0.005 rad/sec). This approach illustrates the increased stiffness and loss of phase angle in the asphalt with aging, similar to the mechanism captured by the outdated ductility test for asphalt binders (ASTM D113). Empirical observations for aged pavements in a Pennsylvania climate (PG 58-28) allowed for development of ductility thresholds defining the binder ductility condition at which (1) damage starts and (2) cracks propagate extensively (Kandhal 1977). Such thresholds could be used in binder specifications to assess long-term durability. Cognizant of the value of the ductility parameter, Glover et al. (2005) correlated ductility to a DSR-based parameter (G'/η'/G'), which enabled researchers to convert Kandhal's ductility thresholds into the black-space approach (Anderson et al. 2011, King et al. 2012); this strategy is being adopted at a fast pace within the pavement community.

Finally, binder chemistry was explored from a qualitative technique (FTIR) from which CA and sulfoxide peaks were compared for the binders aged at various conditions. A thorough comparison among binder and mixture age-hardening processes is provided, with consideration of mechanics, rheology, and chemistry.

CHAPTER III

EFFECTS OF WARM-MIX ASPHALT AND AGING ON SURFACE FREE ENERGY AND POTENTIAL FOR MOISTURE DAMAGE

The surface free energy (SFE) approach has proved effective in ranking binder-aggregate compatibility and mixture performance in relation to moisture damage, as well as providing useful information for performance modeling (Little and Bhasin 2006, Caro et al. 2008a). This chapter reports the findings and conclusions from evaluating the effect of WMA additives and laboratory aging on SFE characteristics with mechanical validation.

A portion of this chapter will be published in a special edition of *Road Materials and Pavement Design* for the 2016 meeting of the Association of Asphalt Pavement Technologists (Garcia Cucalon et al. 2016a).

3.1 Surface Free Energy of Asphalt Binders

This section describes the effects of WMA additives, additive dosage, and aging on the SFE characteristics of asphalt binders. The wettability of the binder over the aggregate fraction and ease of production are discussed, with consideration of binder SFE or surface tension (Equation 1). Decreasing the surface tension of the asphalt binder facilitates the binder spreading over the surface of the aggregate during production, resulting in better coating (Osmari et al. 2015). Additionally, the effect of laboratory aging (RTFOT plus 20 hours of PAV aging) was evaluated in terms of changes in the cohesion work within the asphalt binder (Equation (4)). Previous studies have stated that, in the case

of a binder with higher cohesive bond energy, more work is required for a crack to propagate within the asphalt binder and that a reduction in cohesion work due to oxidative aging implies deterioration of the fracture properties of asphalt binders (Bhasin et al. 2007).

Surface tension of asphalt binders is presented in Figure 20. Results showed that including WMA additives can decrease surface tension of asphalt binders for certain binder-additive combinations, but this is dependent on additive dosage. At production temperatures, these results imply that WMA additives can reduce surface tension, thereby enabling reduction in production temperatures. Nevertheless, the measurements reported within this chapter were taken at room temperature (approximately 20°C), and the surface tension of a material is temperature-dependent. Thus, the rankings of asphalt binders with lower or higher surface tension may not prevail at production temperatures for HMA and WMA. Note also that for both PG binders, modification with WMA Sasobit (nonsurfactant organic wax) resulted in the largest reduction in surface tension, which is consistent with the findings reported by Osmari et al. (2015) at production temperatures.

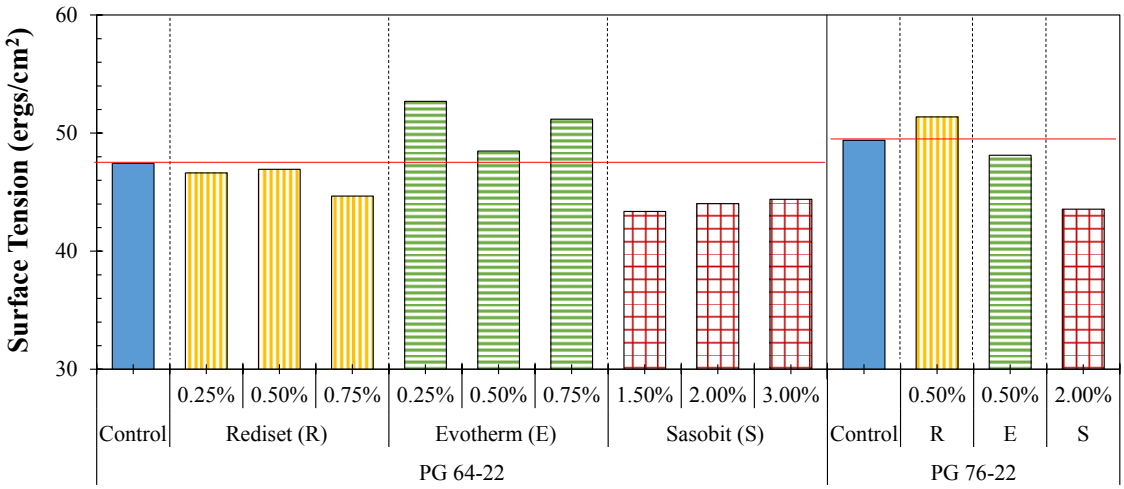

Figure 20. Surface tension of unaged asphalt binders

Current methodologies to evaluate SFE characteristics of asphalt binders and aggregates do not account for experimental variability (i.e, variability in measuring contact angles, spreading pressures, or SSA) when calculating material properties by Equations (1) to (5). There are complexities involved in accounting for the SE of material properties calculated from several experimentally determined values. The standard deviation for SFE components was estimated from the least-squares optimization when solving for x_1, x_2, and x_3 in Equation (11). Average values for SFE components and standard deviations are reported in Table 8, showing that variations were small.

Table 8. SFE components of asphalt binders

Unaged Binders

Binder Type		SFE				Standard Deviation		
		LW	Acid	Base	Total	LW	Acid	Base
PG 64-22	Control	40.5	0.4	28.6	47.4	0.9	0.1	1.3
	Sasobit 1.5%	36.4	0.3	38.1	43.4	0.8	0.1	2.0
	Sasobit 2.0%	40.0	0.1	29.3	44.0	0.5	0.0	1.1
	Sasobit 3.0%	41.0	0.1	28.7	44.4	0.6	0.0	1.5
	Evotherm 0.25%	45.5	0.5	25.4	52.7	0.6	0.1	1.2
	Evotherm 0.50%	44.7	0.1	24.3	48.5	0.9	0.1	0.8
	Evotherm 0.75%	43.3	1.2	13.4	51.2	0.7	0.1	0.7
	Rediset 0.25%	39.1	1.1	13.1	46.6	0.7	0.1	0.6
	Rediset 0.50%	40.0	1.4	8.9	46.9	0.6	0.1	0.7
	Rediset 0.75%	38.4	1.1	8.5	44.7	0.6	0.1	0.6
PG 76-22	Control	45.9	0.1	33.0	49.4	0.8	0.0	1.4
	Sasobit 2.0%	41.8	0.0	30.0	43.6	0.6	0.0	1.1
	Evotherm 0.5%	43.0	0.3	25.9	48.1	0.7	0.1	1.0
	Rediset 0.5%	43.9	1.1	12.5	51.4	0.6	0.1	0.8

RTFOT + 20 hours PAV-Aged Binders

Binder Type		SFE				Standard Deviation		
		LW	Acid	Base	Total	LW	Acid	Base
PG 64-22	Control	40.5	0.4	7.9	44.2	0.6	0.1	0.6
	Sasobit 1.5%	40.5	0.5	19.3	46.5	0.8	0.1	1.0
	Sasobit 2.0%	41.5	0.4	9.1	45.1	0.7	0.1	1.0
	Sasobit 3.0%	39.7	0.1	10.3	41.5	0.5	0.0	0.7
	Evotherm 0.25%	41.4	0.5	11.6	46.4	0.7	0.1	1.2
	Evotherm 0.50%	40.2	0.2	19.0	44.2	0.7	0.1	1.9
	Evotherm 0.75%	41.0	0.4	11.7	45.1	0.7	0.1	0.6
	Rediset 0.25%	41.4	0.3	9.1	44.4	0.6	0.1	0.6
	Rediset 0.50%	40.1	0.3	10.5	43.6	0.7	0.1	0.8
	Rediset 0.75%	35.0	1.1	7.8	40.8	0.5	0.1	0.5
PG 76-22	Control	43.9	0.5	15.7	49.7	0.6	0.1	1.0
	Sasobit 2.0%	40.5	0.4	11.7	44.8	0.6	0.1	0.6
	Evotherm 0.5%	43.5	0.4	21.0	49.5	0.6	0.1	1.3
	Rediset 0.5%	45.2	0.5	22.8	52.2	1.0	0.1	1.3

Figure 21 presents cohesive bond energies of asphalt binders with WMA additives before and after laboratory aging. Note that the legend "PAV" in Figure 21 refers to the

standard RTFOT plus 20 hours of PAV aging, which is the case for all figures herein. Considering the unaged binders, the PG 76-22 binder had higher cohesive bond energies than the PG 64-22 for the HMA control case and the WMA Rediset case. After PAV aging, the cohesive bond of the PG 64-22 binder decreased for most cases, while the polymer-modified materials did not exhibit signs of degradation with aging. These results are consistent with general experience that polymer modifications may improve the fracture resistance of asphalt binders before and after long-term aging. It is possible that further aging may degrade the cohesive bond strength of the polymer-modified binders. It is important to highlight that both binders PG 64-22 and PG 76-22 utilized in this study were of the same crude source and chemical nature, with differences introduced by the polymer modifications, as will be discussed in more detail based on FTIR data in Chapter V. Rheological and chemical changes with binder aging are also discussed in Chapter V.

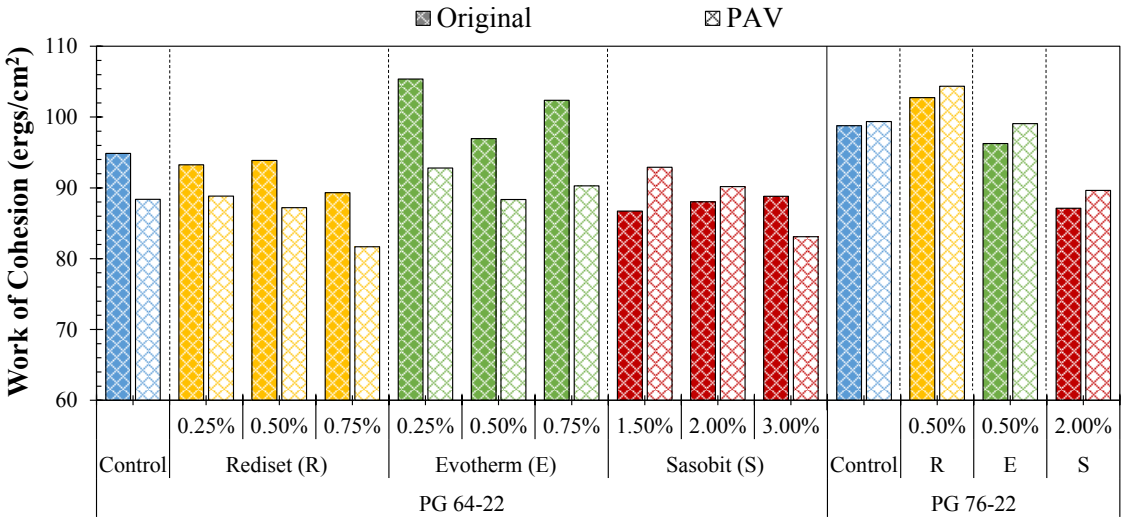

Figure 21. Effect of aging on cohesive bond energy of asphalt binder

To better understand the changes in cohesive bonds with aging, SFE components of asphalt binders were compared before and after aging with consideration of experimental variability. Figure 22 shows the change in nonpolar (a), acid (b), and base (c) components of SFE with laboratory aging; error bars represent the standard deviation from fitted SFE components. The nonpolar, or LW, component (Figure 22a) exhibited minor changes with the inclusion of Rediset and Sasobit WMA additives or with aging. Inclusion of the Evotherm WMA additive and polymer modification increased the LW SFE component. The acid (Figure 22b) and base (Figure 22c) SFE components exhibited proportionally larger changes with technological modifications and with aging, explaining the differences observed in SFE and work of cohesion. The acid component was a very small value for all cases, but it still had great impact on the total contribution of polar components to SFE (Equation 1). The acid component did not show consistent trends with aging, as it may increase or decrease depending on binder type and technological modification. On the other hand, the base component mostly decreased with aging for the PG 64-22 binder and increased for the 76-22 binder. Common oxidation products, ketones and sulfoxides, are weak bases (Branthaver et al. 1993) and are also reported to absorb strongly to the aggregate surface and easily desorb in the presence of water (Curtis et al. 1993). It is important to highlight that total SFE is not a measurement of independent compounds, but the net free energy on the surface of the binder. Though it is possible that the observed changes in binder polar SFE components could have been caused by formation of oxidation products, binder aging also implies volatilization of low-molecular-weight hydrocarbons, contributing to the overall change in binder polarity.

Also, in the case of the PG 76-22 binder, the polymer may have undergone additional chemical changes with aging.

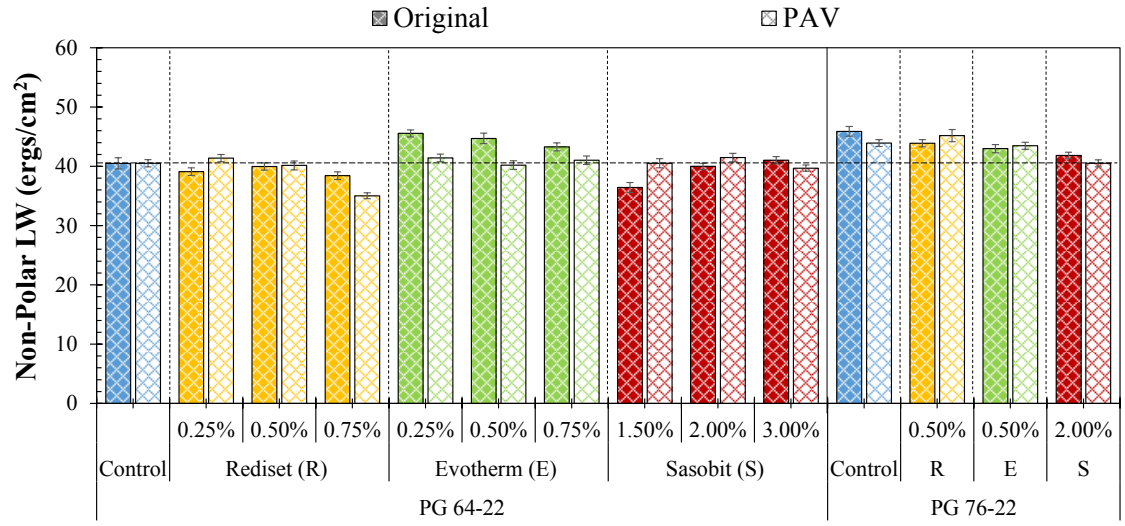

(a) Nonpolar SFE component

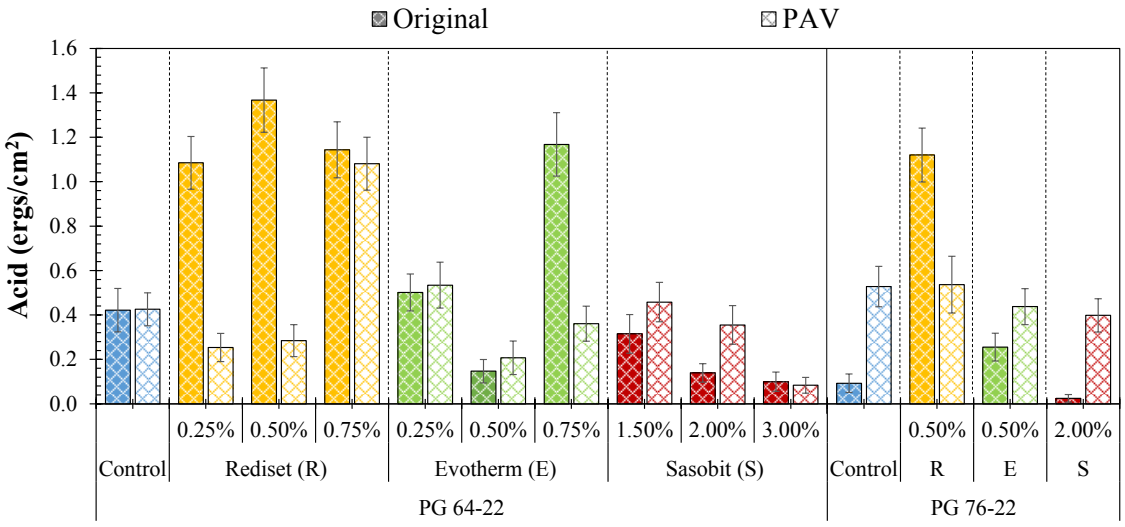

(b) Acid SFE component

Figure 22. Effect of aging on SFE components in asphalt binder

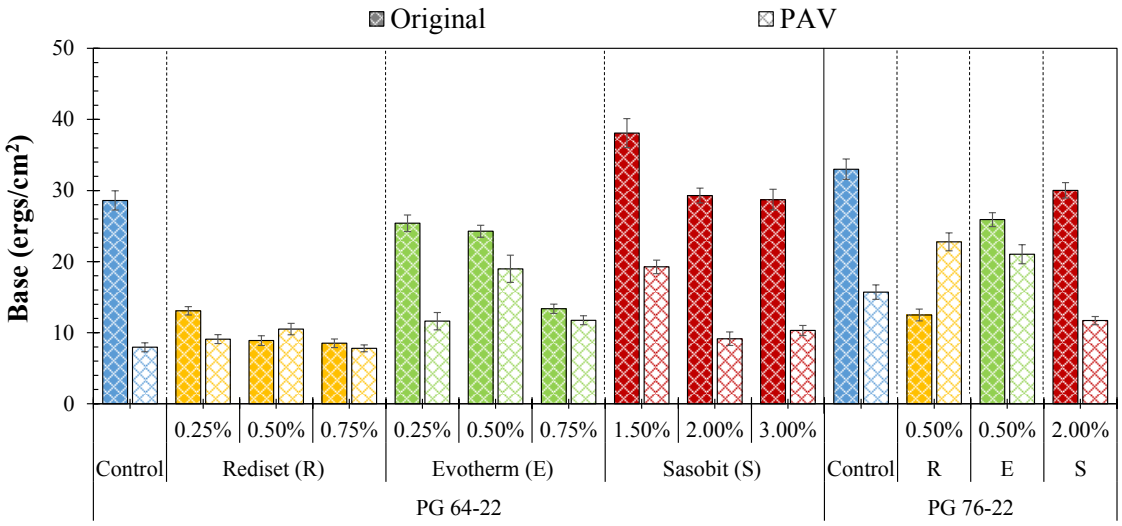

(c) Base SFE component

Figure 22. Continued

3.2 Asphalt Binder-Aggregate Compatibility

Compatibility among constituents is a relevant factor in evaluating moisture damage. This section reports the effect of WMA additives interacting with two different aggregate types. The binder-aggregate work of adhesion (Equation (4)) and ER (Equation (5)) were calculated before and after laboratory aging. The SFE components of the aggregate were calculated from spreading pressure and SSA; the standard deviations from experimental measurements are given in Table 9.

.

Table 9. Spreading pressure and SSA of aggregates

Aggregate	Probe Vapor	Spreading Pressure (erg/cm^2)		SSA (m^2/g)		SFE (erg/cm^2)			
		Avg.	Std. Dev.	Avg.	Std. Dev.	LW	Acid	Base	Total
Limestone	Water	261.78	23.18	3.73	0.41	69.35	0.28	1075.40	104.18
	N-Hexane	33.75	2.67	2.26	0.19				
	MPK	37.65	5.17	2.36	0.22				
Gabbro	Water	743.80	20.72	3.77	0.10	57.37	3.34	6277.96	346.85
	N-Hexane	28.18	1.20	0.58	0.03				
	MPK	44.04	4.57	0.67	0.09				

The binder-aggregate work of adhesion is presented Figure 23 for all binder modifications in combination with both aggregate types. A higher work of adhesion was observed for binders in combination with gabbro aggregates for all cases due to the high polarity observed in the gabbro aggregates from SFE measurements. Work of adhesion, as defined by Equation (2), considers polar and nonpolar components of binders and aggregate; the gabbro evaluated in this study had an extremely large base component (Table 9), which, multiplied by the small acid component in the binder, still contributed largely to the total work of adhesion. The increased polarity of the gabbro can be attributed to metals present in the surface of the gabbro aggregates (Table 3). For both limestone and gabbro aggregates in combination with both PG binders, the inclusion of WMA technologies with adhesion promoters improved the binder-aggregate bond (i.e., Rediset and Evotherm). On the other hand, inclusion of Sasobit resulted in decreased bonding, becoming more obvious as the additive dosage was increased (PG 64-22).

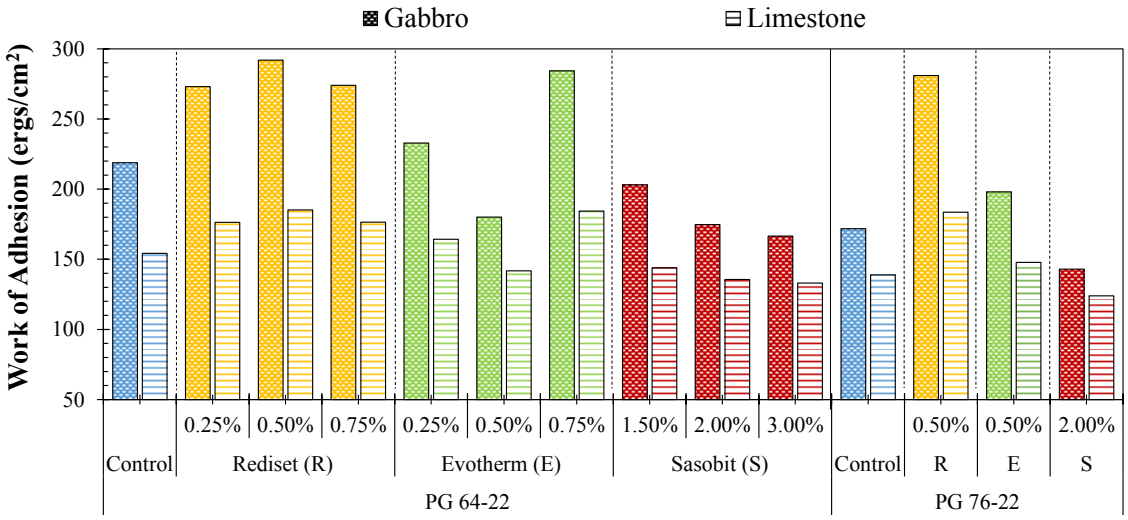

Figure 23. Adhesive bond energy

Highly polar aggregates are also highly hydrophilic; therefore, the potential for moisture damage in asphalt mixtures is greater (Miller et al. 2011, Miller et al. 2012). Similar to the binder-aggregate work of adhesion, the work of debonding (Equation (3)) quantified thermodynamic potential for water to displace asphalt binder from the aggregate surface. The ER parameter described in Equation (5) consisted of an SFE-based approach for ranking asphalt mixture performance considering moisture susceptibility; it considered the work of adhesion, work of cohesion, and work of debonding. The ER parameter for each binder-aggregate combination in this study is reported in Figure 24a. The inclusion of WMA additives with adhesion promoters can reduce the potential for moisture damage in asphalt mixtures, and additive dosages should be optimized for best performance. It was also evident that limestone had higher ER as compared to gabbro in combination with any of the binders considered in this study. Total SFE of the gabbro had a predominant polar SFE components (Table 9); therefore, gabbro resulted in greater work of debonding compared with limestone (Equation (3)).

All SFE parameters were given in units of energy by area (erg/cm^2). In order to account for the surface area of interaction, it is recommended to multiply ER by each aggregate's SSA when comparing various aggregate types (Bhasin et al. 2006, Little and Bhasin 2006). The values in Figure 24a were multiplied by the SSA (n-hexane) of the aggregates, as reported in Table 9, for limestone and gabbro. Results are presented in Figure 24b, highlighting that the limestone aggregates were less likely to experience moisture damage.

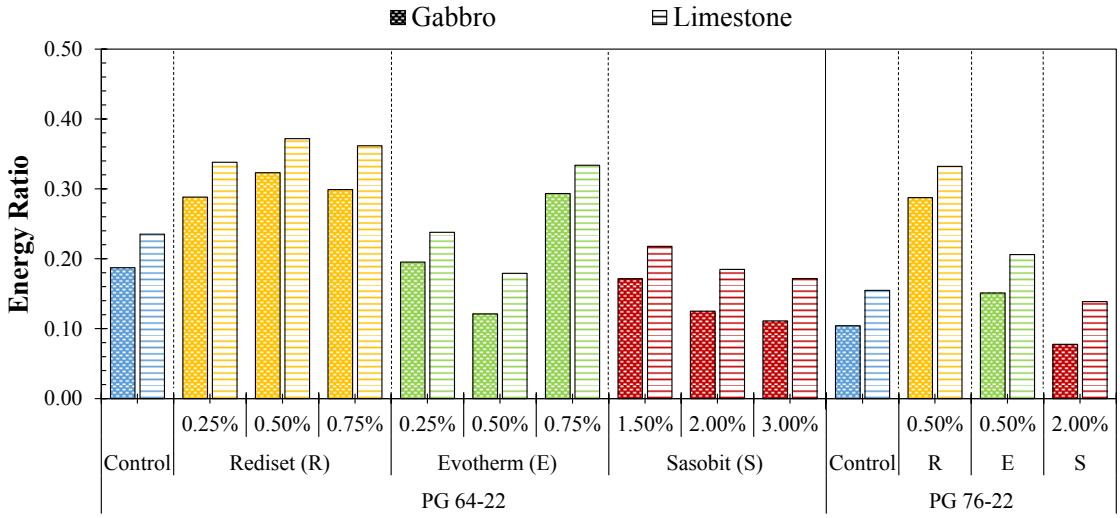

(a) ER

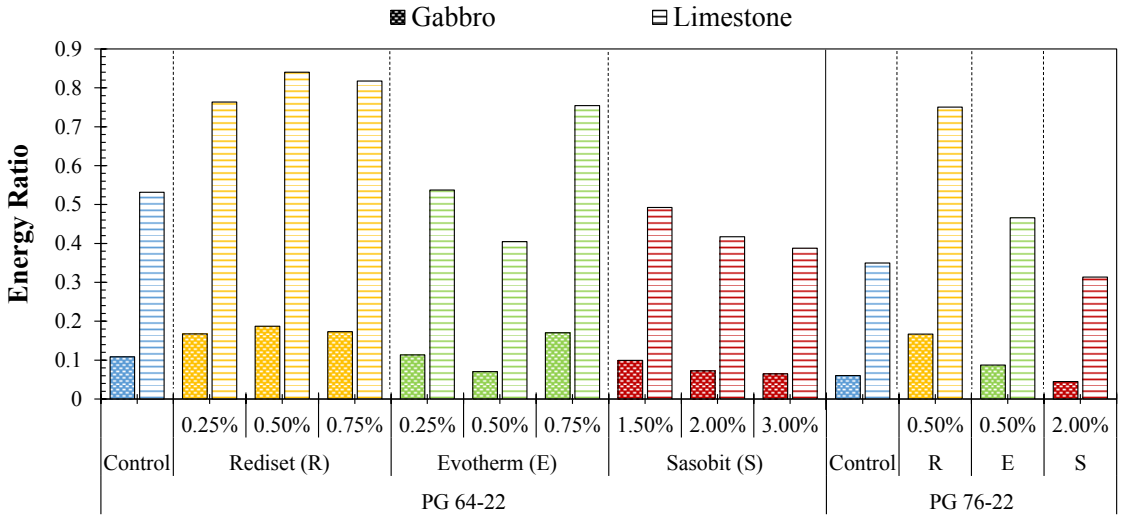

(b) ER×SSA (n-hexane)

Figure 24. ER

The effect of binder aging on binder-aggregate adhesive properties is presented in Figure 25a and Figure 25b for gabbro and limestone, respectively. In most cases, the binder-aggregate work of adhesion was reduced with binder PG 64-22 (except Sasobit) and was increased with binder PG 76-22 (except Rediset).

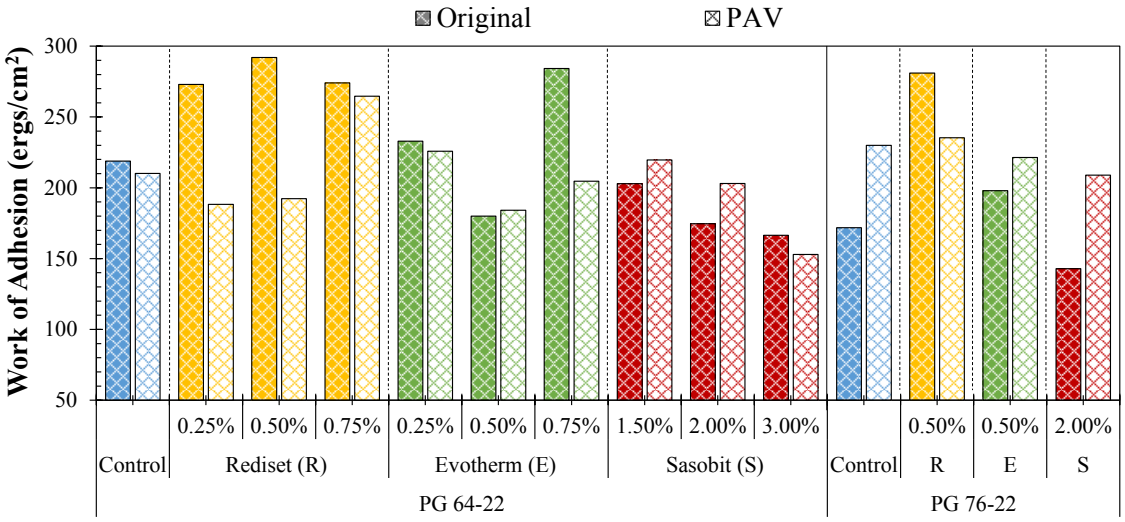

(a) Gabbro

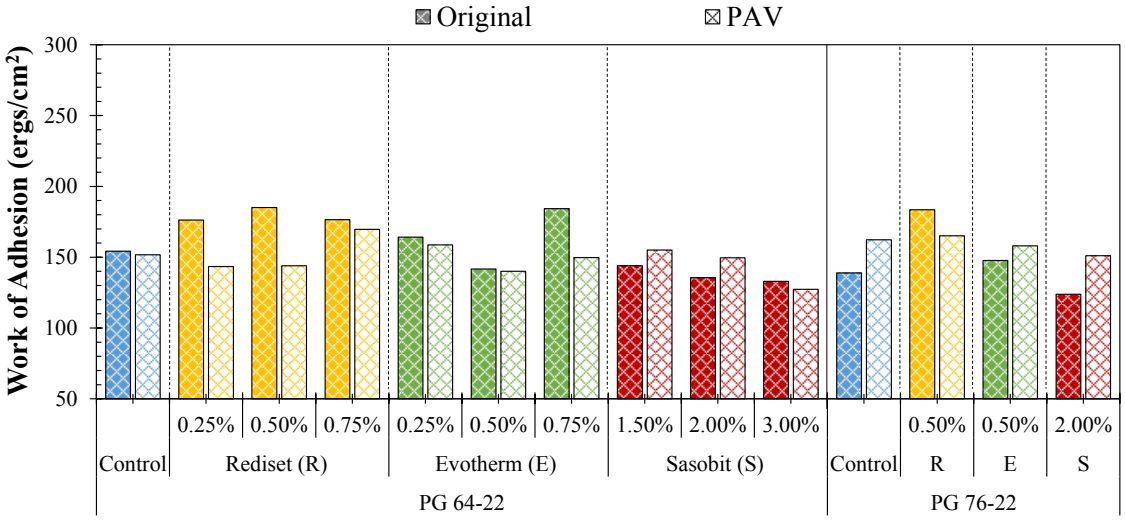

(b) Limestone

Figure 25. Adhesive bond with aging

To consider long-term potential for moisture damage, the changes in ER with aging are presented in Figure 26a and Figure 26b for gabbro and limestone, respectively. ER can increase or decrease upon binder aging, depending on the binder, WMA additive, and additive dosage, while trends are comparable among aggregate type. Based on the

results observed from varying Rediset dosage with binder PG 64-22, it is possible that long-term efficacy of the adhesion promoters depends on additive dosage.

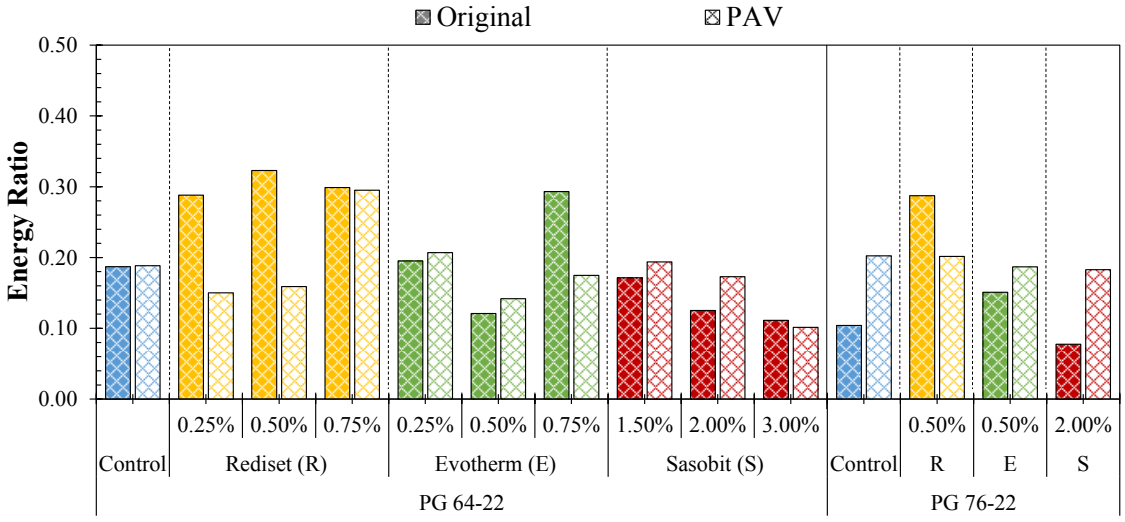

(a) Gabbro

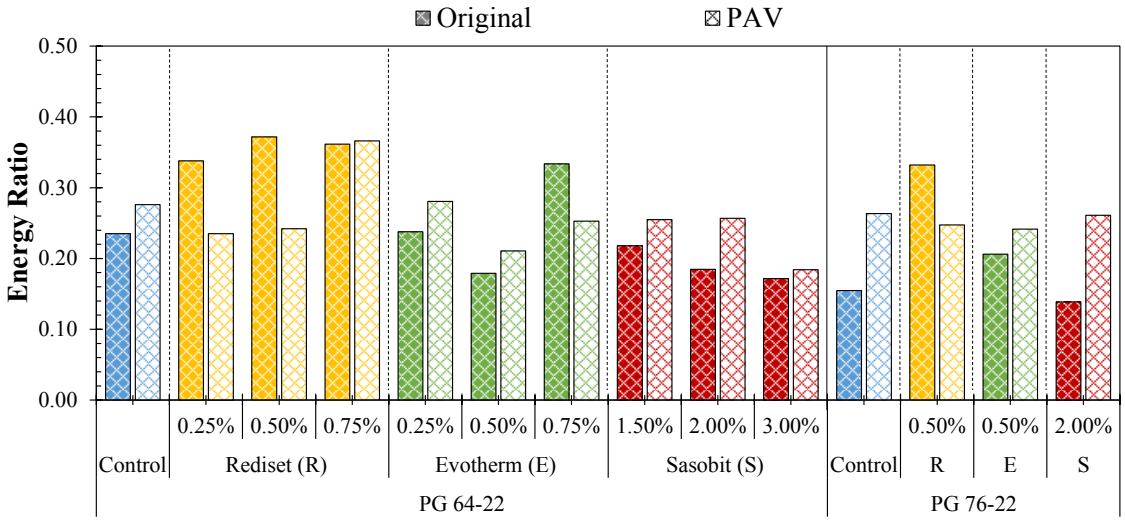

(b) Limestone

Figure 26. ER with aging

Selection of more compatible binder-aggregate combinations should be carefully performed. Selection of aggregates is often restricted by the cost of hauling distances,

while the engineer can select among various adhesion promoters and optimize the dosage for best performance with consideration of long-term asphalt binder properties.

It is important to reiterate that this study considered only one laboratory long-term aging process. Additionally, when absorptive aggregates are utilized (e.g., limestone), it is possible that the binder-aggregate compatibility evaluation with aging is not valid. It has been previously suggested that if selective absorption were to occur, the experimental characterization of binder and aggregate SFE should be representative of such a condition. The SFE components of the aggregate should be measured upon absorption of the lighter compounds from the asphalt binder, followed by evaluation of SFE components of the "incomplete" binder surrounding the aggregate (Luo and Lytton 2012). Experimental conditions for such a case could be extremely difficult to achieve, and ensuring validity of the experimental method would constitute a research project on its own; therefore, it was not considered in this study.

3.3 Mechanical Evaluation of Moisture Damage

Mechanical evaluation was conducted to assess the effect of moisture damage and aging in terms of crack propagation within the FAM portion of an asphalt mixture. Later, results are compared to SFE parameters. The crack growth index (ΔR) calculated from Equation (18) for all test specimens at different conditions is presented in Figure 15. Figure 27a and Figure 27b show examples of the change in crack growth index increasing with number of load cycles under dry and wet conditions, respectively. As one would expect, ΔR in the wet condition was higher (more damage) than in the dry condition. Moisture accelerated the crack growth as it weakened the bond between aggregates and binders. For

further synthesis of the large dataset considered in this study, the crack radius (ΔR) at 5000 load cycles was selected as an indicator parameter. The wet/dry ratio was utilized to assess the effect of moisture-induced damage (Equation (19)).

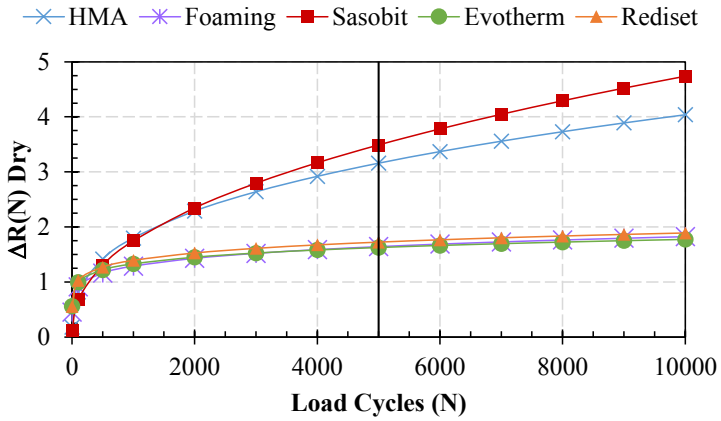

(a) Dry

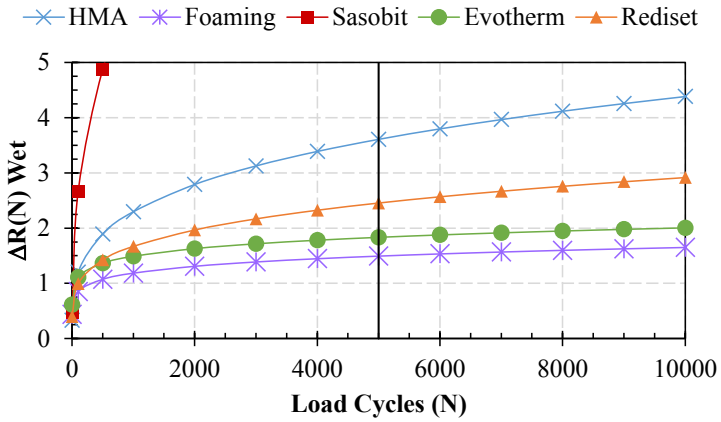

(b) Moisture-Conditioned

Figure 27. Example results of aged limestone: crack radius vs. load cycles

Results from the fatigue test and moisture susceptibility evaluation are summarized and presented in Figure 28 to Figure 31. Arrows on the bar graphs indicate that the obtained values exceeded the limit set by the corresponding y-axis.

Results for the FAM specimens prepared using gabbro aggregates are presented in Figure 28 and Figure 29. Before aging (Figure 28a), most WMAs with PG 64-22 in the dry condition showed increased susceptibility to fatigue cracking compared to HMA, and WMA Evotherm exhibited the fastest crack growth. In terms of moisture susceptibility, HMA was less susceptible to moisture damage compared to any WMA. Considering the polymer-modified binder PG 76-22, WMA Rediset performed similarly to HMA before and after moisture conditioning. After aging (Figure 28b), WMA mixtures with binder PG 64-22 exhibited improved resistance to moisture damage. For binder PG 76-22, WMA foaming exhibited improved fatigue-cracking resistance after aging in both dry and wet conditions. The foaming technology uses water to increase the volume of asphalt binder to provide better coating at lower temperatures, so WMA foaming may hold some moisture after compaction. The authors believe that aging of WMA foaming helped to release any such moisture, promoting better adhesion between the asphalt binder and aggregates. On the other hand, WMA Sasobit and Evotherm exhibited sudden failure after aging when evaluated at the same strain level; therefore, these mixtures could not be compared in a moisture-conditioned state, and results are not available in Figure 28b and Figure 29.

These results indicate that the performance of some WMAs may be improved upon aging, in agreement with previous studies reporting increased stiffness and improved resistance to moisture damage in WMA with laboratory and field aging (Yin et al. 2014b, Garcia Cucalon et al. 2015).

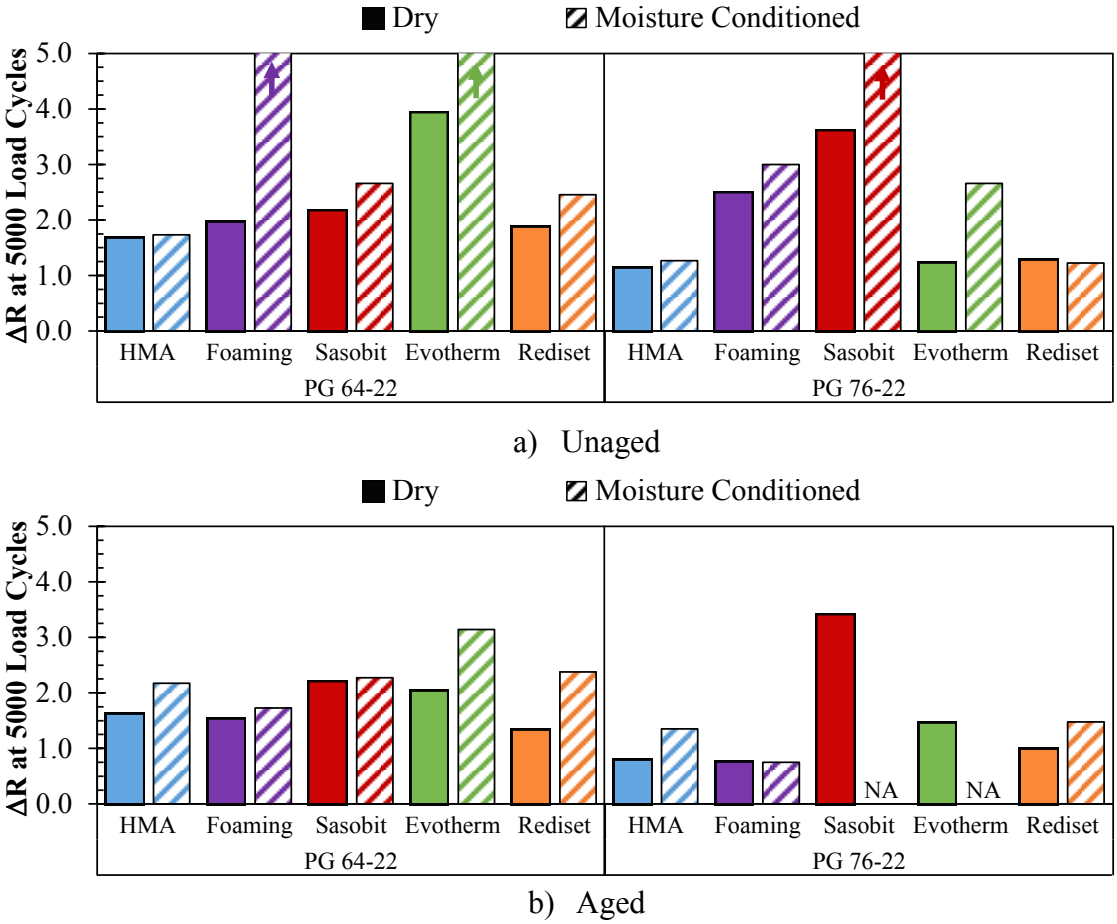

Figure 28. Crack growth—gabbro.

MSR was calculated to quantify the effect of moisture damage (Equation (19)). The larger the MSR was, the greater the moisture susceptibility was. Figure 29 shows the MSR for gabbro materials before and after aging. For the 64-22 binder, most WMAs exhibited a reduction in MSR after aging, with the exception of WMA Rediset, implying that aging improves the moisture damage resistance of some WMAs. It should be highlighted that WMA Rediset exhibited a reduction in ER (Figure 26) after PAV aging. A reduction in ER indicates reduced resistance to moisture damage, which is consistent in this case with the mechanical testing. For the PG 76-22 binder, aging was found to

aggravate the moisture susceptibility for all WMAs, except foaming, which showed slight improvement in moisture damage resistance after aging.

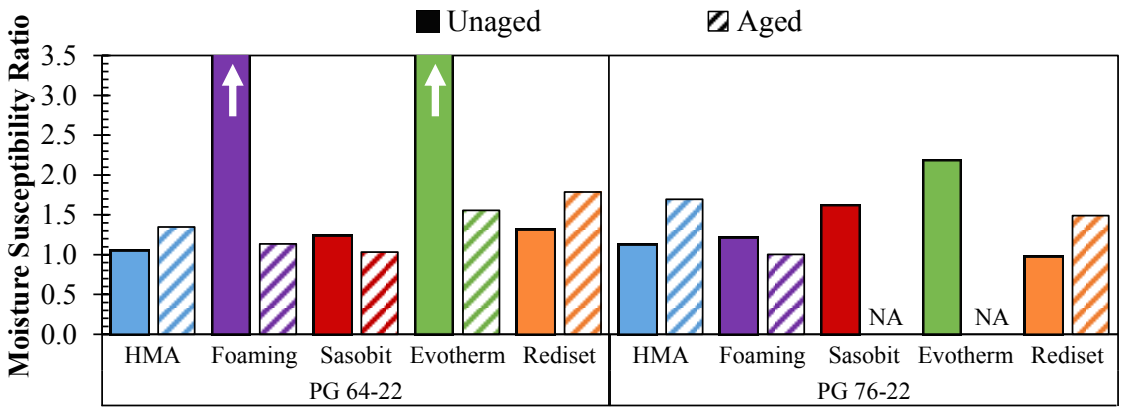

Figure 29. MSR at 5000 cycles—gabbro

The crack growth indexes for limestone mixtures are reported in Figure 30 and Figure 31. Mixtures composed of limestone with unaged PG 64-22 binder (Figure 30a) in the dry condition showed that HMA and WMA Sasobit experienced faster deterioration than other WMA technologies represented herein. Upon moisture conditioning, WMA Sasobit deteriorated the fastest.

In general, results in Figure 28 (gabbro) and Figure 30 (limestone) show that the PG 76-22 binder performed better compared to the unmodified binder (PG 64-22) in the dry condition, highlighting the effectiveness of polymer modification in reducing the potential for fatigue damage before and after aging.

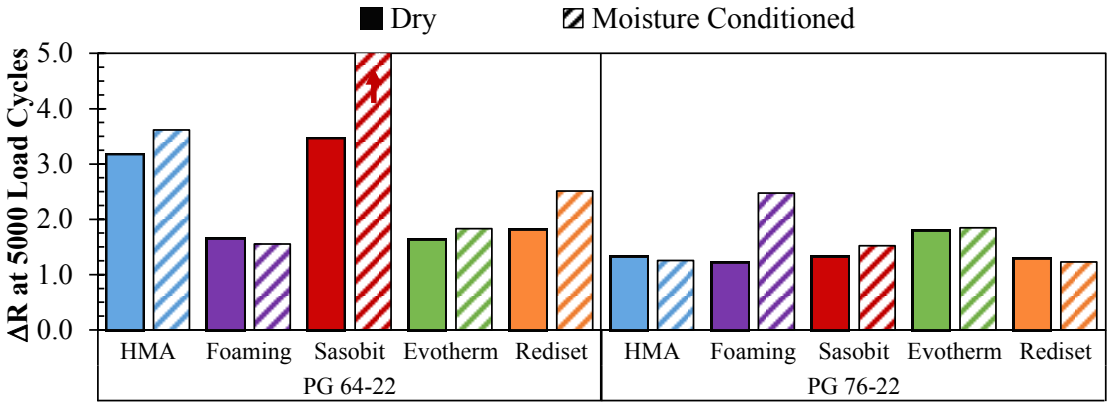

a) Unaged

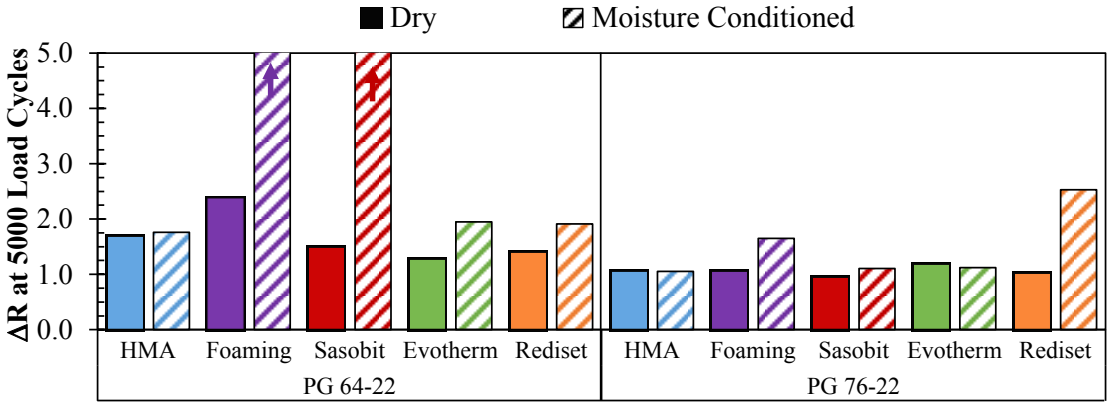

b) Aged

Figure 30. Crack radius at 5000 load cycles—limestone

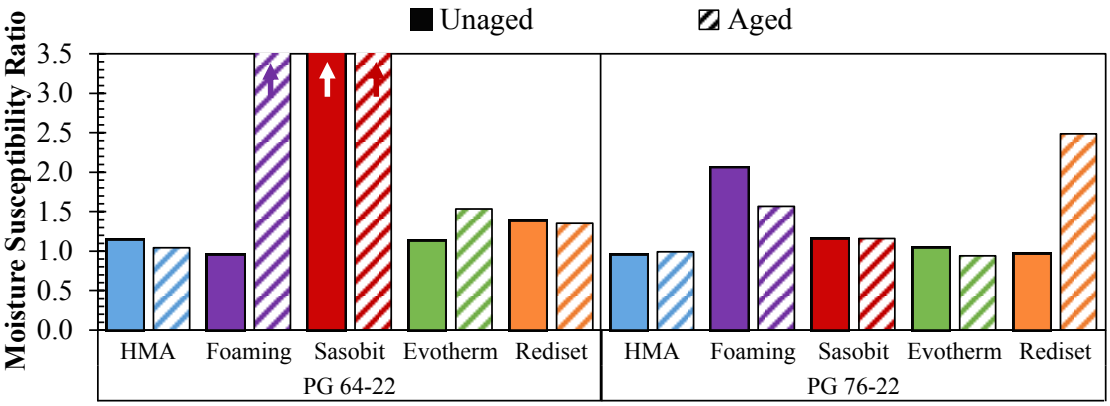

Figure 31. MSR at 5000 cycles—limestone

The MSR for limestone mixtures (Figure 31) indicated a generally lower moisture sensitivity when the polymer-modified binder was utilized, with the exception of WMA Rediset. Aging had less effect for limestone materials versus gabbro materials.

3.4 Surface Free Energy and Moisture Damage

The ER parameter was used as an SFE-based indicator for moisture damage (Equation (5)). This parameter was multiplied by the SSA of each aggregate and plotted against the corresponding indicators from mechanical testing. The DMR (Equation (23)) consisted of an indicator of the retained mechanical property after the moisture condition, for which values were always smaller than 1. The MSR from Equation (19) (wet/dry ΔR) was always larger than 1, given that the crack growth was larger in the wet condition. For ease in comparing both parameters, the MSR was presented as dry/wet ΔR. A 20% loss in mechanical integrity is commonly accepted due to moisture conditioning, resulting in an 80% retained mechanical property (i.e., strength and/or stiffness).

The relationship between ER×SSA and the mechanical indicators of moisture susceptibility are presented in Figure 32 and Figure 33. The DMR (Figure 32) showed gabbro results to be scattered, but the trend of higher ER, implying better resistance to moisture damage, was consistent. For limestone mixtures, most combinations reported good performance in mechanical testing, except for the WMA Sasobit with binder PG 64-22, which fell beneath the 0.8 threshold. The limestone mixtures also exhibited significantly higher values of ER×SSA.

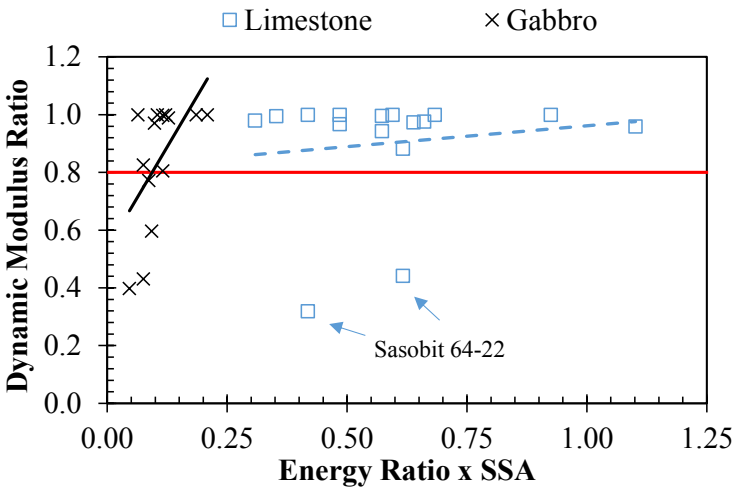

Figure 32. DMR at 1000 cycles vs. ER

The relationship of ER and MSR is presented in Figure 27. Results demonstrated that MSR tended to increase with an increase in ER. For limestone aggregates, a generally good performance was observed, also with higher ER values.

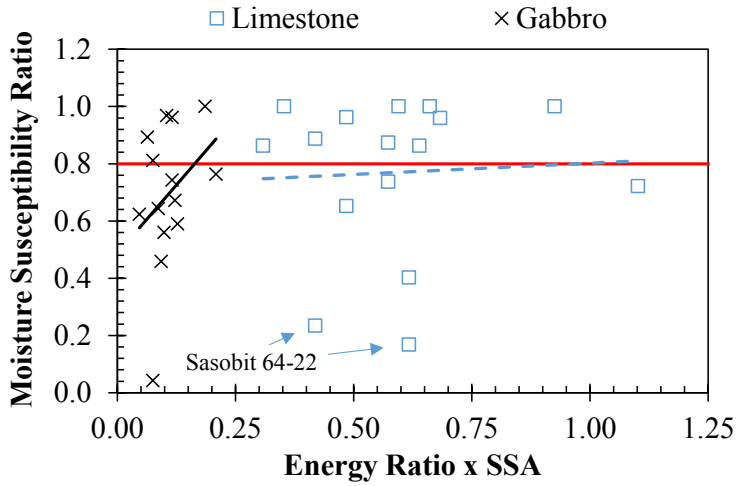

Figure 33. MSR at 5000 cycles vs. ER

ER quantifies the adhesion between asphalt binders and aggregates when their interface is completely dry and when it is wet. Thus, this ratio does not account for any residual or entrapped moisture at the interface (partially wet) due to inadequate aggregate

drying or using moisture or water, as in the foaming technology. In addition, ER is used as a performance indicator and should not be used solely as a performance tool. Other parameters such as VE properties and tensile strength should be considered along with energy parameters to fully evaluate performance (Masad et al. 2008, Kassem et al. 2011).

Further analysis was conducted to assess the effect of aging on binder surface characteristics and implications on moisture susceptibility. PAV was utilized as a qualitative representation of binder aging. The percent changes in calculated adhesive bond energy with aging versus the percent change in FAM mechanical indicators of moisture susceptibility are plotted in Figure 34. The mechanical parameters evaluated were DMR (Equation (23)) and MSR (Equation (19)) on the basis of stiffness and crack growth. Mechanical changes, in terms of moisture susceptibility, trended in the same direction, as dictated by the surface characteristics for most mixtures.

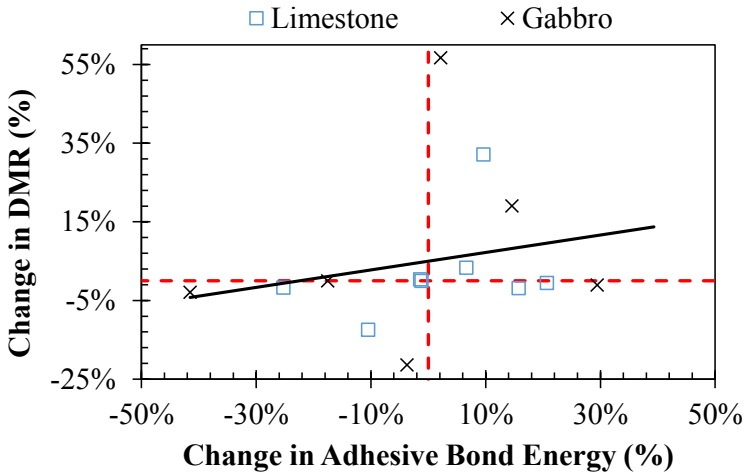

(a) Adhesive Bond Energy vs. DMR

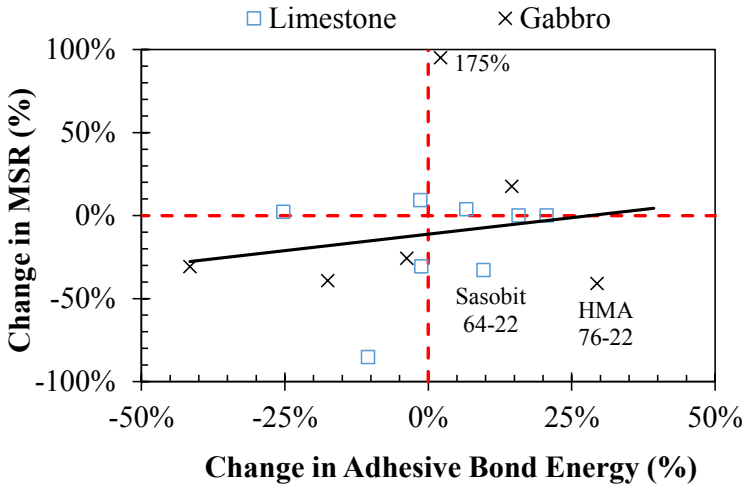

(b) Adhesive Bond Energy vs. MSR at 5000 Cycles

Figure 34. Change in moisture susceptibility parameters with aging.

The aging protocol used in this study was RTFOT plus 20 hours of PAV aging for asphalt binder and 3 months of oven aging at a temperature of 60°C for FAM specimens, after which engineering properties of binder and FAM were determined. During and following the aging process, complex and synergistic reactions occur that impact binder and FAM characteristics. For example, stiffening effects due to oxidative aging can increase fracture strength, yet can also decrease the plastic deformation potential that

occurs beyond the critical stress level. This could translate into an overall loss or gain in fracture toughness, depending on degree of aging. It is possible for asphalt mixtures to exhibit increased resistance to fracture or fatigue after a certain degree of aging, yet exhibit different fracture and fatigue resistance after continued or more severe aging. If further laboratory aging were to be considered, results may vary. Proper aging protocols should be conducted in the laboratory to simulate intermediate- and long-term field aging for improved performance characterization, which is the focus in recent NCHRP studies (9-52 and 9-54).

3.5 Summary

This chapter describes the effect of WMA additives and additive dosage on SFE of asphalt binders and their adhesion with aggregates before and after long-term aging (RTFOT plus 20 hours of PAV aging). Several parameters were considered to quantify the effect of WMA additives on the wettability (or ability to coat) of asphalt binders, adhesive bond energy between asphalt binders and aggregates, and binder-aggregate compatibility related to moisture damage. Additionally, extensive mechanical evaluation of FAM specimens subjected to laboratory moisture conditioning was compared to findings from the SFE-based approach. The main findings within this chapter are summarized as follows:

- WMA additives can reduce the surface tension of asphalt binder, but additive dosage plays a role too. Reduced surface tension allows improved wettability and coating of the aggregate by the binder at production temperatures.

- The binder-aggregate adhesive bond and ER (used as an indicator for moisture damage) can be improved by optimizing WMA additive type and dosage. Aging improves these parameters for some cases.
- Based on SFE and DMA evaluations, mixtures containing gabbro aggregates are more susceptible to moisture damage compared to mixtures with limestone aggregates. However, the moisture sensitivity of gabbro can be improved if combined with certain binder types and WMA additives.
- Available WMA technologies can improve, deteriorate, or have a minimal effect on mixture performance in terms of moisture susceptibility. The selection of modifier type should be optimized for particular binder/aggregate combinations. Aging of WMA generally increases resistance to moisture damage based on the SFE measurements and mechanical testing of FAM.

It is advisable to conduct performance testing and assess constituent compatibility prior to incorporation of any chemical modification to an asphalt mixture. The tools presented in this chapter can be used as screening tools before the design stage to check the compatibility of asphalt binder, WMA additive type, and aggregate type, as well as the sensitivity of such combinations to certain environmental conditions such as moisture and aging.

CHAPTER IV

EFFECTS OF TEMPERATURE AND MOISTURE ON BINDER-AGGREGATE INTERFACIAL BONDING

Various studies have focused on understanding mechanisms for moisture damage, developing experimental methods, and evaluating treatments to minimize moisture damage in asphalt pavements (Little and Jones 2003, Caro et al. 2008a, Caro et al. 2008b). One promising approach is the study of the asphalt binder-aggregate bond based on thermodynamics and physical chemistry by characterizing binder-aggregate work of adhesion (ΔG). Experimental techniques representative of this approach include determination of asphalt binder and aggregate SFE components (Hefer et al. 2006, Bhasin and Little 2007) or evaluation of the wetting process by enthalpy of immersion (Bhasin and Little 2009). Measuring enthalpy of immersion through microcalorimetry is an efficient method that provides a direct measurement of the binder-aggregate interaction. Additionally, this method allows flexibility for the aggregates to be conditioned to mimic realistic production conditions, such as temperature, moisture, and dust (Bhasin and Little 2009, Vasconcelos et al. 2009, Miller et al. 2011). With the asphalt industry continuously evolving and deploying technological alternatives to traditional HMA, simple, fundamental, and versatile experimental techniques are desired.

This chapter presents the findings and conclusions corresponding to the effect of temperature and moisture on binder-aggregate interfacial bonding. Experimental techniques and analysis were adapted to assess the effect of temperature on the binder-

aggregate adhesive bond and on binder-aggregate bonding when a uniform layer of moisture surrounds the aggregate. A control PG 64-22 binder (HMA), two common WMA technologies, and two different aggregate types were investigated (Table 7). SFE components resulting from experimental measurements (Chapter III) are summarized in Table 10, which are relevant to the discussion presented in this chapter.

Table 10. Materials description

	Water	HMA	Sasobit	Evotherm	Gabbro	Limestone
γ (erg/cm^2)	72.8	47.41	44.03	46.95	346.8	104.2
γ^{LW}	24.8	40.48	39.98	39.97	57.4	69.4
γ^+	25.5	0.42	0.14	1.37	3.3	0.3
γ^-	25.5	28.60	29.30	8.89	6278.0	1075.4
SSA (m^2/g					0.58	2.26

4.1 Adhesion at In-Service Temperature Range

Enthalpy of immersion (ΔH) was determined experimentally for various binder-aggregate combinations (Table 7) at four different temperatures (10°C, 20°C, 35°C, and 50°C), covering a representative range for asphalt pavement in-service temperatures. $\Delta G(T)$ was modeled upon selection of a ΔG_{ref}, as discussed in Section 2.3.2, consisting of (1) $\Delta G_{ref} = \Delta G_{AS}$ and (2) $\Delta G_{ref} = \frac{1}{2}\Delta H_{300K}$. The effect of using different aggregate types is reported in Figure 35 for the measured ΔH (Figure 35a) and the modeled ΔG (Figure 35b and c), where the assumption for ΔG_{ref} is marked by a dashed line. At each temperature, three replicate tests were conducted (standard deviation is represented by error bars in Figure 35a). A linear fit was applied, as explained in Figure 16, in order to

obtain the heat capacity (ΔC_p), described in Equation (36). Both enthalpy (ΔH) and entropy (ΔS) increased with temperature as a function of specific heat capacity, as described in Equations (39) and (40), resulting in reduced energy available to do work (ΔG), which is modeled by Equation (41).

The experimental measurements for ΔH, shown in Figure 35a, considered the control PG 64-22 binder and wetting gabbro and limestone aggregates. It was observed that temperature variation had a substantial influence on the interaction between the control binder and the gabbro aggregate, while the effect was minimal for the asphalt-limestone interaction. Figure 35b and Figure 35c show the modeled ΔG based on the two available estimations for ΔG_{ref}. An effective reduction of binder-aggregate ΔG could be explained based on reduction in binder surface tension with increasing temperature. Thus, ΔG versus temperature, shown in Figure 35b and Figure 35c, should have shown parallel lines, which was not the case. It is possible that the difference observed was related to a change in entropy. Regardless of the physicochemical and/or mechanical phenomena responsible, it is clear that the aggregate fraction had a significant effect on the magnitude of the binder-aggregate bond and the rate of change over the temperature range. Different assumptions for ΔG_{ref} may rank binder-aggregate combinations comparably, but they can also result in widely different magnitudes of ΔG with temperature.

It is important to consider that field and laboratory experience with limestone indicates that limestone is generally more resistant to moisture damage than most other noncalcareous aggregates (Parker Jr and Wilson 1986, Hunter and Ksaibati 2002, Birgisson et al. 2004). This generalized trend has been attributed to the limestone being a

more porous, adsorptive aggregate with relatively higher SSA as compared to other aggregates used in asphalt mixtures. It is also generally considered that the calcium bond with asphalt acids is relatively durable and strong (Little et al. 2006).

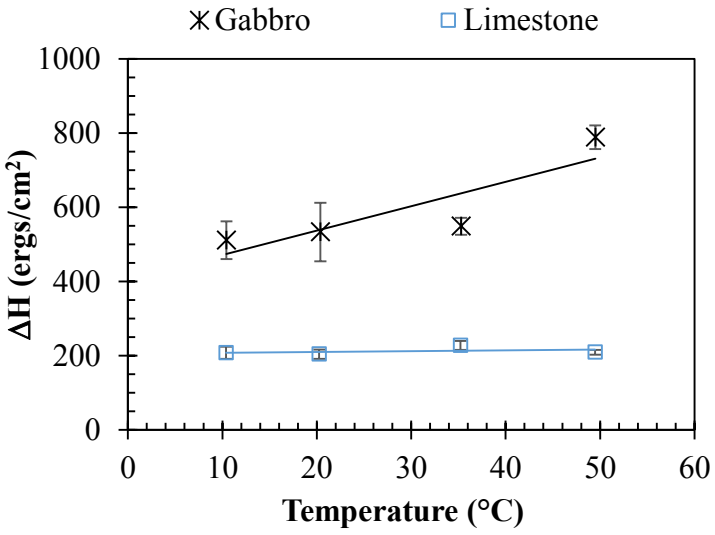

(a) Enthalpy of Immersion

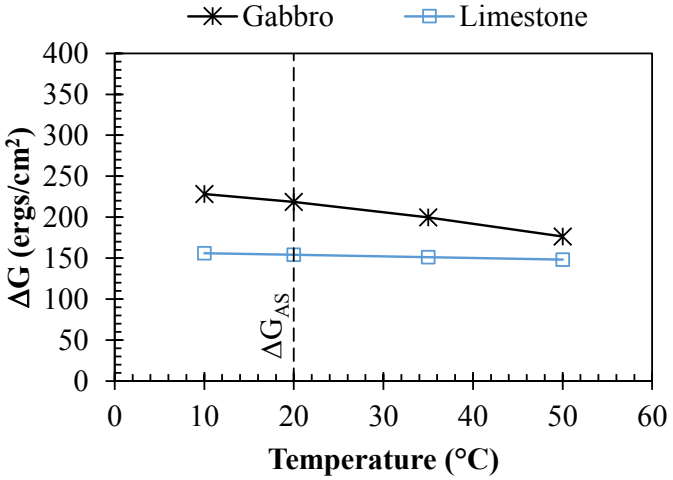

(c) Work of Adhesion ($\Delta G_{ref} = \Delta G_{AS}$)

Figure 35. Effect of aggregate type on ΔH and ΔG with temperature

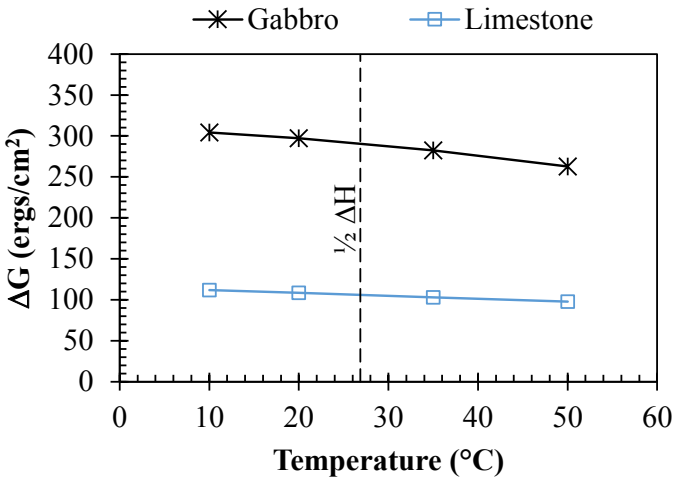

(c) Work of Adhesion (ΔG_{ref} = ½ ΔH_{300K})

Figure 35. Continued

The asphalt industry offers a wide range of technological alternatives for production of asphalt mixtures. In this study, the effect of common WMA additives on binder-aggregate adhesive properties was investigated. The enthalpy of immersion (ΔH) was measured and the temperature-dependent ΔG was calculated for all binder-aggregate pairs upon estimation of ΔG_{ref}. Results are presented in Figure 36, considering ΔG_{ref} = ΔG_{AS}, and in Figure 37, assuming ΔG_{ref} = ½ ΔH_{300K}. Results in Figure 36a and Figure 36b show the effect of common WMA additives on the binder-aggregate adhesive bond with gabbro and limestone aggregates, respectively. Figure 36 shows that inclusion of WMA additives modified ΔG over the 10°C to 50°C temperature range and that ranking prevailed for WMAs and control binders in combination with both aggregate types. The inclusion of WMA additive with adhesion promoter (Rediset) resulted in an overall increase in ΔG, while the inclusion of the wax (Sasobit) resulted in reduced ΔG. Additional comparisons can be made from the total loss in ΔG from 10°C to 50°C, reported in Table 11. All the

binder-gabbro combinations had a larger loss of ΔG compared to the limestone counterpart, with the largest reduction observed for the gabbro-Sasobit combination.

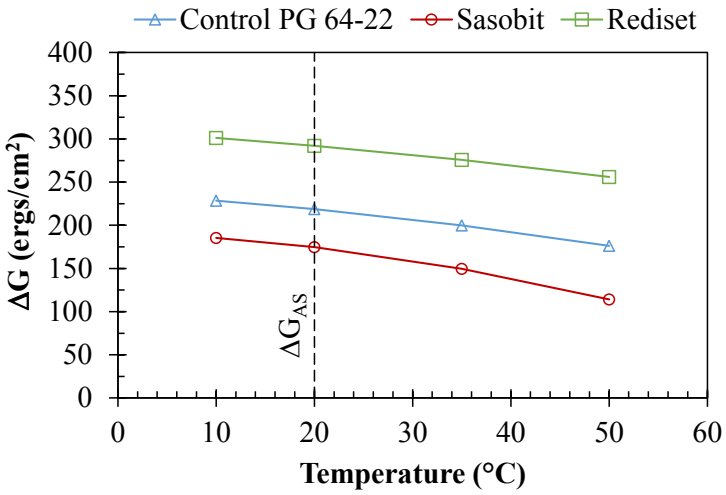

(a) Gabbro

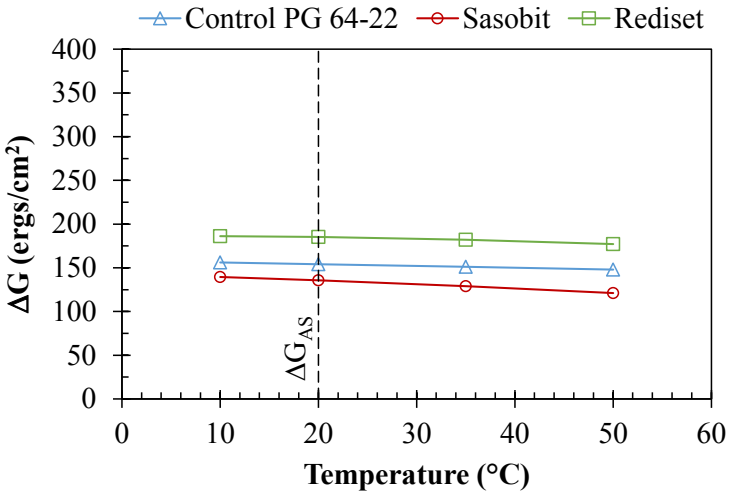

(b) Limestone

Figure 36. Effect of WMA additives ($\Delta G_{ref} = \Delta G_{AS}$)

Table 11. Loss in ΔG with increasing temperatures

ΔG_{ref}	Loss ΔG 10 to 50°C	Gabbro			Limestone		
		HMA	Sasobit	Rediset	HMA	Sasobit	Rediset
ΔG_{AS}	Total loss	52.1	71.4	45.3	8.0	18.4	9.0
	% loss	23%	38%	15%	5%	13%	5%
½ ΔH (300K)	Total loss	41.4	49.5	42.5	14.2	18.3	17.3
	% loss	14%	15%	13%	13%	13%	14%

Figure 37 shows the modeled ΔG with the assumption $\Delta G_{ref} = ½ \Delta H_{300K}$; in this case, both WMAs had higher ΔG over the temperature range in combination with both aggregate types. For the control PG 64-22 binder and the WMA Rediset, the rankings were comparable to those presented in Figure 36, while WMA Sasobit® showed an overall higher ΔG in combination with either aggregate type. Additional comparisons by considering the total loss in ΔG from 10°C to 50°C (Table 11) indicate that all the asphalt binder-gabbro combinations had a larger total loss of ΔG, but percentage-wise were comparable to those from the asphalt binder-limestone combinations.

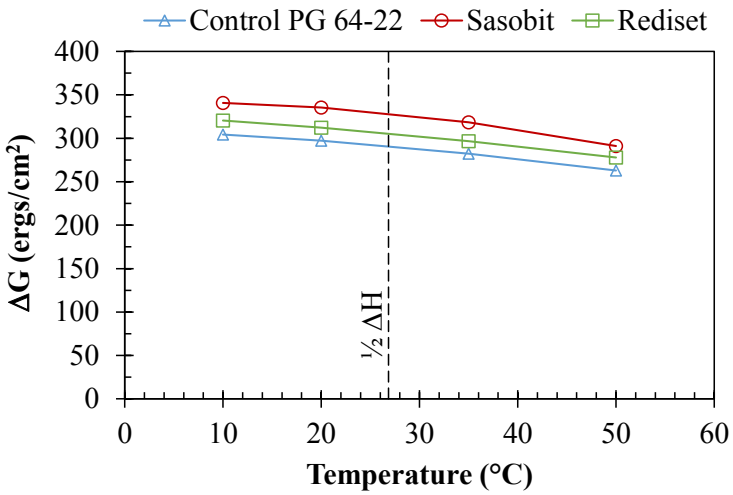

(a) Gabbro

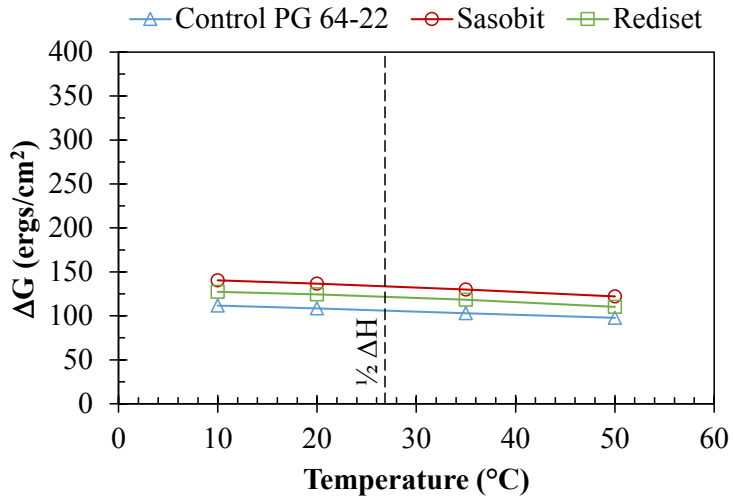

(b) Limestone

Figure 37. Effect of WMA additives ($\Delta G_{ref} = ½\ \Delta H_{300K}$)

It is clear that these two methodologies for estimating ΔG_{ref} may not necessarily provide comparable conclusions in terms of overall rankings, and the total magnitude of ΔG may differ. It is important to recall the advantages and disadvantages from both assumptions considered: (1) $\Delta G_{ref} = ½\ \Delta H_{ref}$ is an assumption that has been reported to be reasonable based on experimental measurements for minerals in combination with

different probe liquids by Doulliard et al. (1995). On the other hand, (2) $\Delta G_{ref} = \Delta G_{AS}$ corresponds to calculated values based on experimentally determined SFE components, which can be considered a more reasonable assumption. However, there are limitations from such an approach, given that binder-aggregate adhesion is calculated based on the van Oss–Chaudhury-Good theory considering only LW and acid-base interactions. In other words, each method has shortcomings (Bhasin and Little 2009). Further work is needed to accurately determine ΔG_{ref} , preferably by microcalorimetry experiments for ease and practicality.

4.2 Effect of Moisture at the Aggregate Interface

Aggregate hydrophilicity contributed to the potential for moisture to disrupt the binder-aggregate bond. ΔH and ΔG at 20°C for water-aggregate systems are significantly larger than ΔH and ΔG for binder-aggregate systems. Both aggregates evaluated in this study were hydrophilic. Figure 38 shows aggregate hydrophilicity evaluated by both microcalorimeter measurement (ΔH) and the acid-based theory calculating work of adhesion (ΔG), which were compared to ΔH and ΔG for a binder-aggregate systems. Gabbro (Figure 38a) had a much larger affinity for water compared to limestone (Figure 38b). This can be explained by the large polar SFE component for this aggregate type (Table 10). The inclusion of WMA additives may have impacted the binder-aggregate ΔG. However, the values were much smaller compared to the aggregate hydrophilicity, implying that it is thermodynamically favorable for water to displace or detach the binder film from the aggregate surface.

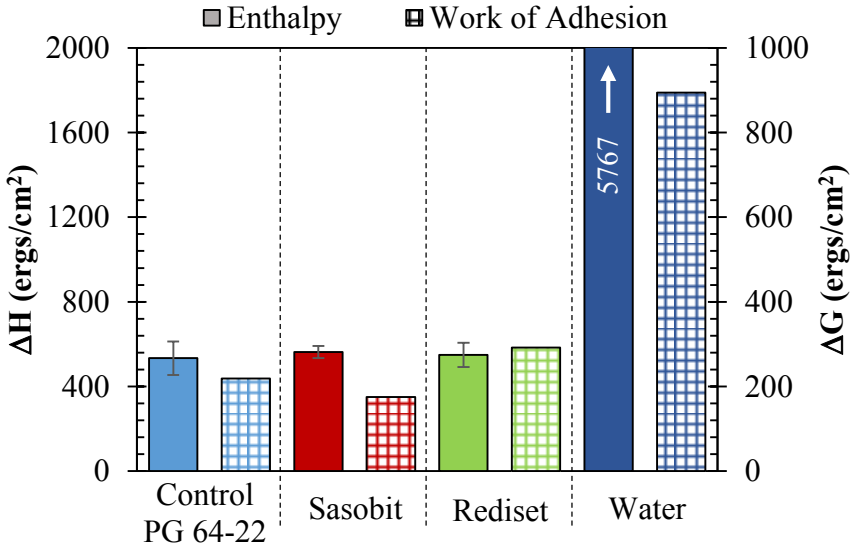

(a) Gabbro

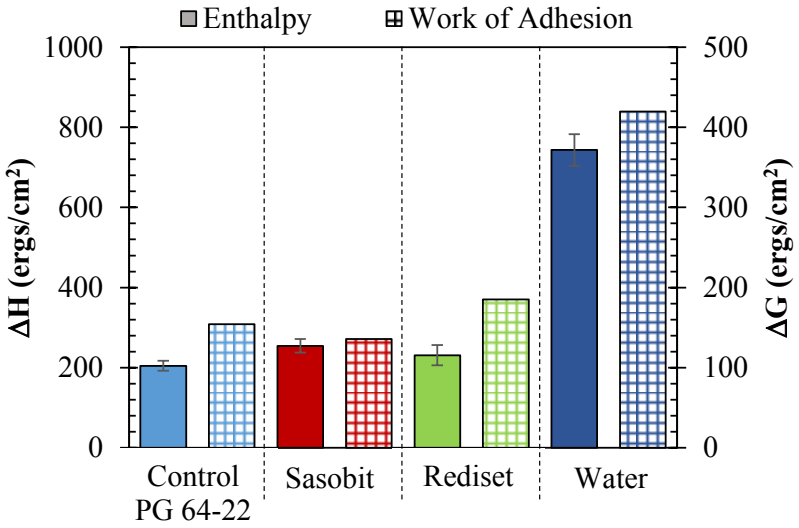

(b) Limestone

Figure 38. Water-aggregate affinity (20°C)

Results from measuring heat of immersion with aggregates preconditioned at a specified RH are presented in Figure 39. In the dry condition, the results were always exothermic, implying significant heat generated in the reaction cell upon contact between binder and aggregate fractions (Figure 39a and Figure 39d). Measurements conducted with aggregates conditioned at 33% and 76% RH were variable and inconsistent for both

aggregate types (Figure 39c and Figure 39d). The RH at which a monolayer of water is formed around the surface of an aggregate can be estimated based on USD measurements. For both aggregates, limestone and gabbro, a monolayer of water was already formed at 33% RH. The results observed in Figure 39c and Figure 39d can be interpreted as virtually zero energy transaction, implying there was no quantifiable adhesive bond when moisture was present at the binder-aggregate interface. One unusual observation was the endothermic reaction when binder solution was injected into aggregates conditioned at 100% RH (Figure 39e and Figure 39f). This observation implies greater heat produced in the reference cell than in the reaction cell. This kind of response is common when vaporization of water molecules occurs, as this removes heat from a system. The experimental data obtained in this study resulted as largely variable for the 100% RH condition.

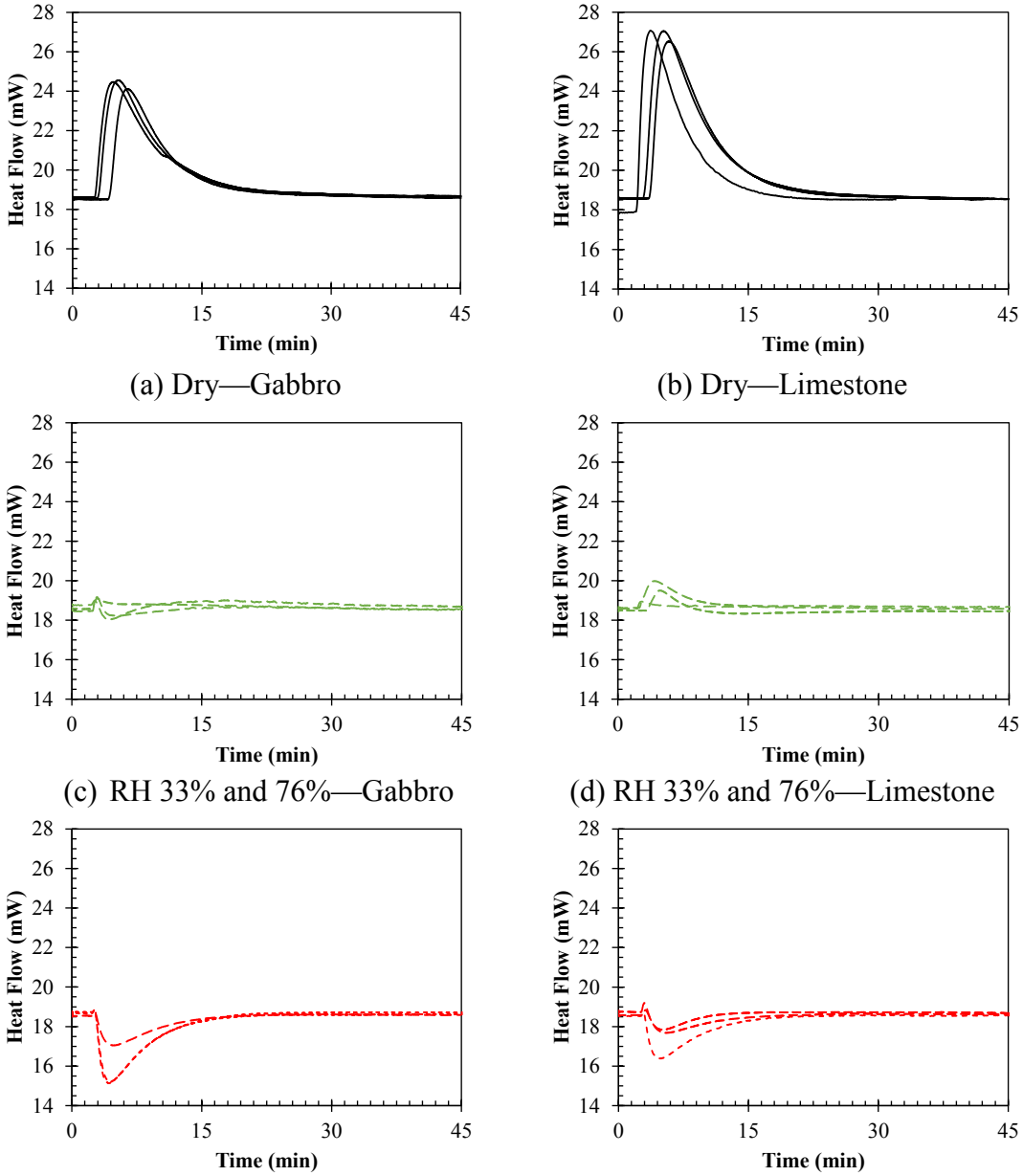

(a) Dry—Gabbro (b) Dry—Limestone

(c) RH 33% and 76%—Gabbro (d) RH 33% and 76%—Limestone

(e) RH 100%—Gabbro (f) RH 100%—Limestone

Figure 39. Enthalpy of immersion with moisture-conditioned aggregates

Moisture prevents binder-aggregate bonding, and the microcalorimetry technique provides an experimental means to measure and validate bonding (or lack of bonding). The endothermic reaction observed for aggregates conditioned at 100% RH could have

resulted from vaporization of free water molecules; nevertheless, the possibility of aggregate type having an impact on this value cannot be dismissed. Further research is recommended in order to confirm observations and conclusions regarding which variables contributed to the observed endothermic reaction.

4.3 Summary

This chapter presents an experimental procedure and analysis methodology capable of assessing the effect of temperature on the binder-aggregate adhesive bond and binder-aggregate bonding when a uniform layer of moisture surrounds the aggregate. The main findings of this study are as follows:

- The asphalt binder-aggregate adhesive bond decreases with increasing temperature, most likely due to the reduction in binder SFE. Adhesive bond strength reductions with temperature are dependent on the specific binder-aggregate combination.
- The assumption for ΔG_{ref} affects the overall ranking of the binder-aggregate bond for a particular binder-aggregate system and the total reduction of bond energy with increasing temperature.
- Type of aggregate has a greater influence on the adhesion-versus-temperature relationship, i.e., sensitivity to temperature than that from binder modification.
- A relative humidity of 30% or higher can inhibit formation of bonds between asphalt binder and aggregate surface. The experiments regarding aggregate hydrophilicity based on enthalpy of immersion are consistent with the predicted

bond strength based on SFE measurements and calculated water-aggregate work of adhesion (ΔG).

The literature reports mixtures with limestone aggregates to be more resistant to moisture damage (Parker Jr and Wilson 1986, Hunter and Ksaibati 2002, Birgisson et al. 2004). This generalized trend can be attributed to strong bonding between the calcium in limestone and the acids in asphalt binders (Little et al. 2006). Additionally, the relatively open surface morphology and higher SSA allow more binder to be adsorbed and strongly bonded to the aggregate surface by interfacial adhesion and mechanical interlock. Based on the experimental results from this study, it is also possible that the binder-aggregate bond for limestone materials is less susceptible to temperature changes, adding to the benefits previously identified. The end result is a reliable mixture that is highly resistant to moisture damage.

Knowing that the binder-aggregate adhesive bond changes over the range of in-service temperatures and that particular binder-aggregate combinations may contribute to larger variations of ΔG with temperatures, local climate conditions should be considered when evaluating moisture susceptibility of asphalt mixtures. For example, if the main concern for a specific location is a hot and rainy summer, it would be reasonable to utilize a test such as the Hamburg Wheel Tracking Test in order to evaluate potential for moisture damage. Conversely, for extremely cold weather, experiments involving freezing cycles may be more accurate in ranking mixtures comparably to field experience.

CHAPTER V

AGE-HARDENING OF ASPHALT MIXTURES AND BINDERS

This chapter describes the evolution of the linear viscoelastic (LVE) response of asphalt mixtures and binders as they undergo age-hardening. The experimental plan considered 20 asphalt mixtures at three aging conditions. Asphalt binders were extracted and recovered from eight mixtures at two aging conditions in order to conduct rheological and chemical characterization, as previously detailed in Section 2.3.3. Additionally, mixture and binder age-hardening processes were compared to changes in binder chemistry.

5.1 Age-Hardening of Asphalt Mixtures

The aging state variable (A) was utilized in this study to compare the age-hardening effect on various asphalt mixtures, including two aggregate sources, two binder types, and four WMA technologies, as previously described (Figure 17). Age-hardening of mixtures with gabbro aggregates after 3 months and 6 months at 60°C is presented in Figure 40. Results show that after 3 months and 6 months, the PG 64-22 HMA control binder experienced greater age-hardening than most of the WMA, except the foaming technology. For binder PG 76-22, all WMA mixtures showed more age-hardening as compared to the HMA counterpart.

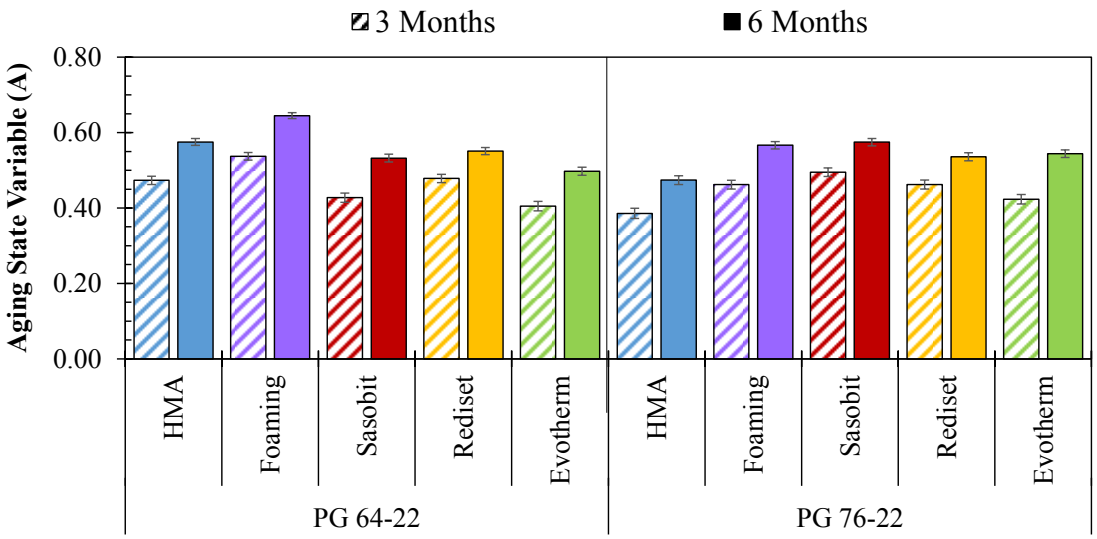

Figure 40. Age-hardening of gabbro mixtures

For the limestone mixtures (Figure 41), WMA technologies experienced greater age-hardening effect than the corresponding HMA counterpart at 3 months and 6 months of laboratory aging, with either binder type.

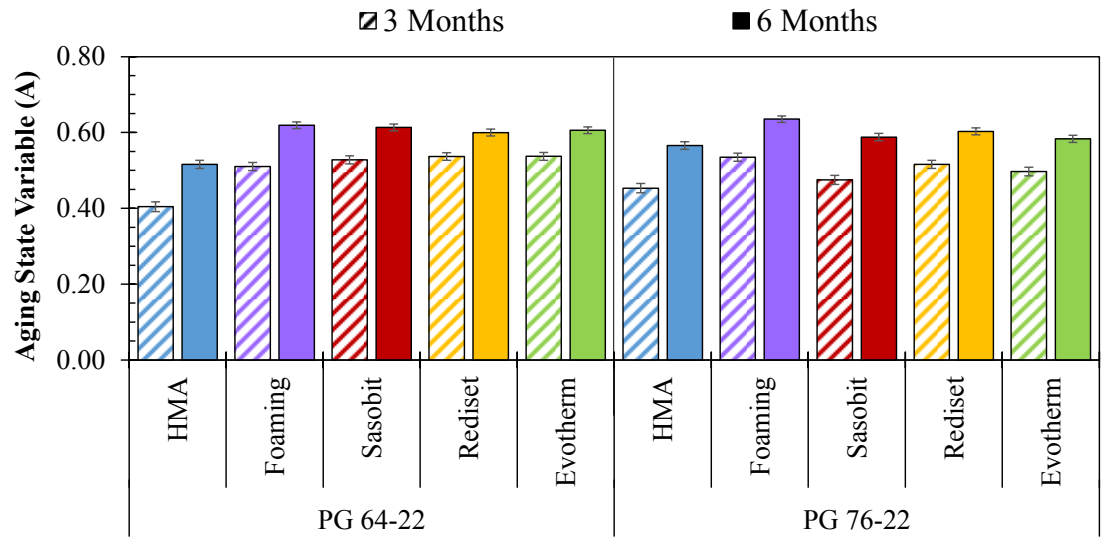

Figure 41. Age-hardening of limestone mixtures

Three main variables were considered for comparison within the mixtures and aging conditions presented in Figure 40 and Figure 41: (1) aggregate type, (2) binder PG, and (3) WMA versus HMA. Using the calculated 95% CI, conclusions resulted as following:

1) Limestone versus gabbro: Considering the 10 technological variables and the two aging conditions (3 months and 6 months), in 14 of 20 cases (70%) the mixtures with limestone aggregate experienced greater age-hardening as compared to those with gabbro aggregates.
2) WMA versus HMA: Considering the four WMA alternatives, both binder types, both aggregate types, and the two aging conditions, 24 of 32 WMA mixtures (75%) experienced more age-hardening than the HMA counterpart.
3) PG 64-22 versus PG 76-22: No clear trend was observed. These binders were of the same crude source, so they may have exhibited similar aging characteristics. Discussion regarding binder chemistry follows in the next section.

WMA may exhibit an initially faster stiffening effect with aging as compared to HMA, but these may be comparable in the long-term (Yin et al. 2014b). To better discriminate among possible initial differences overcome at relatively early aging stages, the change in A from 3 months to 6 months was evaluated for all mixtures. It can be observed in Figure 42 that, with both limestone and gabbro aggregates, the change in A was proportional (or smaller) for WMA as compared to the HMA counterpart in most cases. Also, the limestone mixtures did not necessarily continue to have increased age-

hardening as compared to gabbro. In the first 3 months, WMA mixtures might have experienced more significant stiffening effect than the HMA counterpart, especially in combination with the limestone aggregate, which may change in the long-term.

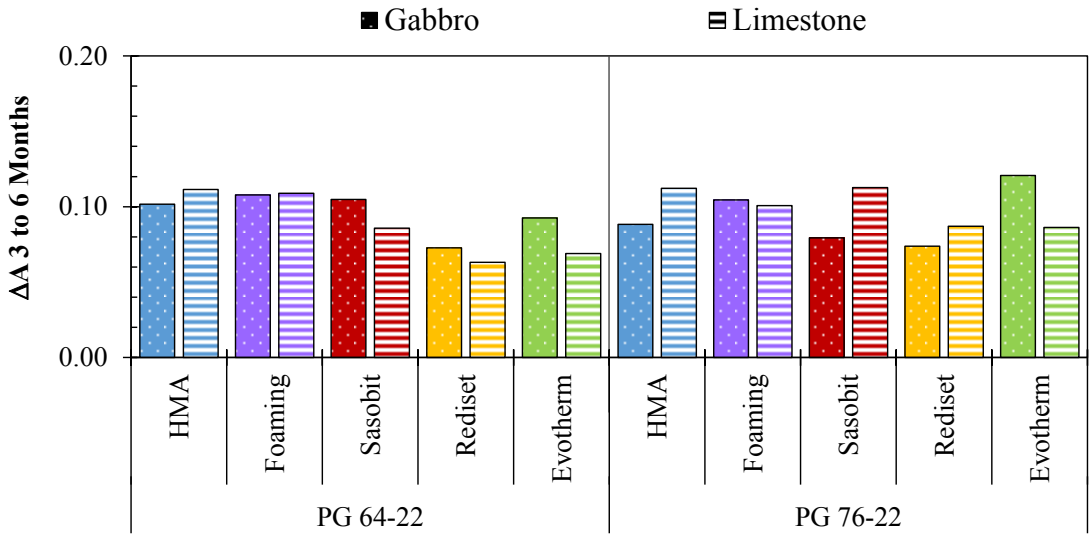

Figure 42. Age-hardening from 3 months to 6 months

It is important to recall that age-hardening effect was captured from the initial condition of each mixture using the aging state variable (A). Previous research states that WMA may be softer than HMA at the initial stage due to lower production temperatures (Yin et al. 2013), but with time WMA reaches stiffness levels of HMA and may continue to stiffen equivalently for most cases (Yin et al. 2014b, Newcomb et al. 2015). The initial lower stiffening may be caused mainly by two situations: (1) reduced binder age-hardening due to lower production temperatures or (2) reduced binder absorption at an early stage for WMA. It has been reported that the reduced mixing temperatures in WMA are not a determining factor contributing to the initial stiffness of the mixture, but curing temperature has a much greater impact (Newcomb et al. 2015). Lower binder absorption

has been identified at an early stage for WMA, but absorption continues to occur in WMA with extended curing times, affecting performance properties (Estakhri et al. 2010). Part of the stiffening or age-hardening effect in WMA can be possibly explained by changes in the binder, but especially at early stages the age-hardening process can be explained by changes in a binder-aggregate interphase region. The mechanical characteristics of this interphase may depend on binder-aggregate interfacial bonding (interstitial forces at boundary of two ideal surfaces, i.e., an interface) and mechanical interlock, provided mainly by microtextural features of the aggregate and effective surface area of binder and aggregate in contact. Within the asphalt mixture, the interphase occupies a volume and possesses mechanical properties different from those of binder or aggregate (Garcia Cucalon et al. 2016b). Note that the concept of the interphase as referred to in this study does not consider long-term chemical reactions; such a scenario has been previously disproved based on experimental measurements by Curtis et al. (1991).

Figure 43 illustrates an idealized interphase of an asphalt mixture at the initial condition (a) and after aging (b). At the initial condition (Figure 43a), it is expected that the binder has coated all the aggregate surface upon mixing and there should be some level of mechanical interlock between binder and aggregate, but it is possible that the binder hasn't reached every irregularity of the aggregate surface. With time and temperature (Figure 43b), the binder is expected to keep flowing into the aggregates' microtextural features or diffuse into the aggregate in the case of selective absorption. The differences reported in this study for WMA versus HMA and limestone versus gabbro aggregates could be possibly explained with understanding the interphase and its evolution.

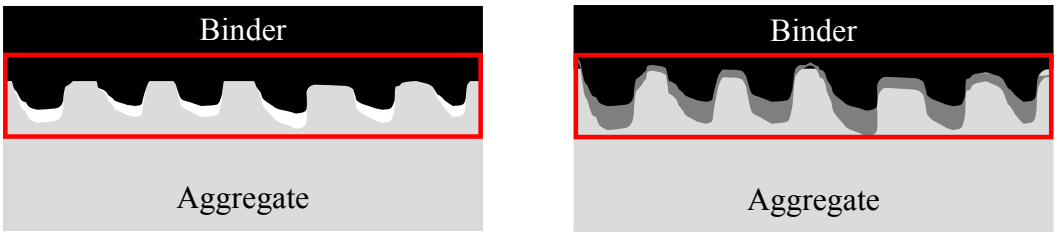

(a) Initial condition (b) With time/temperature

Figure 43. Depiction of the interphase with age-hardening

Figure 44 presents photographs of small aggregates compared to aged mixtures taken under natural and ultraviolet (UV) light. Due to the dark color of the gabbro aggregate, it was impossible to distinguish binder from rock under natural or UV light (Figure 44a). For the limestone aggregate, absorption was extremely evident after 6 months of aging, reaching the small aggregate entirely (Figure 44b). It is reasonable to attribute part of the age-hardening effect observed in the asphalt mixtures to changes in the binder-aggregate interphase region, so it is important to quantify the age-hardening effect of the asphalt binders.

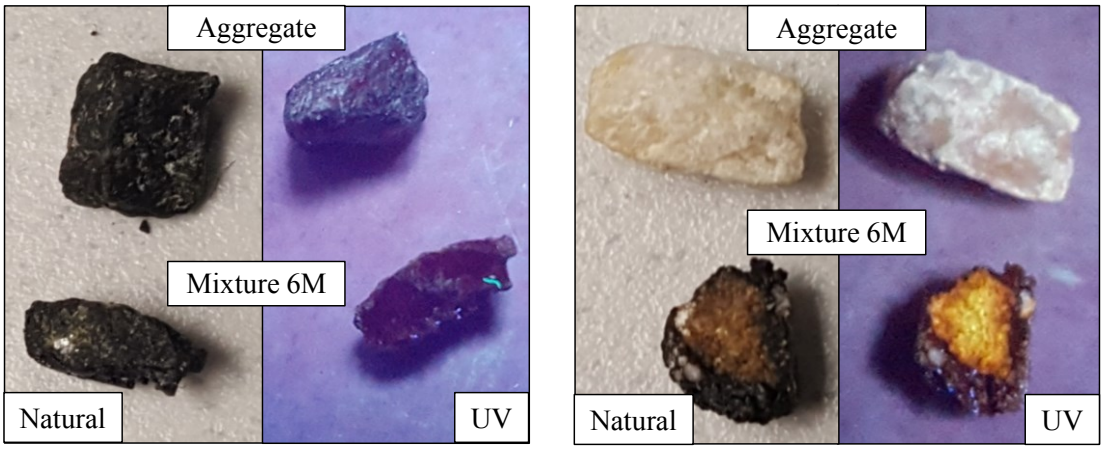

(a) Gabbro (b) Limestone

Figure 44. Visual comparison of aggregate absorption under natural and UV lights

5.2 Age-Hardening of Asphalt Binder

Asphalt binders undergo chemical and mechanical changes due to oxidative aging that affect the asphalt mixture. The previous section quantifies age-hardening of 20 asphalt mixtures; this section quantifies the age-hardening effect of asphalt binders extracted from eight of those asphalt mixtures after aging for 3 months and 6 months at 60°C. The aging state variable A_1 was fitted to modify the compliance (Equation (8)) and retardation times (Equation (9)) using the storage compliance (J') Equation (33). Upon fitting A_1, A_2 was fitted to modify the viscosity of the dashpot (Equation (45)) using the loss compliance (J") Equation (34). The aging state variable A_1 accounted for the changes in the compliance and retardation times of the Kelvin elements, while A_2 modified the viscosity of the dashpot in Equation (45).

Figure 45 shows the age-hardening effect on asphalt binders extracted from aged mixtures and for binders after standardized short- and long-term laboratory aging protocols. With consideration of both aging state variables A_1 and A_2, comparisons were made considering the extracted binders in terms of (1) aggregate type, (2) binder PG, and (3) WMA versus HMA. Analogous to the comparisons presented for the asphalt mixtures, conclusions resulted as follows:

1) Limestone versus gabbro: PG 64-22 control and Rediset binders aged more in combination with gabbro aggregate, while PG 76-22 aged more within the limestone mixtures after 3 months and 6 months of aging.
2) WMA versus HMA: For seven of eight combinations, WMA binder did not age more than HMA.

3) PG 64-22 versus PG 76-22: PG 76-22 experienced more age-hardening in combination with either aggregate type.

The conclusions obtained based on binder age-hardening were not in agreement with those obtained from mixture age-hardening, suggesting that binder age-hardening is not the exclusive factor affecting age-hardening of asphalt mixtures.

Figure 45 also shows that the changes in A_2 were greater than the changes in A_1 for all cases. The A_2 parameter (Figure 45b) presented in this study is capable of quantifying changes in viscosity of the Maxwell dashpot (Figure 13b), representative of binder rheology at 20°C and a large range of frequencies. Comparing alternative asphalt technologies, the polymer-modified PG 76-22 binder showed the largest increase in A_2 under all aging processes. The WMA Sasobit experienced a larger increase in A_2 with RTFOT aging as compared to the control PG 64-22 binders. With extended aging protocols, Sasobit experienced relatively smaller changes in A_2 as compared to the other binders. A previous study in microstructural characterization using atomic force microscopy (AFM) of asphalt binders with aging concluded that binder including 3% Sasobit WMA additive does not exhibit changes in microstructure after long-term aging (Menapace et al. 2015). The binders in Menapace's study correspond to the PG 64-22 (Pen 60/70) and PG 76-22 in this study.

Evaluating the effect of aging method for each technological alternative, it was observed that the control PG 64-22 and the Rediset binders showed greater hardening effect after 6 months of aging in the gabbro mixtures, while the Sasobit and the polymer-modified PG 76-22 had greater age-hardening in combination with the limestone

aggregates after 6 months of aging. In general, the PAV aging resulted in an age-hardening effect somewhere between 3 months and 6 months of mixture aging at 60°C.

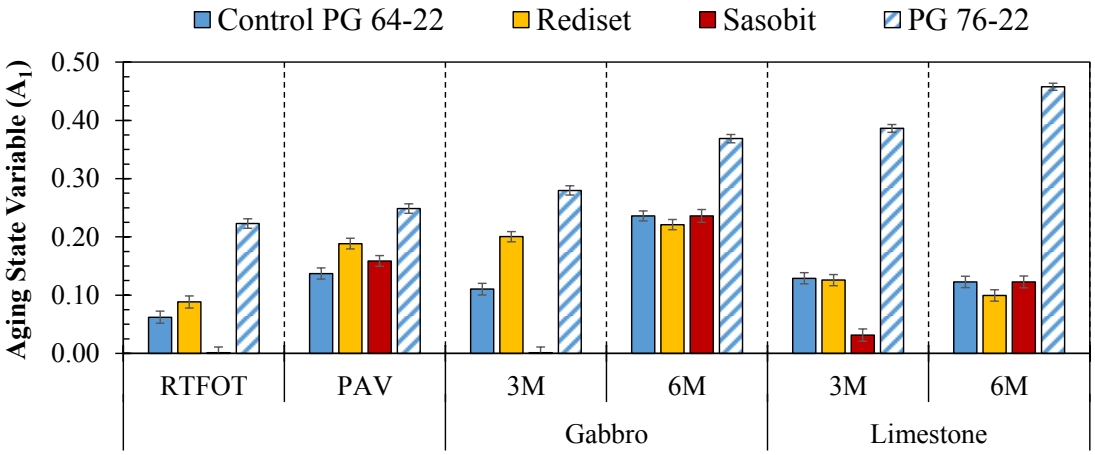

(a) A_1

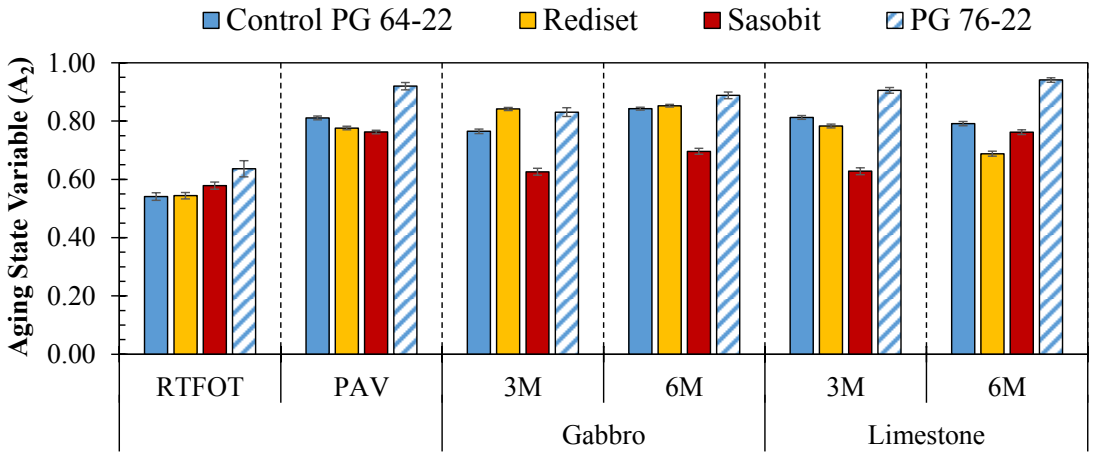

(b) A_2

Figure 45. Aging state variable for asphalt binders

The parameters A_1 and A_2 provided information about the changes in storage (J') and loss (J") compliances independently. For ease in visualizing a global age-hardening effect, the change in dynamic shear modulus with aging was evaluated by the use of an aging index (ratio of dynamic shear modulus before and after aging) at two different

temperatures representative of high and intermediate pavement temperatures (60°C and 20°C). The aging index at 60°C is presented in Figure 46a, where the PAV aging protocol showed that binder modifications (i.e., WMA and polymer) resulted in equivalent or improved aging characteristics, with the largest reduction in aging index attributed to the inclusion of polymer. On the other hand, the binders extracted from the laboratory-aged mixtures showed largely varying aging indexes depending on the binder-aggregate combinations, highlighting the possible impact of the aggregate in binder age-hardening. For an instance, the control PG 64-22 and Rediset binders had a more significant stiffening effect in combination with the gabbro aggregates after 6 months, while the PG 76-22 stiffened the most in combination with the limestone aggregates after 6 months. The aging index at 20°C (Figure 45b) provided similar conclusions as the 60°C aging index for rankings of the PG 64-22 control and WMA binders, while the PG 76-22 had a relatively larger aging index at 20°C (can be explained by the increased A_1). Considering both aging indexes, WMA Sasobit exhibited the least aging within the mixtures in combination with both aggregate types after 3 months and 6 months.

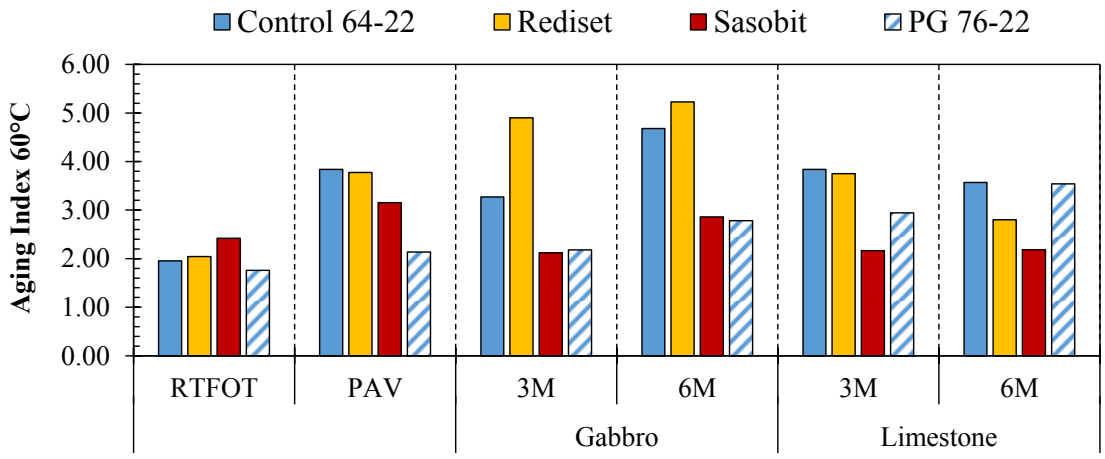

(a) | G* | ratio at 60°C, 10 Hz

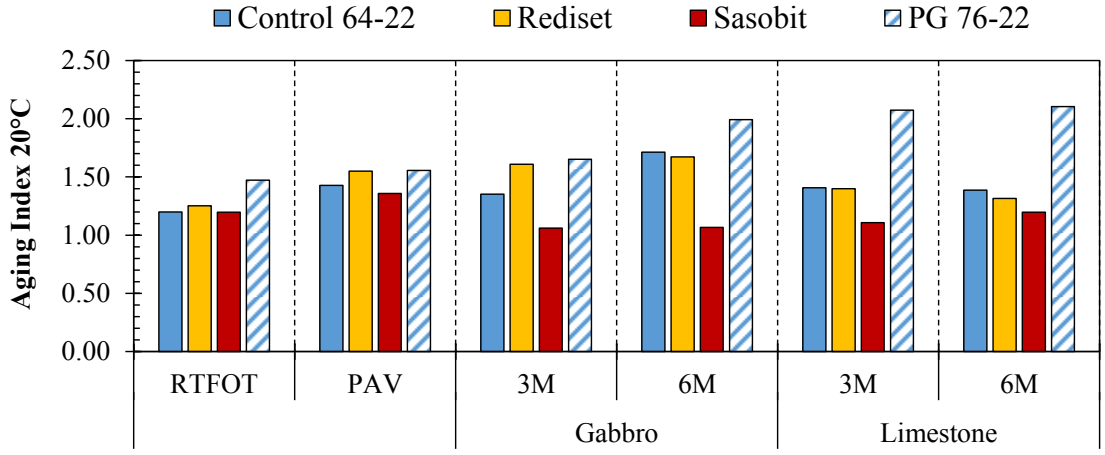

(b) | G* | ratio at 20°C, 10 Hz

Figure 46. Aging index

Within asphalt literature, it is common to find various adjectives to describe changes in mechanical behavior of asphalt mixtures and binders over time (e.g. aging, age-hardening, embrittlement, stiffening, loss of ductility). The principal concern with aging is excessive pavement cracking, which is promoted not solely by increased stiffness, but by embrittlement of the asphalt binder (and subsequently mixture) with time. The GR parameter was proposed to address the issue of binder embrittlement and was used in this study for comparison purposes; results are presented in Figure 47. The data were plotted

in the black space and were compared to the empirically determined damage thresholds (Figure 47a), from which it can be said that none of the aging protocols considered in this study were sufficient to degrade the binder to the extent of reaching the damage region. It is becoming a common practice to compare binders in terms of how much aging it takes for a specific binder-additive combination to fall into the damage region; such comparison was not possible within this study. From Figure 47a, it can be observed that none of the WMA additives altered the "path" for binder aging, while the polymer modification significantly modified the rheological properties of the binder (as expected). It is important to recall that the damage regions were defined empirically for neat binders; therefore, binders involving polymer modifications could not be evaluated by this approach. To address the effect of aggregate type and inclusion of WMA additives, the GR is presented as a bar graph in Figure 47b, where a material expected to be more susceptible to cracking would show higher numbers. The WMA Sasobit binder exhibited the highest GR at all aging conditions, while Rediset showed the lowest in most cases. WMA Sasobit was always portrayed as the less aging-susceptible binder, with the smallest A_1 and A_2 (Figure 45) and the smallest aging indexes (Figure 46). It is important to highlight that the inclusion of the Sasobit resulted in significantly stiffer binder at the original condition, which explains the apparent lack of agreement between the approaches considered.

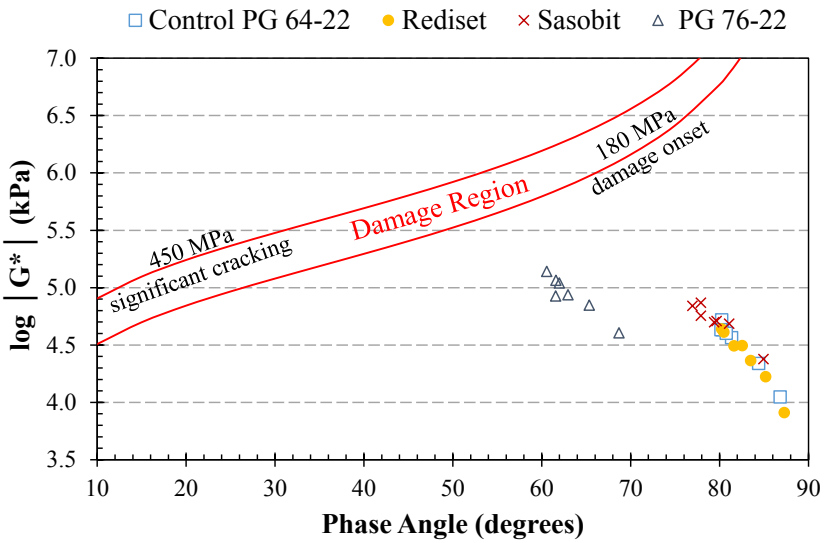

(a) Black-space diagram

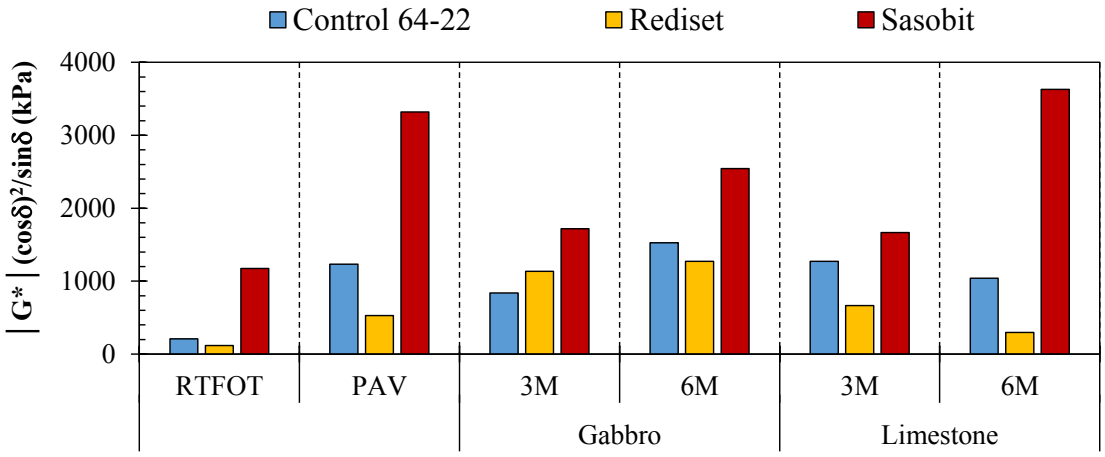

(b) $|G^*|(\cos\delta)^2/\sin\delta$

Figure 47. GR parameter

5.3 Binder Chemistry

The previous section characterizes the age-hardening of 20 asphalt mixtures and eight binders extracted from those mixtures. In this portion of the study, a qualitative chemical was presented based on FTIR measurements considering the extracted binders and laboratory-aged materials, including technological alternatives such as the control PG

64-22, WMA Rediset, WMA Sasobit, and polymer-modified PG 76-22. The Rediset and Sasobit modifications were performed by the author in the laboratory by mixing the control PG 64-22 binder with 0.5% Rediset and 2% Sasobit over the weight of binder. The polymer-modified PG 76-22 binder was modified at the terminal (Woqod—Middle East). Both binders PG 64-22 and PG 76-22 were received from the same provider; comparing the FTIR spectra (Figure 48), it is a reasonable assumption that both PG 64-22 and PG 76-22 were of similar chemical nature, possibly from the same crude source. Figure 48 presents the FTIR spectra for both binders, showing differences at 995 cm^{-1}, 967 cm^{-1}, 910 cm^{-1}, 748 cm^{-1}, and 699 cm^{-1}, which can be attributed to the addition of SBS polymer (Table 6). Based on these results, binders PG 64-22 and PG 76-22 were treated as being of the same nature, with a difference of the polymer modification for PG 76-22. Literature on asphalt aging commonly reports that the most significant differences in binder age-hardening and oxidation are found within binders from different crude sources; such a variable was not included in this study. The focus of this chapter is to determine the impact of binder modification and aggregate type in the age-hardening process of asphalt mixtures.

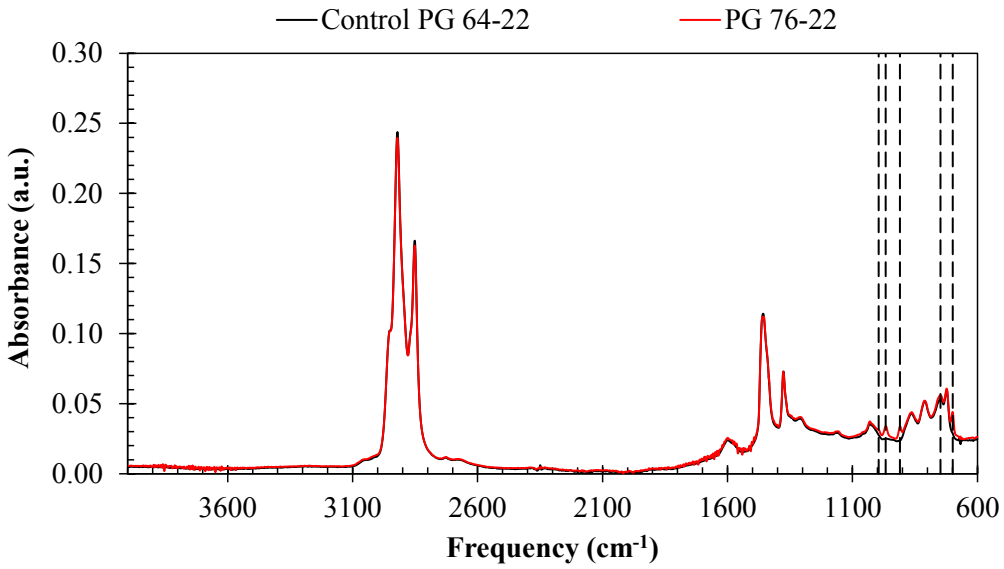

(a) Full Spectra

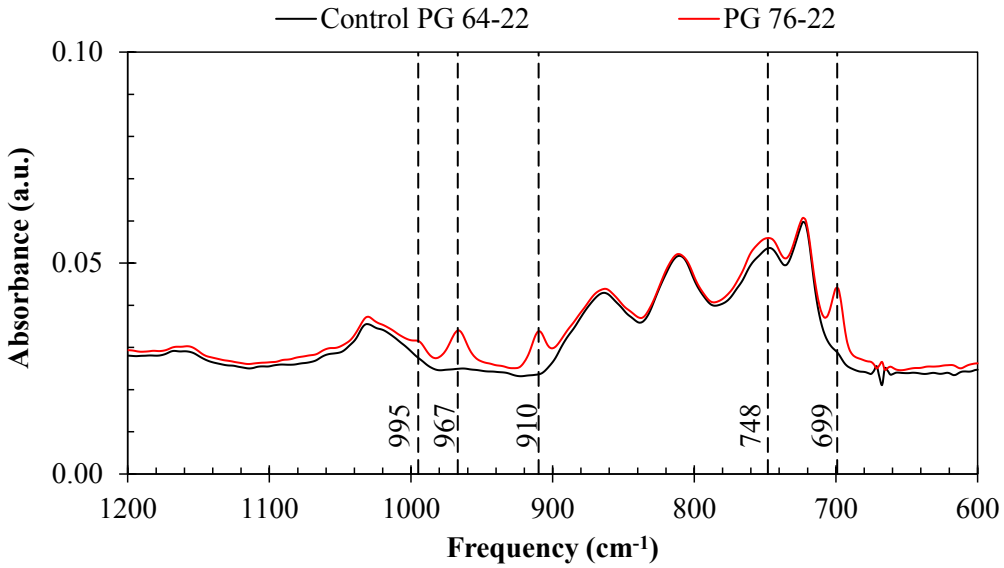

(b) 1200 cm^{-1} to 600 cm^{-1}

Figure 48. FTIR spectra for binders PG 64-22 and PG 76-22

The most common parameter to quantify binder oxidation and kinetics is the CA, which represents the increase in oxidation products containing carbonyl groups (e.g., ketones and carboxylic acids). CA results are presented in Figure 49; the bar graphs

present the average value from two replicates, while the average difference is presented as error bars. The binder PG 64-22 with WMA Rediset had the largest CA before aging, which could possibly be introduced by the composition of the chemical additive. From original to RTFOT aging, all binders observed minimum changes in CA. After PAV aging (implying RTFOT plus 20 hours PAV aging), all binders observed a clear increase in CA, with Rediset having the largest CA. Considering the asphalt binders extracted from mixtures after 3 months and 6 months of aging, 3 months of aging with either limestone or gabbro rendered comparable results, except for WMA Sasobit, which had a larger CA in combination with the gabbro aggregate. After 6 months of aging, most binders aged within the gabbro aggregates had a larger CA, except for the polymer-modified PG 76-22, which continued to age similarly with either aggregate type. Based on previous research studies, it is possible that iron and aluminum ions present on the surface of the gabbro (Table 3) could be catalyzers for binder oxidation (Petersen 1974, Petersen 2009, Wu et al. 2014). The PAV aging resulted in binders with similar or lesser CA than that of binders extracted after 3 months of aging in the mixtures.

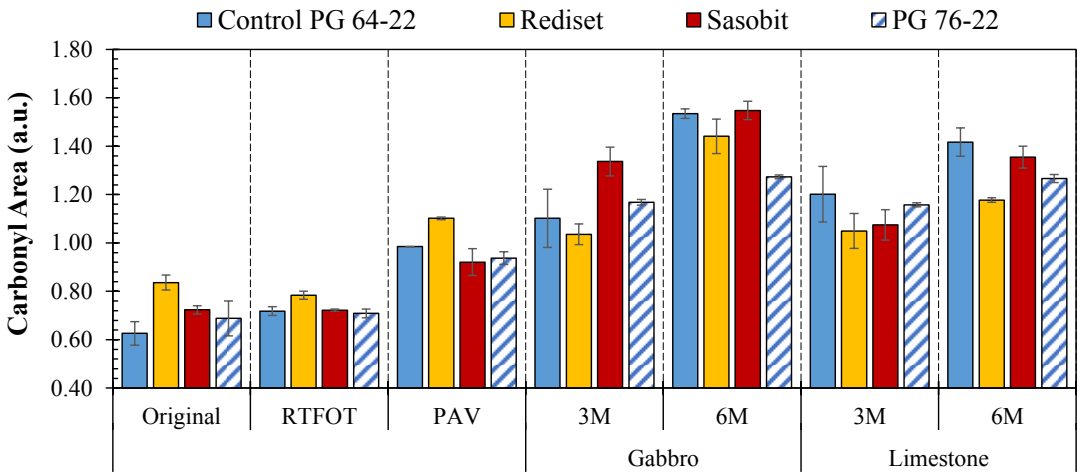

Figure 49. CA

Another oxidation product commonly considered in evaluating binder aging is sulfoxide, which peaks at a frequency around 1030 cm^{-1} on the FTIR spectrum. Several research studies have highlighted the importance of considering sulfoxide formation to quantify binder aging and oxidation kinetics (Petersen and Harnsberger 1998, Petersen and Glaser 2011). The sulfoxide peak for all binders evaluated within this study are summarized in Figure 50. Minor changes were observed in the height of sulfoxide peaks after RTFOT and PAV aging. Significantly larger sulfoxide peaks were observed for the extracted binders, especially in combination with limestone aggregates after 3 months and 6 months. It was previously discussed that carbonyl formation may occur faster when the binder is adjacent to the gabbro aggregates, possibly due to a catalytic effect, while the opposite trend is observed in terms of sulfoxide formation. It is important to highlight that limestone materials are highly absorptive, which could also alter the oxidation process.

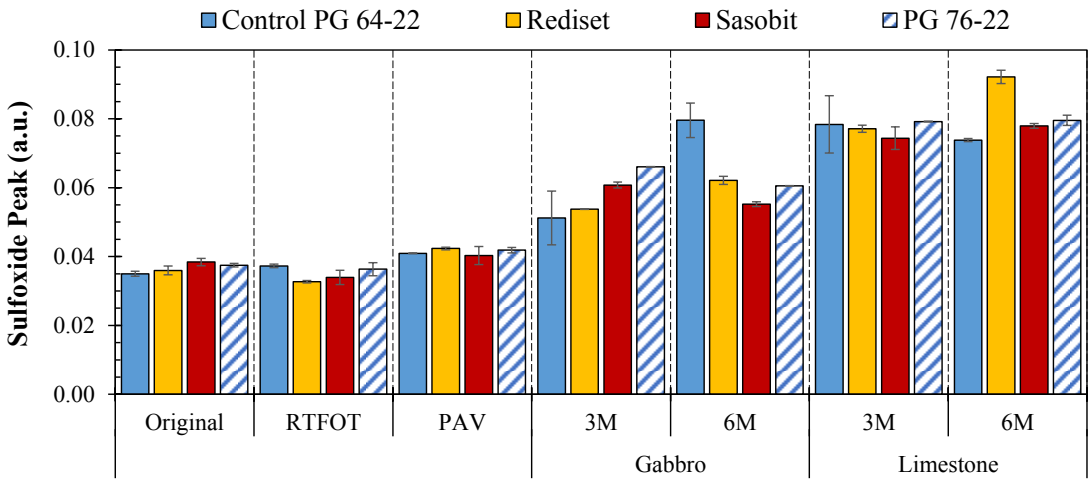

Figure 50. Sulfoxide peak

Literature on asphalt binder oxidation mechanisms has reported that ketones (identified in FTIR spectra by CA increase) are formed mainly from benzylic carbon chain reactions (Petersen 2009). Elevated temperatures increase the molecular mobility of these highly polar moieties, promoting oxidation and ketone formation, while at lower temperatures these are highly associated and not so readily oxidized. On the other hand, sulfides (while available) are highly reactive with hydroperoxides to form sulfoxides, a reaction likely to occur at lower temperatures (Petersen 2009). In this study, the aging of asphalt mixtures was conducted at 60°C to be consistent with realistic pavement aging temperatures. This relatively lower aging temperature can explain the increased sulfoxide peaks observed in the binders extracted from aged mixtures as compared to the RTFOT- and PAV-aged binders. Petersen (2009) also summarized how, after the initial spurt, sulfoxides and ketones can be formed from the same precursor, hydroperoxides. Sulfoxides are most probably formed from the reaction of akylarylhydroperoxides with asphalt sulfides, which is promoted by the presence of acidic molecules. Additionally,

decomposition of hydroperoxides provides an alternate route for ketone formation, which can be induced by a catalytic amount of metal ions or a basic reaction medium (Petersen 2009). The gabbro aggregates considered in this study contained significant amounts of iron and other metals (Table 3), which could catalyze hydroperoxide decomposition and ketone formation, as stated in previous studies. If more hydroperoxides are decomposed and ketones are formed, then less hydroperoxides would be available to react with sulfides and forming sulfoxides. It is reasonable to calculate a carbonyl-to-sulfoxide ratio based on peak height in order to evaluate this possibility; the higher this carbonyl-to-sulfoxide ratio, it could be inferred that more hydroperoxides have been decomposed into ketone formation due to the aggregate's catalytic effect. Results are presented in Figure 51, confirming that binders aged in gabbro mixtures had a higher production of carbonyl (very likely ketones) than sulfoxides.

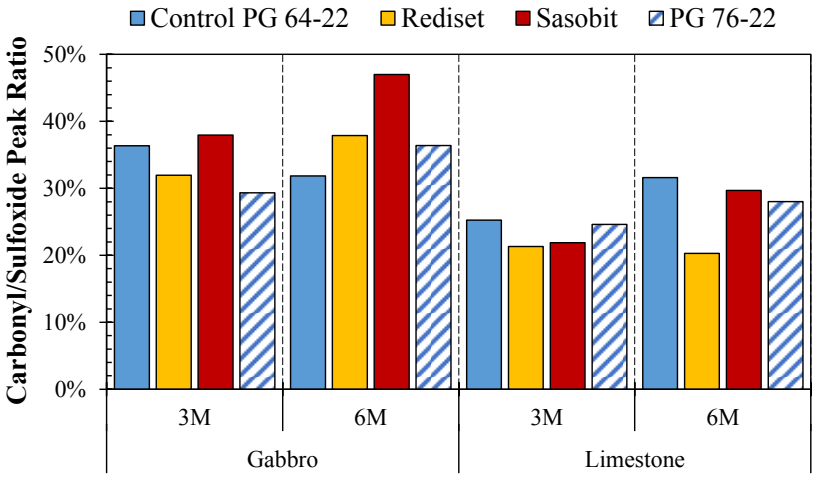

Figure 51. Carbonyl-to-sulfoxide ratio

Given the binder modifications and different aggregate types introduced in this aging study, it was considered important to "scan" through the FTIR spectra for changes in binder chemistry outside of the commonly studied carbonyl and sulfoxide formation. Regarding the binder modifications, it was found that the peaks corresponding to the presence of polymers (Table 6) changed with aging. The FTIR peaks at 995 cm^{-1}, 967 cm^{-1}, 910 cm^{-1}, and 699 cm^{-1} corresponding to the polymer-modified binder were found to change with aging (Figure 52). All these polymer peaks increased with short-term aging (RTFOT) and exhibited minor changes after further PAV aging or materials extracted from aged mixtures. Peak 967 cm^{-1} fell in an area of baseline upshift for the extracted materials, limiting conclusions beyond PAV aging. A previous study by Cortizo et al. (2004) reported that, during the degradation of process of polymer-modified asphalt (with SBS copolymer), free radical reactions produce chain scission and subsequent radical addition to some asphalt components; such a process would be a reasonable explanation for the changes in polymer peaks with aging. The increased absorbance in the FTIR peaks could be explained from chain scissions. From the mechanical evaluation of asphalt binder age-hardening, it was observed that the polymer-modified binder PG 76-22 experienced the largest increase in A_1, caused by the largest shift in the storage (elastic) component of the dynamic response with RTFOT aging. With further laboratory aging, changes in the mechanical response for the PG 76-22 followed a similar range as the PG 64-22 binders. This initial change in the PG 76-22 binder could be related to chemical changes in the polymer with short-term aging.

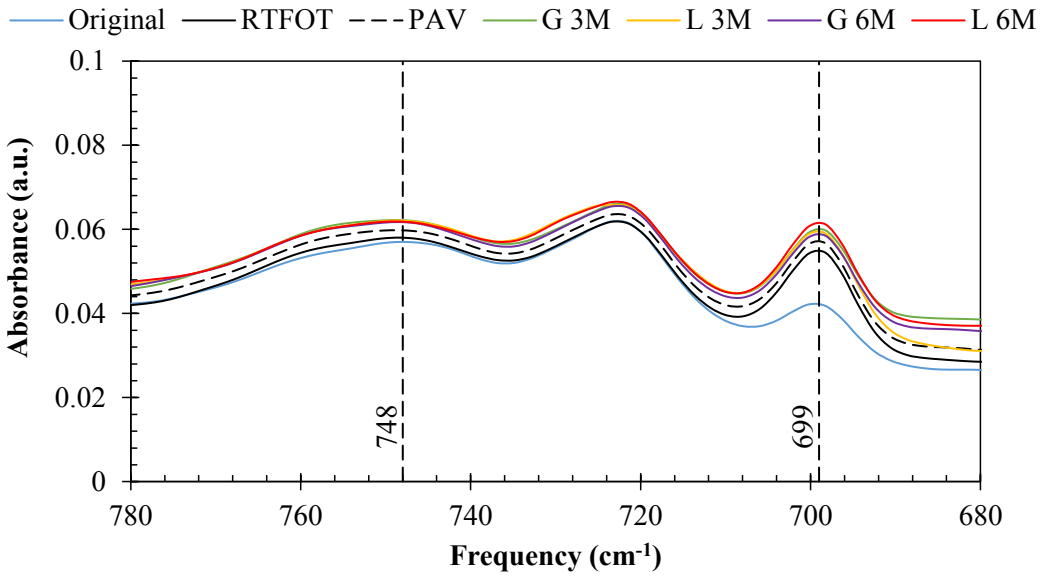

(a) Peaks at 748 cm^{-1} and 699 cm^{-1}

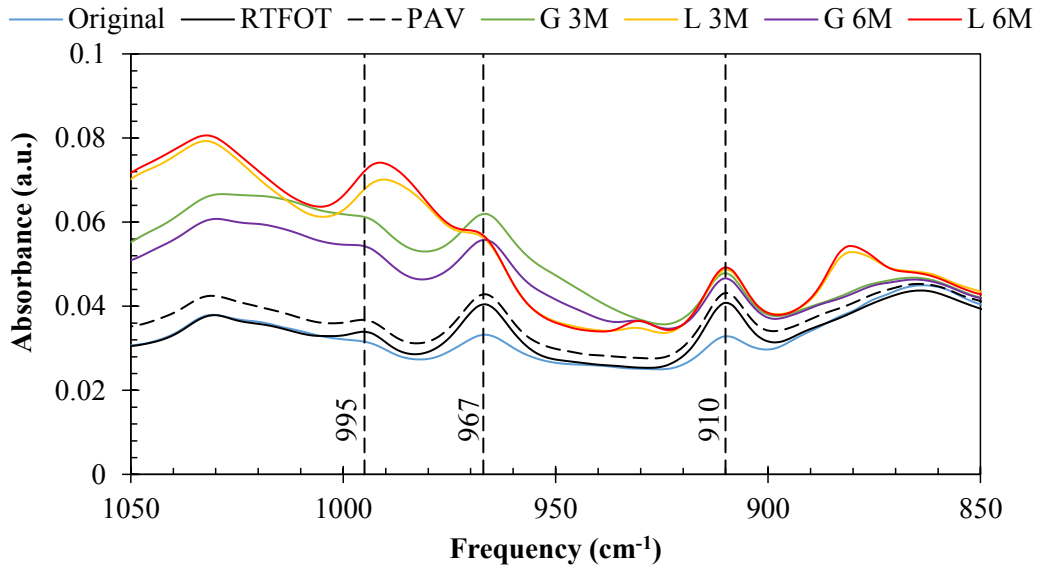

(b) Peaks at 967 cm^{-1} and 910 cm^{-1}

Figure 52. Polymer-modified binders with aging

Regarding the different aging protocols, including laboratory and mixture aging, variations were found, specifically for binders extracted from limestone mixtures. Figure 53 shows the peaks identified in this study around 880 cm^{-1}, 985 cm^{-1}, 1090 cm^{-1}, and

1120 cm^{-1}, exclusively for materials aged in limestone mixtures. Sulfur-containing compounds are found in the region from around 1000 cm^{-1} to 1320 cm^{-1} (Usmani 1997); it could be speculated that sulfur-containing compounds have formed when aging with limestone aggregates. Determining the nature of these compounds and chemical reactions leading to their formation could constitute a research project on its own. Additionally, the effect of such compounds on binder rheology and potential influence on the mechanical behavior of asphalt mixtures should be determined. From the data available within this study, it is clear that the peaks around 880 cm^{-1}, 985 cm^{-1}, 1090 cm^{-1}, and 1120 cm^{-1} increased with aging only within the limestone mixtures, regardless of binder modification. WMA Rediset exhibited the largest peaks, while WMA Sasobit had the lowest.

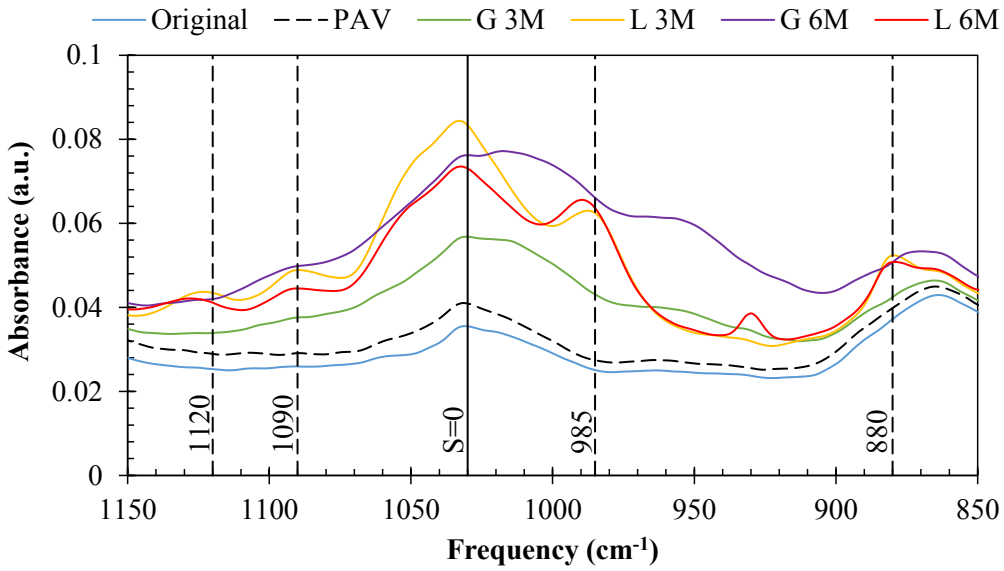

(a) Control PG 64-22 HMA

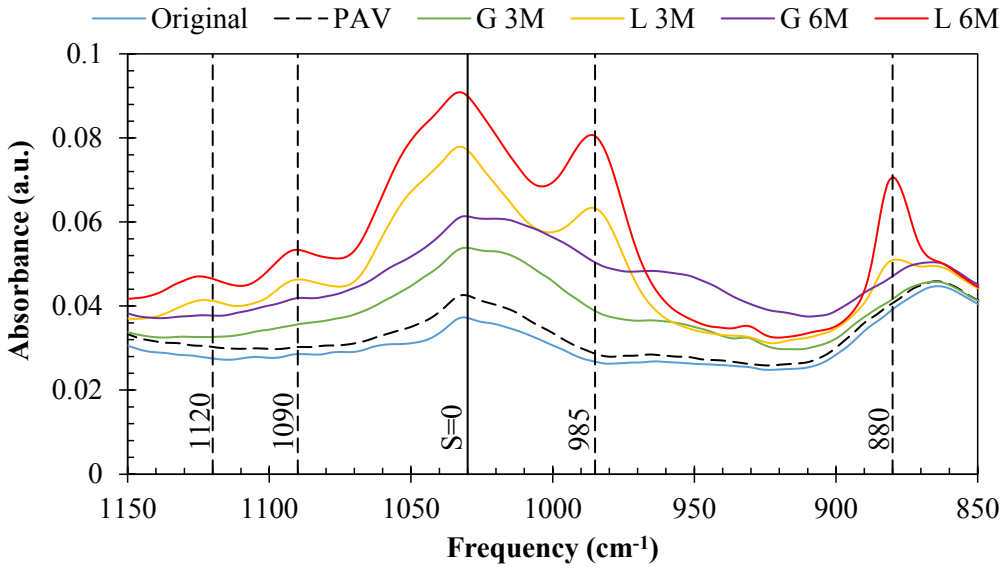

(b) PG 64-22 Rediset

Figure 53. Other compounds with aging

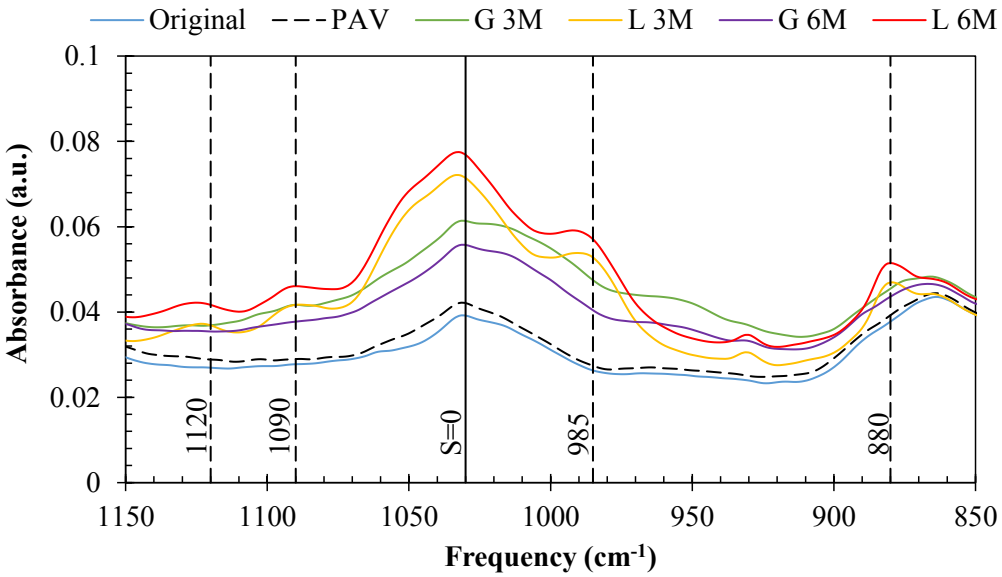

(c) PG 64-22 Sasobit

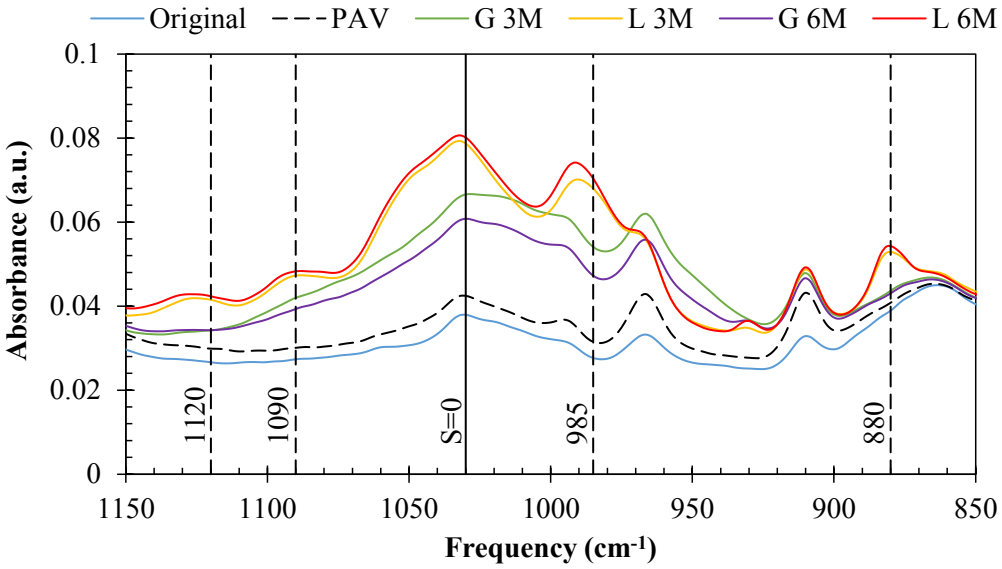

(d) Polymer-modified PG 76-22

Figure 53. Continued

Figure 54 shows that all binders extracted from aged limestone mixtures also exhibited changes at the 1460-cm^{-1} peak, which is related to the methyl and methylene functional groups (Table 6). These compounds are not expected to change with binder aging (Liu et al. 2013). Other peaks related to the presence of methyl and methylene (i.e., CH_2 and CH_3 from 3000 cm^{-1} to 2800 cm^{-1}) were evaluated, and no changes were found with aging. From Figure 53, it was speculated that some sulfur-containing compounds could be responsible for the additional peaks observed around the sulfoxide area, possibly such a compound also provoked the change at 1460 cm^{-1}.

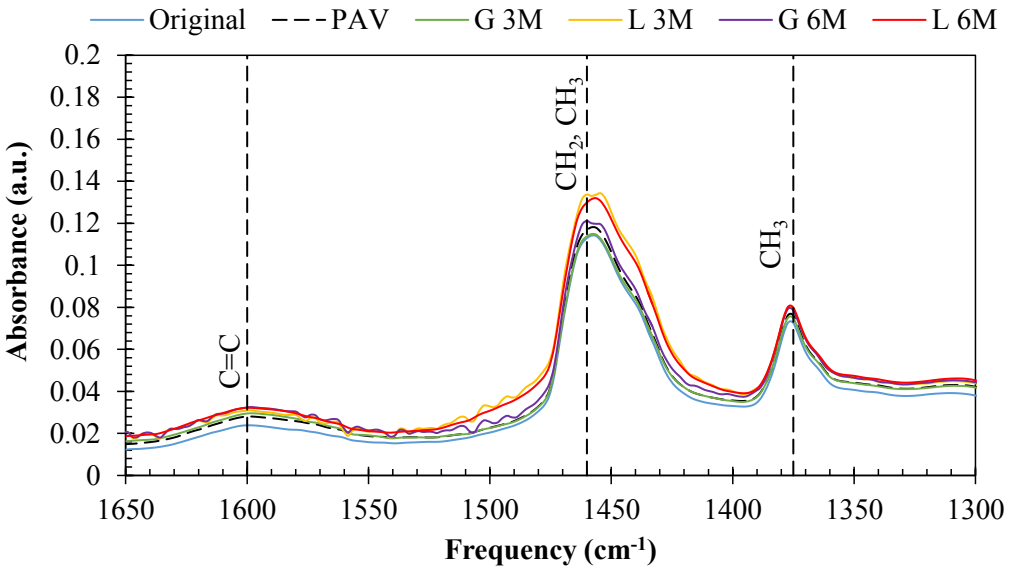

(a) Control PG 64-22 HMA

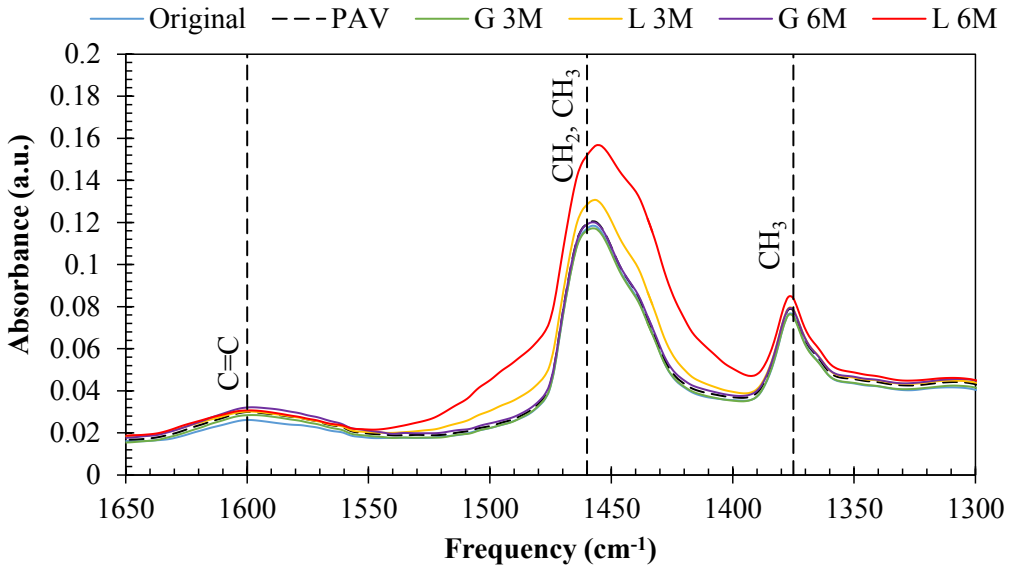

(b) PG 64-22 Rediset

Figure 54. Methylene and methyl groups with aging

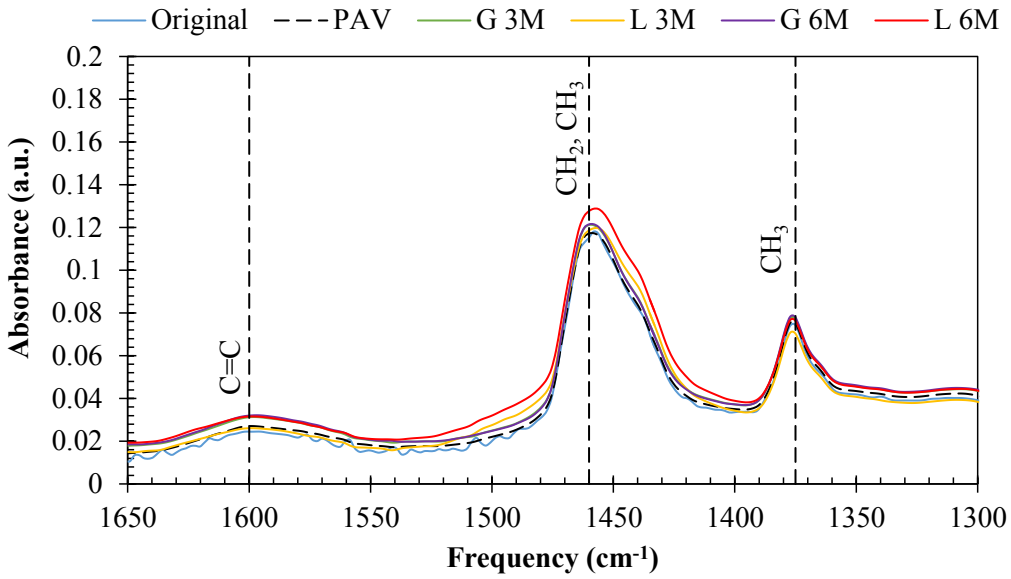

(c) PG 64-22 Sasobit

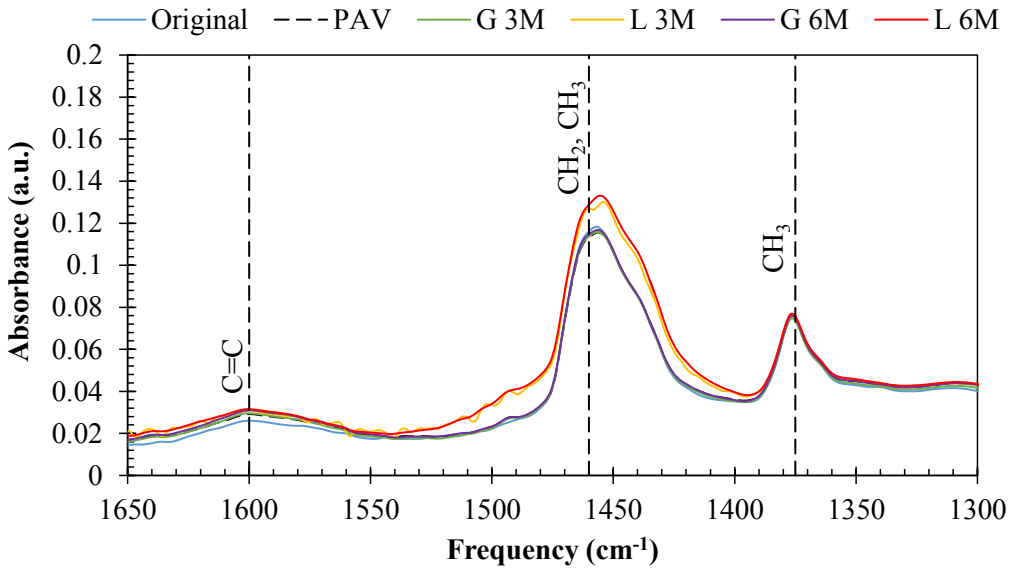

(d) Polymer-modified PG 76-22

Figure 54. Continued

5.4 Summary

A full factorial experiment was conducted to evaluate the long-term properties of asphalt mixtures, with a focus on quantifying the effect of binder modifications and

aggregate types on age-hardening characteristics of the mixtures. A total of 20 mixtures was evaluated, including two aggregate types, two asphalt binders, and five technological alternatives. The VE behavior of asphalt mixtures was evaluated at three different aging stages (initial stage, 3 months, and 6 months) in a controlled-temperature room at 60°C. Mixtures were fabricated based on recommendations from Yin et al (2013) to mimic recently constructed materials. A subset of four asphalt binders, including the control PG 64-22, two WMAs (Rediset and Sasobit), and polymer-modified PG 76-22 binders, was characterized in terms of rheological and chemical changes after standard laboratory aging (i.e., RTFOT and PAV aging) and after extraction from aged mixtures (i.e., 3 months and 6 months at 60°C).

It was found that WMA technologies may exhibit a larger age-hardening effect during the first 3 months of aging in the 60°C environmental room, while from 3 months to 6 months, the age-hardening effect was comparable to that from HMA. Aggregate type had a significant effect on the age-hardening process. The age-hardening of asphalt mixtures is commonly attributed to binder age-hardening, and binder age-hardening is explained by changes in binder chemistry. Most specifically, binder age-hardening has been correlated to the formation of ketones, which are carbonyl-containing compounds. Within this study, comparisons were made at two different levels: (1) binder rheology and chemistry and (2) mixture and binder.

Figure 55 compares binder rheology to carbonyl formation. Binder rheology was defined by the viscosity of the dashpot corresponding to the mechanical analog model for binder (Figure 55a) and the dynamic shear modulus at 60°C and 10 Hz (Figure 55b). The

control PG 64-22 and polymer-modified PG 76-22 binders exhibited rheological changes, which can be reasonably explained from carbonyl formation, while correlations were not very clear for the WMA-modified binders. It is important to highlight that the various data points plotted in Figure 55 correspond to different aging protocols, involving different temperatures and/or pressures. Adding the inherent variability introduced by the extraction process, the resulting correlations are not sufficiently precise, but the trends are still useful for comparison purposes.

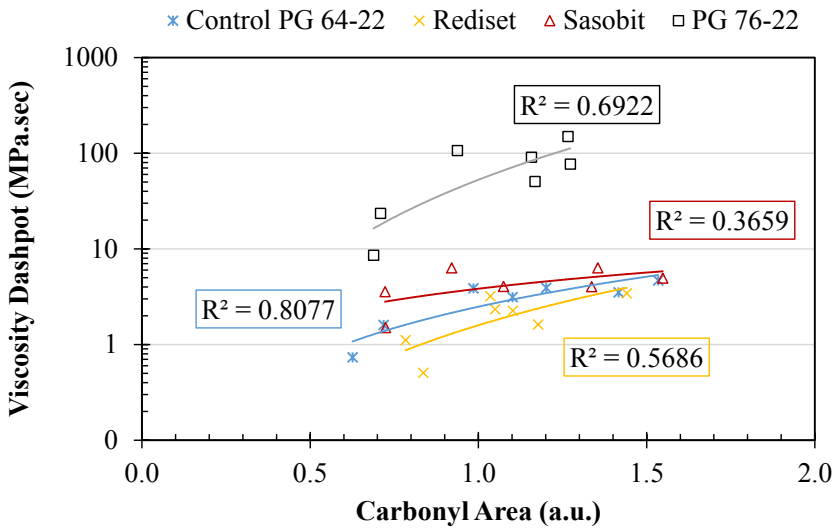

(a) Viscosity dashpot

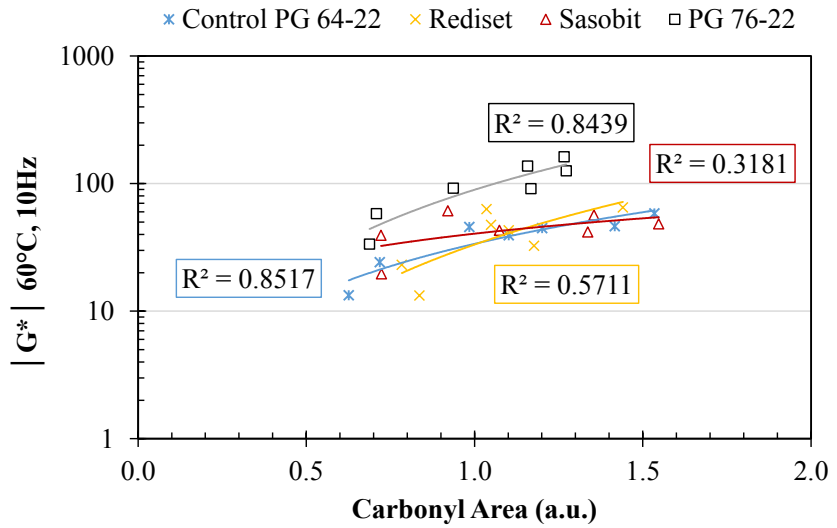

(b) Dynamic shear modulus at 60°C, 10 Hz

Figure 55. CA vs. binder rheology

The process of mixture age-hardening was compared to that of the extracted binders at two different levels, binder rheology and binder chemistry. For comparison of mixtures and binder rheology, the aging state variable (A) of asphalt mixtures was compared to the aging state variables (A_1 and A_2) of the asphalt binders (Figure 56). Considering exclusively the gabbro materials (Figure 56a), it was observed that A_1 and A_2

increased when mixture A increased, which was not the case for limestone mixtures (Figure 56b). In general, A_1 and/or A_2 did not have a direct strong correlation to mixture age-hardening. A_1 and A_2 modified the binders from J' and J" separately such that neither parameter was solely responsible for the global age-hardening of the asphalt binder. Additionally, parameters A, A_1, and A_2 required an initial condition in order to quantify age-hardening. For the mixtures, the initial condition was the mixture prior to aging, while for the binders it was taken prior to mixing, and these may not be comparable to produce good correlations.

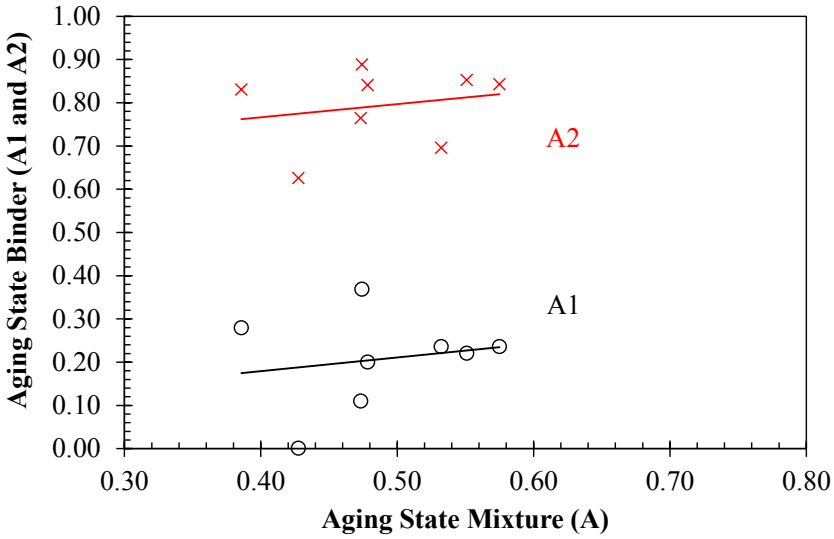

(a) Gabbro

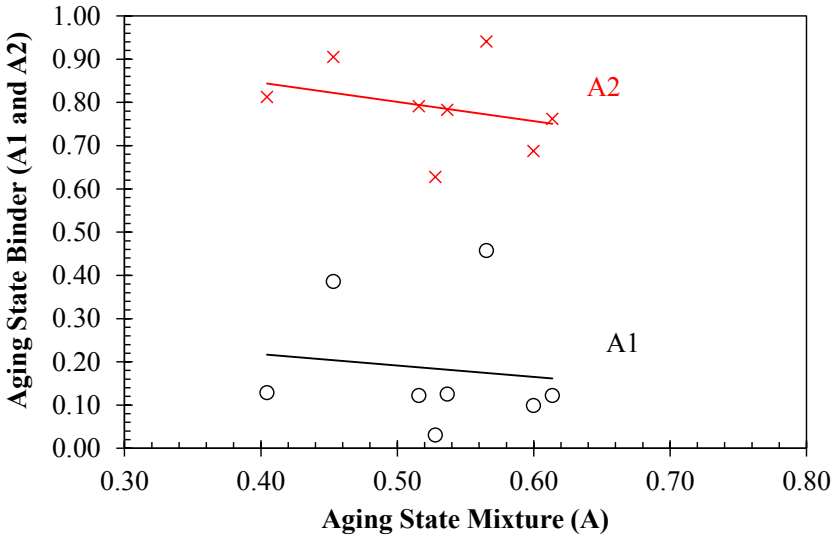

(b) Limestone

Figure 56. Aging state variable: mixture vs. binder

To eliminate the concern regarding the initial condition, CA was compared to mixture age-hardening. Figure 57 shows that gabbro mixtures exhibited increased age-hardening analogous to the increase in carbonyl formation, while limestone mixtures did not show such correlation. Several factors could contribute to the lack of correlation for

limestone age-hardening and carbonyl formation. First, any mechanical change at the interphase could not be explained from the increase in carbonyl groups. Second, the aged binders extracted from the limestone materials observed larger production of sulfoxides, and the presence of unidentified functional groups contributing to age-hardening was unknown and was not quantifiable within the scope of this study. And finally, considering the scenario of selective absorption, the binder extracted and evaluated would not accurately represent the binder crust around the limestone aggregate within the mixture.

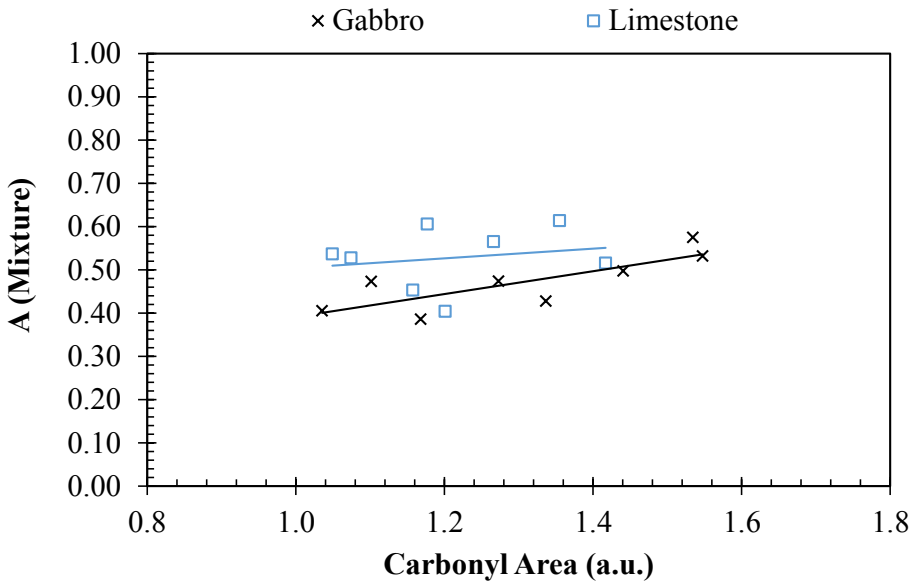

Figure 57. CA vs. mixture age-hardening (A)

In general, this study suggests that that mixture age-hardening cannot be explained from binder age-hardening exclusively, especially when absorptive aggregates are considered. Based on the FTIR CA results, it is likely that the gabbro materials act like a catalyst in the formation of carbonyl-containing compounds. Based on LVE evaluation, mixtures with limestone aggregates experience increased age-hardening, while binder

rheology and FTIR CA are not in agreement. The observed mixture response could be affected by changes in the interphase region with aging and/or caused by selective absorption of the asphalt binder into the aggregate's surface morphology. The possible selective absorption in the limestone mixtures raises concerns about how accurately the rheology of the extracted binder represents that of the effective binder surrounding the limestone aggregates within the mixture (i.e., binder not absorbed by the aggregate). Age-hardening of asphalt mixtures is a complex phenomenon involving many variables. Binder oxidation is a major concern, but it is not the only factor by which mixture age-hardening could be explained. For improved modeling of the age-hardening of asphalt mixtures, further understanding and quantification are required on how aggregate morphology and mineralogy may alter rheological properties of the effective binder and its aging characteristics.

CHAPTER VI

CONCLUSIONS AND RECOMMENDATIONS FOR FUTURE RESEARCH

This chapter presents conclusions based on the results of this study and provides recommendations for future research.

6.1 Conclusions

Asphalt mixtures degrade with time due to weathering, reducing the service life of the wearing course and the pavement structure. Moisture damage and oxidative age-hardening are the main concerns in ensuring material durability. Pursuing a fundamental understanding of weathering degradation will enable pavement engineers and scientists to evaluate mixtures and pavement performance effectively. It is important to continue to develop experimental and analytical tools for designers to provide cost-efficient recommendations with consideration of long-term performance. This study focused on investigating physicochemical interactions at the binder-aggregate interface contributing to moisture damage and oxidative age-hardening processes.

Evaluation of binder-aggregate adhesive properties is reported in Chapters III and IV. Chapter III focuses on the effect of incorporating WMA additives and varying additive dosages on the SFE of WMA binders before and after laboratory aging. Adhesion to the aggregate fraction and moisture susceptibility were evaluated based on SFE parameters for a total of 28 binder-aggregate combinations. Additionally, mechanical degradation of the FAM with moisture damage and aging was evaluated for 20 of these mixtures for comparison with the SFE-based moisture susceptibility parameters. Chapter IV presents a

microcalorimeter technique to evaluate the change of binder-aggregate adhesive bond at an in-service temperature range and to assess the binder-aggregate bond in the presence of water.

Based on the SFE analysis, it was found that WMA additives can increase the binder-aggregate adhesive bond and improve the ER, potentially improving resistance to moisture damage. Additive dosage can be optimized for best results. Additionally, WMA additives can reduce binder surface tension, and an asphalt binder with lower surface tension results in improved coating of aggregate particles. Based on the mechanical evaluation, it can be concluded that the surface energy parameters and mechanical evaluation for moisture damage result in similar trends. The ER and FAM evaluation provide a good toolset for screening moisture-susceptible mixtures. Additional findings from this study are as follows:

- From SFE and DMA evaluations, mixtures containing gabbro aggregates are more susceptible to moisture damage compared to mixtures with limestone aggregates. Meanwhile, the moisture sensitivity of gabbro can be improved if combined with certain binder types and WMA additives.
- Available WMA technologies can improve, deteriorate, or have a minimal effect on mixture performance. The selection of modifier type should be optimized for particular binder/aggregate combinations.
- SFE parameters such as adhesive bond energy and ER prove effective in ranking mixtures most resistant to moisture damage as compared to mechanical evaluation of FAM.

Considering the effect of temperature in binder-aggregate adhesive characteristics, it was found that the asphalt binder-aggregate adhesive bond becomes weaker with increasing temperature. The magnitude of the bond reduction is dependent on the particular binder-aggregate combinations, with the aggregate type having a greater impact. The assumption that ΔG_{ref} has a significant effect on ranking binder-aggregate combinations makes it is important to continue to study thermodynamics of adhesion and wetting processes for improved accuracy in analysis methodologies. Experimental data confirm that conditioning aggregates at relative humidity levels of 30+% can inhibit binder-aggregate bonding. The experiments regarding aggregate hydrophilicity based on enthalpy of immersion are consistent with the predicted bond strength based on SFE measurements and calculated water-aggregate work of adhesion (ΔG).

Chapter V presents a full study on age-hardening of asphalt mixtures and binders with consideration of mechanics, rheology, and chemistry. Mixture age-hardening could not be fully explained from binder age-hardening; inconsistencies are attributed to changes in the binder-aggregate interphase with aging, which cannot be fully characterized at this time. Changes in binder rheology could be explained by changes in binder chemistry, specifically from the formation of carbonyl compounds. Based on the experimental data, gabbro aggregates are a catalyst for binder oxidation, while limestone aggregates have a greater impact on mixture age-hardening, possibly based on selective absorption and/or changes at the interphase. The standard laboratory long-term aging protocol (RTFOT plus 20 hours of PAV aging) does not produce comparable binders to those extracted from the asphalt mixtures. Consideration of the asphalt binders near the aggregate surface, or

diffusing into it, could improve the accuracy of mechanical modeling for asphalt mixture age-hardening.

Based on the results presented in this study with respect to both weathering degradation processes (i.e., moisture damage and aging), aggregate type has a larger impact than WMA additives on the short- and long-term performance of asphalt mixtures in terms of moisture susceptibility and mixture age-hardening. Synergistic effects of moisture damage and aging should be carefully considered in evaluating asphalt mixtures and pavement design approaches. An aggregate that may be poor in terms of wearing resistance, such as limestone, could also be highly resistant to moisture damage and possibly long-term age-hardening if sufficient binder is incorporated into the mixture.

6.2 Recommendations for Future Research

The Wilhelmy plate and USD methods for assessment of SFE consist of measuring material properties at ambient temperature separately for binders and aggregates and then calculating the interaction using the acid-base theory. Conversely, the microcalorimeter is capable of directly measuring binder-aggregate interaction, but requires an assumption of ΔG_{ref} in order to obtain full thermodynamic characterization of interactions at the interface. In this study, ΔH was measured at various temperatures and ΔG had to be assumed at one reference temperature. Considering an alternative to this approach, if ΔG experiments were conducted at various temperatures, ΔH could be calculated based on the following Gibbs-Helmholtz Equation (48), whose derivation is explained by Wilson (1966).

$$\Delta \mathrm{H} = \Delta \mathrm{G} - \mathrm{T}\left(\frac{\partial \Delta G}{\partial T}\right)_P \quad (48)$$

The temperature-dependent evaluation of the binder-aggregate interface could be a powerful tool for assessing WMA effectiveness in reducing mixing and compaction temperatures. Several studies have evaluated binder viscosity (Sadeq et al. 2016b; Garcia Cucalon 2010; Wasiuddin et al. 2007; Hurley,Prowell 2005) and binder surface tension (Osmari et al. 2015) without conclusive recommendations on how to select production temperatures for a given combination of WMA technology, binder, and aggregate. Oftentimes, wax-based WMA additives are the most effective in reducing mixing and compaction temperatures by evaluating binder viscosity or binder surface tension, while in practice other chemical additives also allow for lower production temperatures without sacrificing coatability. Findings from this study suggest that aggregate type has an impact on the temperature dependency of the binder-aggregate bond at in-service temperatures, so the wettability or coatability at production temperatures is likely also affected by the binder-aggregate interaction as opposed to being controlled solely by binder surface tension. The next step in evaluating and optimizing WMA mixing temperature reduction should include the aggregate as part of the experimental process, and a microcalorimetry study in the production temperature range could be a promising fundamental approach.

The flexibility for aggregate conditioning within microcalorimetry experiments provides a powerful tool to assess the effectiveness of chemical additives such as adhesion promoters or lime treatments. The effect of temperature and moisture could also be applied for evaluating cold asphalt mixtures (or surface treatments), in which experimental

conditions could be modified to mimic field climatic conditions and/or construction operations.

The asphalt mixtures undergo age-hardening as a result of changes in the binder chemistry and rheology plus the changes at the interphase region. Aging of the asphalt binder may occur at different rates (faster or slower) depending on the aggregate fraction it neighbors. It would be complex, excessively time-consuming, and probably impractical to include the aggregate as part of any standardized binder laboratory-aging method. Recent NCHRP projects are oriented toward laboratory protocols for age-hardening of asphalt mixtures and evaluating the mixture mechanical response with aging. Such an approach is accurate, but still somewhat impractical, with the increased number of technological alternatives currently available. It would be appropriate to accompany such studies with in-depth evaluation of the binder-aggregate neighboring region, continuing to move forward with micromechanics-based modeling.

It is important to continue exploring fundamental properties enabling the pavement community to understand interactions among constituent materials in asphalt mixtures and their relation to performance of the composite. Such a fundamental research approach leads to a more efficient assessment of current and emerging asphalt technologies. Research studies should consider initial, intermediate-term, and long-term characteristics of asphalt materials with relation to field performance.

REFERENCES

Airey, G.: State of the art report on ageing test methods for bituminous pavement materials. International Journal of Pavement Engineering 4(3), 165-176 (2003)

Airey, G., Wu, J.: The influence of aggregate interaction and aging procedure on bitumen aging. Journal of Testing and Evaluation 37(5), 1-8 (2009)

Al-Ansary, M., Iyengar, S.R.: Physiochemical characterization of coarse aggregates in Qatar for construction industry. International Journal of Sustainable Built Environment 2(1), 27-40 (2013)

Alavi, M.Z., Hajj, E.Y., Hanz, A., Bahia, H.U.: Evaluating Adhesion Properties and Moisture Damage Susceptibility of Warm-Mix Asphalts, Bitumen Bond Strength and Dynamic Modulus Ratio Tests. Transportation Research Record No. 2295, 44-53 (2012)

Anderson, D.A., Christensen, D.W., Bahia, H.U., Dongre, R., Sharma, M., Antle, C.E., Button, J.: Binder characterization and evaluation, volume 3: Physical characterization. Strategic Highway Research Program, National Research Council, Report No. SHRP-A-369 (1994)

Anderson, R.M., King, G.N., Hanson, D.I., Blankenship, P.B.: Evaluation of the relationship between asphalt binder properties and non-load related cracking. Journal of the Association of Asphalt Paving Technologists 80 (2011)

Austerman, A.J., Mogawer, W.S., Bonaquist, R.: Evaluating the Effects of Warm Mix Asphalt Technology Additive Dosages on the Workability and Durability of Asphalt. In: 88th Annual Meeting of the Transportation Research Board, Washington DC (2009)

Barbour, F.A., Barbour, R.V., Peterson, J.C.: A study of asphalt-aggregate interactions using inverse gas-liquid chromatography. Journal of Applied Chemistry and Biotechnology 24(11), 645-654 (1974)

Bell, C.A.: Summary report on aging of asphalt-aggregate systems. SHRP-A-305. Strategic Highway Research Program, (1989)

Bell, C.A., AbWahab, Y., Cristi, M., Sosnovske, D.: Selection of laboratory aging procedures for asphalt-aggregate mixtures. vol. SHRP-A-383. Strategic Highway Research Program, (1994)

Bennert, T., Maher, A., Sauber, R.: Influence of Production Temperature and Aggregate Moisture Content on the Performance of Warm Mix Asphalt. Transportation Research Record No. 2208, 97-107 (2011)

Bhasin, A., Howson, J., Masad, E., Little, D.N., Lytton, R.L.: Effect of Modification Processes on Bond Energy of Asphalt Binders. Transportation Research Record 1993, 29-37 (2007)

Bhasin, A., Little, D.: Characterization of Aggregate Surface Energy Using Universal Sorption Device. Journal of Materials in Civil Engineering 19(8), 634-641 (2007)

Bhasin, A., Little, D.N.: Application of microcalorimeter to characterize adhesion between asphalt binders and aggregates. Journal of Materials in Civil Engineering 21(6), 235-243 (2009)

Bhasin, A., Masad, E., Little, D., Lytton, R.: Limits on Adhesive Bond Energy for Improved Resistance of Hot-Mix Asphalt to Moisture Damage. Transportation Research Record No. 1970, 3-13 (2006)

Birgisson, B., Roque, R., Page, G.: Performance-based fracture criterion for evaluation of moisture susceptibility in hot-mix asphalt. Transportation research record: journal of the transportation research board(1891), 55-61 (2004)

Bonaquist, R.: Mix Design Practices for Warm Mix Asphalt. In: NCHRP Report 691. Advanced Asphalt Technologies, LLC, Sterling, VA, (2011)

Bower, N., Wen, H., Willoughby, K., Weston, J., DeVol, J.: Evaluation of Performance of Warm Mix Asphalt in Washington State. In. Washington State University, (2012)

Branthaver, J., Petersen, J., Robertson, R., Duvall, J., Kim, S., Harnsberger, P., Mill, T., Ensley, E., Barbour, F., Scharbron, J.: Binder characterization and evaluation. Volume 2: Chemistry. No. SHRP-A-368. (1993)

Caro, S., Beltran, D., Alvarez, A., Estakhri, C.: Analysis of moisture damage susceptibility of warm mix asphalt (WMA) mixtures based on Dynamic Mechanical Analyzer (DMA) testing and a fracture mechanics model. Construction and Building Materials 35, 460-467 (2012)

Caro, S., Masad, E., Bhasin, A., Little, D.: Coupled micromechanical model of moisture-induced damage in asphalt mixtures. Journal of Materials in Civil Engineering 22(4), 380-388 (2009)

Caro, S., Masad, E., Bhasin, A., Little, D.N.: Moisture susceptibility of asphalt mixtures, Part 1: mechanisms. International Journal of Pavement Engineering 9(2), 81-98 (2008a)

Caro, S., Masad, E., Bhasin, A., Little, D.N.: Moisture susceptibility of asphalt mixtures, Part 2: characterisation and modelling. International Journal of Pavement Engineering 9(2), 99-114 (2008b)

Cortizo, M., Larsen, D., Bianchetto, H., Alessandrini, J.: Effect of the thermal degradation of SBS copolymers during the ageing of modified asphalts. Polymer Degradation and Stability 86(2), 275-282 (2004)

Cui, Y., Jin, X., Han, R., Glover, C.: An Accelerated Method for Determining Asphalt Oxidation Kinetics Parameters for Use in Pavement Oxidation and Performance Modeling. Petroleum Science and Technology 32(22), 2691-2699 (2014)

Curtis, C.W., Ensley, K., Epps, J.: Fundamental properties of asphalt-aggregate interactions including adhesion and absorption. In. National Research Council Washington, DC, USA, (1993)

Curtis, C.W., Perry, L., Brannan, C.: Investigation of asphalt-aggregate interactions and their sensitivity to water. No. VTI Rapport 372A, Part 4. (1991)

D'Angelo, J., Anderson, R.M.: Material production, mix design, and pavement design effects on moisture damage. Moisture Sensitivity of Asphalt Pavements (2003): 187-201.

Davidson, R.R., Bullin, J.A., Glover, C.J., Jr., B.L.B., Jemison, H.B., Kyle, A.L.G., Cipione, C.A.: Development of Gel Permeation Chromatography, Infrared and Other Tests to Characterize Asphalt Cements and Correlate with Field Performance. In., vol. FHWA/TX-90/458-1F, p. 453. Texas Transportation Institute, College Station, Texas, (1989)

Diefenderfer, S., Clark, T.M.: Warm-Mix Asphalt Heating Up in Virginia. In: TR News. vol. 274. (2011)

Douillard, J., Zoungrana, T., Partyka, S.: Surface Gibbs free energy of minerals: some values. Journal of Petroleum Science and Engineering 14(1), 51-57 (1995)

Doyle, J.D., Mejias-Santiago, M., Brown, E.R., Howard, I.L.: Performance of High RAP-WMA Surface Mixtures. Asphalt Paving Technology 80, 419-458 (2011)

Epps, J., Berger, E., Anagnos, J.N.: Treatments. In: Proceedings of the Moisture Sensitivity of Asphalt Pavements–A National Seminar 2003

Epps Martin, A., Arambula, E., Yin, F., Garcia Cucalon, L., Chowdhury, A., Lytton, R., Epps, J., Estakhri, C., Park, E.S.: Evaluation of Moisture Susceptibility of WMA Technologies. In: Board, T.R. (ed.) NCHRP Report 763. Texas A&M Transportation Institute, Washington D.C., (2014)

Estakhri, C.: Laboratory and Field Performance Measurements to support the Implementation of Warm Mix Asphalt in Texas. In., vol. FHWA/TX-12/5-5597-01-1, p. 77. Texas Transportation Institute, College Station, TX, (2012)

Estakhri, C., Button, J., Alvarez, A.: Field and Laboratory Investigation of Warm Mix Asphalt in Texas. In., p. 144. Texas Transportation Institute, College Station, Texas, (2010)

Farrar, M., Loveridge, J.L., Rovani, J.: The Limit of Detection (LOD) Method: An FTIR Screening Tool for Evaluating Solvent Remaining after Extraction. In: Fundamental Properties of Asphalts and Modified Asphalts III Product: FP 03. p. 18. Western Research Institute, Laramie, WY, (2015)

Garcia Cucalon, L.: Comparación del comportamiento mecánico de mezcla asfáltica tibia y mezcla asfáltica caliente. "Comparison of mechanical performance of WMA and HMA". Catholic University of Guayaquil (2010)

Garcia Cucalon, L., Epps Martin, A., Arambula, E., Yin, F., Estakhri, C.K., Park, E.S., Epps, J.: Moisture susceptibility of Warm-Mix Asphalt. In: Asphalt Pavements. pp. 691-700. CRC Press, (2014)

Garcia Cucalon, L., Kassem, E., Little, D.N., Masad, E.: Fundamental Evaluation of Moisture Damage in Warm-Mix Asphalts. Road Materials and Pavement Design (Special Issue: Papers from the 91st Association of Asphalt Paving Technologists' Annual Meeting "In press") (2016a)

Garcia Cucalon, L., Rahmani, E., Little, D.N., Allen, D.H.: A multiscale model for predicting the viscoelastic properties of asphalt concrete. Mechanics of Time-Dependent Materials, 1-18 (2016b). doi:10.1007/s11043-016-9303-2

Garcia Cucalon, L., Yin, F., Epps Martin, A., Arambula, E., Estakhri, C., Park, E.S.: Evaluation of Moisture Susceptibility Minimization Strategies for Warm-Mix Asphalt: Case Study." Journal of Materials in Civil Engineering 28, no. 2 (2015).

Glover, C.J., Davison, R.R., Domke, C.H., Ruan, Y., Juristyarini, P., Knorr, D.B., Jung, S.H.: Development of a new method for assessing asphalt binder durability with field validation. No. FHWA/TX-05/1872-2. (2005)

Glover, C.J., Liu, G., Rose, A.A., Tong, Y., Gu, F., Ling, M., Arambula, E., Estakhri, C.K., Lytton, R.L.: Evaluation of Binder Aging and Its Influence in Aging of Hot Mix Asphalt Concrete. In. (2014)

Goh, S.W., You, Z.: Moisture Damage and Fatigue Cracking of Foamed Warm Mix Asphalt Using a Simple Laboratory Setup. Journal of Materials in Civil Engineering (2011): 1338-1345.

Hearon, A., Diefenderfer, S.: Laboratory Evaluation of Warm Asphalt Properties and Performance. In: Airfield and Highway Pavements: Efficient Pavements Supporting Transportation’s Future, Bellevue, Washington, October 2008, pp. 182-194

Hefer, A.W., Bhasin, A., Little, D.: Bitumen Surface Energy characterization Using a Contact Angle Approach. Journal of Materials in Civil Engineering 18(6), 759-767 (2006)

Howson, J., Masad, E.A., Bhasin, A., Branco, V.C., Arambula, E., Lytton, R.L., Little, D.N.: System for The Evaluation of Moisture Damage Using Fundamental Material Properties. In. (2007)

Hunter, E.R., Ksaibati, K.: Evaluating moisture susceptibility of asphalt mixes. Mountain-Plains Consortium, (2002)

Hurley, G.C., Prowell, B.D.: Evaluation of Sasobit for use in warm mix asphalt. NCAT report 5(06) (2005)

Hurley, G.C., Prowell, B.D.: Evaluation of Potential Processes for Use in Warm Mix Asphalt. Asphalt Paving Technology 75, 41-90 (2006)

Izzo, R., Tahmoressi, M.: Use of the Hamburg wheel-tracking device for evaluating moisture susceptibility of hot-mix asphalt. Transportation Research Record: Journal of the Transportation Research Board(1681), 76-85 (1999)

Jensen, P.A.: Operations Research Models and Methods. http://staff.ulsu.ru/semushin/_index/_pilocus/_gist/docs/mycourseware/9-linprogram/6-tools/simplex-DemoCD/_SIMPLEX-DemoTools/t6/index-7.html (2004). Accessed 4/26/201 2016

Jones, D., Wu, R., Tsai, B.W.: Key Results from a Comprehensive Accelerated Loading, Laboratory, and Field Testing Study on Warm-Mix Asphalt in California. In: 2nd International Warm-Mix Asphalt Conference, St. Louis, Missouri 2011

Kandhal, P.: Low-temperature ductility in relation to pavement performance. In: Low-Temperature Properties of Bituminous Materials and Compacted Bituminous Paving Mixtures. ASTM International, (1977)

Kassem, E., Masad, E., Lytton, R., Chowdhury, A.: Influence of air voids on mechanical properties of asphalt mixtures. Road Materials and Pavement Design 12(3), 493-524 (2011)

Kim, Y.-R., Baek, C., Lee, J., Bacchi, C.: Evaluation of Moisture Susceptibility in a Warm Mix Asphalt Pavement: US 157, Hurdle Mills, NC. In: 2nd International Warm-Mix Asphalt Conference, St. Louis, Missouri 2011

Kim, Y.-R., Little, D.N., Lytton, R.L.: Effect of Moisture Damage on Material Properties and Fatigue Resistance of Asphalt Mixtures. Transportation Research Record No. 1832, 48-54 (2004)

King, G., Anderson, M., Hanson, D., Blankenship, P.: Using black space diagrams to predict age-induced cracking. In: 7th RILEM International Conference on Cracking in Pavements 2012, pp. 453-463. Springer

Larsen, D.O., Alessandrini, J.L., Bosch, A., Cortizo, M.S.: Micro-structural and rheological characteristics of SBS-asphalt blends during their manufacturing. Construction and Building Materials 23(8), 2769-2774 (2009). doi:http://dx.doi.org/10.1016/j.conbuildmat.2009.03.008

Lau, C., Lunsford, K., Glover, C., Davison, R., Bullin, J.: Reaction rates and hardening susceptibilities as determined from pressure oxygen vessel aging of asphalts. Transportation Research Record(1342) (1992)

Lee, D.-Y., Guinn, J.A., Khandhal, P.S., Dunning, R.L.: Absorption of asphalt into porous aggregates. In. (1990)

Little, D.N., Bhasin, A.: Using Surface Energy Measurements to Select Materials for Asphalt Pavement. In., vol. Web-Only Document 104, p. 90. National Cooperative Highway Research Program, Washington, D.C., (2006)

Little, D.N., Epps, J.A., Sebaaly, P.E.: Hydrated Lime in Hot Mix Asphalt. National Lime Association (2006).

Little, D.N., Jones, D.: Chemical and mechanical processes of moisture damage in hot-mix asphalt pavements. In: Proceedings of the Moisture Sensitivity of Asphalt Pavements–A National Seminar 2003, pp. 37-71

Liu, H., Hao, P., Wang, H., Adhikair, S.: Effects of physio-chemical factors on asphalt aging behavior. Journal of Materials in Civil Engineering 26(1), 190-197 (2013)

Liu, M., Ferry, M.A., Davidson, R.R., glover, C.J., bullin, J.A.: Oxygen Uptake As Correlated to Carbonyl Growth in Aged Asphalts and Asphalt Corbett Fractions. Industrial and Engineering Chemistry Research 37, 4669-4674 (1998)

Lu, X., Isacsson, U.: Chemical and rheological evaluation of ageing properties of SBS polymer modified bitumens. Fuel 77(9), 961-972 (1998)

Luo, R., Lytton, R.L.: Selective absorption of asphalt binder by limestone aggregates in asphalt mixtures. Journal of Materials in Civil Engineering 25(2), 219-226 (2012)

Lytton, R., Uzan, J., Fernando, E.G., Roque, R.: Development and validation of performance prediction models and specifications for asphalt binders and paving mixes. In: Strategic Highway Research Program. Washington DC, (1993)

Masad, E., Branco, V.C., Little, D.N., Lytton, R.: A unified method for the analysis of controlled-strain and controlled-stress fatigue testing. International Journal of Pavement Engineering 9(4), 233-246 (2008)

Masad, E., Kassem, E., Little, D.: Characterization of Asphalt Pavement Materials in the State of Qatar. Road Materials and Pavement Design 12:4, 739-765 (2011). doi:10.1080/14680629.2011.9713893

Mastrofini, D., Scarsella, M.: The application of rheology to the evaluation of bitumen ageing. Fuel 79(9), 1005-1015 (2000)

McGennis, R.B., Kennedy, T.W., Machemehl, R.B.: Stripping and moisture damage in asphalt mixtures. In. (1984)

McPhail, D., Cooper, A.: Thermodynamics and kinetics of dissociation of ligand-induced dimers of vancomycin antibiotics. Journal of the Chemical Society, Faraday Transactions 93(13), 2283-2289 (1997)

Mejias-Santiago, M., Doyle, J., Howard, I., Brown, R.: Moisture Damage Potential for Warm Mix Asphalt Containing Reclaimed Asphalt Pavement. In: 2nd International Warm Mix Conference, St. Louis, Missouri 2011

Menapace, I., Masad, E., Bhasin, A., Little, D.: Microstructural properties of warm mix asphalt before and after laboratory-simulated long-term ageing. Road Materials and Pavement Design 16 (2015)

Miller, C., Little, D., Bhasin, A., Gardner, N., Herbert, B.: Surface Energy Characteristics and Impact of Natural Minerals on Aggregate-Bitumen Bond Strengths and Asphalt Mixture Durability. Transportation Research Record: Journal of the Transportation Research Board(2267), 45-55 (2012)

Miller, C., Vasconcelos, K.L., Little, D.N., Bhasin, A.: Investigating aspects of aggregate properties that influence asphalt mixtures performance. In. Research Report for DTFH61-06-C-00021, Texas A & M University at College Station and The University of Texas at Austin, Texas, (2011)

Mogawer, W.S., Austerman, A.J., Kassem, E., Masad, E.: Moisture Damage Characteristics of Warm Mix Asphalt Mixes. Asphalt Paving Technology 80 (2011)

Mogawer, W.S., Austerman, A.J., Kluttz, R., Roussel, M.: High-Performance Thin-Lift Overlays with High Reclaimed Asphalt Pavement Content and Warm-Mix Asphalt Technology. Transportation Research Record(2293), 18-28 (2012)

Morian, N., Hajj, E., Glover, C., Sebaaly, P.: Oxidative aging of asphalt binders in hot-mix asphalt mixtures. Transportation Research Record: Journal of the Transportation Research Board(2207), 107-116 (2011)

NAPA: https://www.asphaltpavement.org/index.php?option=com_content&view=article&id=14&Itemid=33. Accessed 7/22/2015 2015

Newcomb, D., Martin, A.E., Yin, F., Arambula, E., Park, E.S., Chowdhury, A., Brown, R., Rodezno, C., Tran, N., Coleri, E.: Short-Term Laboratory Conditioning of Asphalt Mixtures. In. (2015)

Osmari, P.H., Arega, Z., Bhasin, A.: Wetting Characteristics of Asphalt Binders at Mixing Temperatures. In: 94th Annual Meeting of the Transportation Research Board, Washington, D.C. 2015

Parker Jr, F., Wilson, M.S.: Evaluation of boiling and stress pedestal tests for assessing stripping potential of Alabama asphalt concrete mixtures. Transportation Research Record(1096) (1986)

Pauli, A.T., Huang, S.-C.: Relationship between asphalt compatibility, flow properties, and oxidative aging. International Journal of Pavement Research and Technology 6(1), 1-7 (2013)

Petersen, J., Barbour, F., Dorrence, S.: Catalysis of asphalt oxidation by mineral aggregate surfaces and asphalt components. In: Association of Asphalt Paving Technologists Proc 1974

Petersen, J., Harnsberger, P.: Asphalt aging: dual oxidation mechanism and its interrelationships with asphalt composition and oxidative age hardening. Transportation Research Record: Journal of the Transportation Research Board(1638), 47-55 (1998)

Petersen, J., Robertson, R., Branthaver, J., Harnsberger, P., Duvall, J., Kim, S., Anderson, D., Christiansen, D., Bahia, H.: Binder Characterization and Evaluation, Volume 1, vol. 1. vol. SHRP-A-367. SHRP-A-367, Strategic Highways Research Program, National Research Council, Washington, DC, (1994)

Petersen, J.C.: A Review of the Fundamentals of Asphalt Oxidation. Transportation Research Circular E-C140, vol. E-C140. Transportation Research Board, Washington, DC, (2009)

Petersen, J.C., Glaser, R.: Asphalt oxidation mechanisms and the role of oxidation products on age hardening revisited. Road Materials and Pavement Design 12(4), 795-819 (2011)

Prowell, B.D., Hurley, G.C., Crews, E.: Field Performance of Warm Mix Asphalt at the NCAT Test Track. Transportation Research Record(1998), 96-102 (2007)

Rahmani, E.: Continuum-Based Constitutive Modeling of Coupled Oxidative Aging-Mechanical Response pf Asphalt Concrete. Texas A&M University (2015)

Rahmani, E., Darabi, M.K., Al-Rub, R.K.A., Kassem, E., Masad, E.A., Little, D.N.: Effect of confinement pressure on the nonlinear-viscoelastic response of asphalt concrete at high temperatures. Construction and Building Materials 47, 779-788 (2013)

Rashwan, M., Williams, R.C.: An Evaluation of Warm Mix Asphalt Additives and Reclaimed Asphalt Pavement on Performance Properties of Asphalt Mixtures. In: 91st Annual Meeting of the Trasnportation Research Board, Washington, D.C. 2012, p. 16

Robertson, R.E., Branthaver, J.F., Harnsberger, P.M., Petersen, J.C., Dorrence, S.M., McKay, J.F., Turner, T.F., Pauli, A.T., Huang, S.-C., Huh, J.-D.: Fundamental properties of asphalts and modified asphalts, volume I: Interpretive report. In. (2001)

Sadeq, M., Al-Khalid, H., Masad, E., Sirin, O.: Comparative evaluation of fatigue resistance of warm fine aggregate asphalt mixtures. Construction and Building Materials 109, 8-16 (2016a)

Sadeq, M., Masad, E., Al-Khalid, H., Sirin, O., Little, D.: Rheological Evaluation of Short- and Long-Term Performance for Warm Mix Asphalt (WMA) Binders. In: 8th RILEM International Symposium on Testing and Characterization of Sustainable and Innovative Bituminous Materials. pp. 129-139. Springer Netherlands, (2016b)

Schapery, R.A.: Correspondence Principles and a Generalized J-integral for Large Deformation and Fracture Analysis of Viscoelastic Media. International Journal of Fracture 25, 195-223 (1984)

Shakiba, M., Darabi, M.K., Abu Al-Rub, R.K., Masad, E.A., Little, D.N.: Microstructural modeling of asphalt concrete using a coupled moisture–mechanical constitutive relationship. International Journal of Solids and Structures 51(25–26), 4260-4279 (2014). doi:http://dx.doi.org/10.1016/j.ijsolstr.2014.08.012

Solaimanian, M., Harvey, J., Tahmoressi, M., Tandon, V.: Test methods to predict moisture sensitivity of hot-mix asphalt pavements. In: Transportation Research Board National Seminar. San Diego, California 2003, pp. 77-110

Solaimanian, M., Milander, S., Boz, I., Stoffels, S.M.: Development of Guidelines for Usage of High Percent RAP in Warm-Mix Asphalt Pavements. In. The Thomas D. Larson Pennsylvania Transportation Institut, University Park, PA, (2011)

Sousa, P., Kassem, E., Masad, E., Little, D.: New design method of fine aggregates mixtures and automated method for analysis of dynamic mechanical characterization data. Construction and Building Materials 41, 216-223 (2013)

Thomas, K.P., McKay, J.F., Branthaver, J.F.: Surfactants in aged asphalt and impact μ on moisture susceptibility of laboratory-prepared mixes. Road materials and pavement design 7(4), 477-490 (2006)

Usmani, A.: Asphalt science and technology. CRC Press, (1997)

Van Oss, C.J., Chaudhury, M.K., Good, R.J.: Interfacial Lifshitz-van der Waals and polar interactions in macroscopic systems. Chemical Reviews 88(6), 927-941 (1988)

Vasconcelos, K.L., Bhasin, A., Little, D.N.: Influence of reduced production temperatures on the adhesive properties of aggregates and laboratory performance of fine aggregate-asphalt mixtures. Road Materials and Pavement Design 11(1), 47-64 (2010)

Wasiuddin, N., Selvamohan, S., Zaman, M., Guegan, M.: Comparative laboratory study of Sasobit and aspha-min additives in warm-mix asphalt. Transportation Research Record: Journal of the Transportation Research Board (2007)

Wasiuddin, N.M.: Effect of Sasobit and Aspha-Min on Wettability and Adhesion between Asphalt Binders and Aggregates. Transportation Research Record(2051), 80-89 (2008)

Wilson, A.H.: Thermodynamics and statistical mechanics. Thermodynamics and Statistical Mechanics, by AH Wilson, Cambridge, UK: Cambridge University Press, 1957 1 (1957)

Wu, J., Han, W., Airey, G., Yusoff, N.I.M.: The influence of mineral aggregates on bitumen ageing. International Journal of Pavement Research and Technology 7(2), 115 (2014)

Xiao, F., Shivaprasad, P.V., Amirkhaian, S.N.: Low Volume WMA Mixtures: Moisture Susceptibility of Mixtures Containing Coal Ash and Roofing Shingle with Moist Aggregate. In: 90th Annual Meeting of the Transportation Research Board, Washington, D.C. 2011

Yin, F., Arambula, E., Newcomb, D., Bhasin, A.: Workability and coatability of foamed Warm-Mix Asphalt. In: Asphalt Pavements. pp. 721-730. CRC Press, (2014a)

Yin, F., Epps Martin, A., Arámbula-Mercado, E.: Warm-Mix Asphalt Moisture Susceptibility Evaluation for Mix Design and Quality Assurance. Transportation Research Record: Journal of the Transportation Research Board(2575), 39-47 (2016)

Yin, F., Garcia Cucalon, L., Epps Martin, A., Arambula, E., Chowdhury, A., Park, E.: Laboratory Conditioning Protocols for Warm-Mix Asphalt. Asphalt Paving Technology 82, 177-211 (2013)

Yin, F., Garcia Cucalon, L., Epps Martin, A., Arambula, E., Park, E.: Performance Evolution of Hot-Mix and Warm-Mix Asphalt with Field and Laboratory Aging. Asphalt Paving Technology 83, 109-141 (2014b)